Light Regulation of Zeaxanthin Epoxidase in Plants

Inaugural-Dissertation

for attaining the title of Doctor (Dr. rer. nat.)
in the faculty of Mathematics and Natural Sciences
at Heinrich Heine University Düsseldorf

Presented by

Stephanie Tanja Bethmann

From Neuss

Düsseldorf, May 2022

From the Institute of Plant Biochemistry,
Heinrich Heine University Düsseldorf

Printed with the permission from the Faculty of Mathematics and Natural Sciences,
Heinrich Heine University Düsseldorf

Supervisor: Prof. Dr. Peter Jahns

Co-Supervisor: Prof. Dr. Georg Groth

Date of Oral Examination: June 30th, 2022

STATEMENT OF DECLARATION

I, Stephanie Tanja Bethmann, hereby declare that I have fully and independently written the submitted dissertation without additional unauthorized support and consultation beyond that permitted and specified in the dissertation to include the necessary and appropriate cited literary resources. The dissertation in its present or similar form has not been previously submitted under the same or otherwise specified institution and department name. Previous unsuccessful oral examinations have not been registered or attempted.

Düsseldorf, May 19th, 2022

Table of contents

1. Summary

Plants are frequently exposed to fluctuating light conditions. Proper acclimation to such light conditions is essential for the competitiveness of plants in the field. Photo-oxidative stress is one of the most challenging stress factors for plants since reactive oxygen species (ROS) are inevitably formed upon photosynthetic light utilization. Hence, plants have developed several photoprotective mechanisms to prevent the formation of ROS and to detoxify already existing ROS. The photoprotective pigment zeaxanthin (Zx) contributes to both strategies. Zx is formed upon high light (HL) in the xanthophyll cycle by the enzyme violaxanthin (Vx) de-epoxidase (VDE), which converts Vx to Zx. The reconversion of Zx to Vx, which occurs predominantly in the dark as well as in low light (LL), is catalyzed by Zx epoxidase (ZEP). Zx has a dual function in photoprotection: bound to antenna of photosystem II (PSII), Zx is involved in the energy-dependent (qE) and in the Zx-dependent (qZ) mechanism of non-photochemical quenching (NPQ) of excitation energy. In these photoprotective mechanisms, excessively absorbed light energy is dissipated as heat and thereby the formation of ROS is prevented. As free pigment in the lipid phase of the thylakoid membrane, Zx contributes to the detoxification of already existing ROS. In *A. thaliana,* ZEP activity and hence Zx epoxidation was shown to be gradually downregulated in parallel with increasing photoinhibition of PSII in response to HL exposure.

In this work, the concerted regulation of ZEP and PSII activity in response to short- and long-term acclimation to HL was characterized in detail in different plant species (*A. thaliana*, N*. benthamiana*, *P. sativum* and *S. oleracea*). Moreover, the molecular basis of the light-regulation of ZEP activity was addressed under *in vitro* conditions. The experimental results reveal that the co-regulation of ZEP and PSII activity represents a common feature of all studied species and under all growth light conditions. Severe HL stress resulted not only in complete inactivation of PSII and ZEP, but also in the degradation of ZEP protein in parallel with D1. As a consequence of ZEP inactivation and degradation, high amounts of Zx are retained in the thylakoid membrane during photoinhibition of PSII, indicating an important photoprotective role of Zx during photoinhibition and repair of PSII under long-lasting HL conditions. Species-specific differences in HL sensitivity and thus different HL acclimation properties were shown to be predominantly determined by differences in the leaf thickness, the pool size of xanthophyll cycle pigments (Vx, antheraxanthin (Ax) and Zx) and the qE capacity. Analyses of the light-regulation of ZEP activity under *in vitro* conditions revealed a similar high activity of ZEP in the dark- and light-acclimated state. Moreover, ZEP activity could generally not be stimulated by reductants, such as dithiothreitol, suggesting that ZEP is not light-regulated by thiol-modification. Treatment of ZEP with different ROS showed, that ZEP is irreversibly inhibited by hydrogen peroxide (H_2O_2) in a time- and concentration-dependent manner, but not by singlet oxygen and superoxide. This implies that the observed HL induced inactivation of ZEP under *in vivo* conditions is likely based on an oxidation of ZEP by H_2O_2.

2. Zusammenfassung

Pflanzen sind häufig fluktuierenden Lichtbedingungen ausgesetzt. Die geeignete Anpassung an solche Lichtbedingungen ist essentiell für die Konkurrenzfähigkeit von Pflanzen. Photooxidativer Stress stellt einen der herausforderndsten Stressfaktoren für Pflanzen dar, da die Bildung reaktiver Sauerstoffspezies (ROS) bei der Nutzung der Lichtenergie in der Photosynthese unvermeidbar ist. Pflanzen haben daher verschiedene Mechanismen der Photoprotektion entwickelt, um der Bildung von ROS vorzubeugen und gebildete ROS zu entgiften. Das photoprotektive Pigment Zeaxanthin (Zx) ist an beiden Strategien beteiligt. Zx wird bei Starklicht im Xanthophyllzyklus von dem Enzym Violaxanthin (Vx) De-epoxidase (VDE), welches Vx zu Zx umwandelt, gebildet. Die Rückumwandlung von Zx zu Vx, die überwiegend im Dunkeln und bei Schwachlicht (LL) stattfindet, wird von der Zx Epoxidase (ZEP) katalysiert. Zx trägt auf zwei Arten zum Lichtschutz bei: Gebunden an die Antennenproteine von Photosystem II (PSII) ist Zx am pH-abhängigen (qE) und Zx-abhängigen (qZ) Mechanismus der nicht-photochemischen Löschung (NPQ) von Anregungsenergie beteiligt. Dabei wird im Überschuss absorbierte Lichtenergie in Form von Wärme abgeführt und dadurch die Entstehung von ROS verhindert. Als freies Pigment in der Lipidphase der Thylakoidmembran ist Zx an der Entgiftung bereits gebildeter ROS beteiligt. In *A. thaliana* wird die Epoxidation von Zx bei langanhaltendem Starklicht schrittweise herunterreguliert, parallel zur ansteigenden Photoinhibition von PSII.

In dieser Arbeit wurde die gemeinsame Regulation von ZEP und PSII Aktivität im Zusammenhang mit der kurz- und langfristigen Anpassung an Starklicht in verschiedenen Pflanzenspezies (*A. thaliana*, N. *benthamiana*, *P. sativum* and *S. oleracea*) eingehend charakterisiert. Darüber hinaus wurde die molekulare Grundlage der Lichtregulation der ZEP-Aktivität unter *in vitro* Bedingungen untersucht. Die Ergebnisse zeigen, dass die Koregulierung von ZEP und PSII Aktivität die Photoinhibition in allen Spezies und unter allen Wachstumsbedingungen erfolgt. Ausgeprägter Starklicht-Stress führte nicht nur zu einer vollständigen Inaktivierung von ZEP und PSII, sondern auch zum Abbau der ZEP parallel zum Abbau von D1. Die aus Inaktivierung und Abbau der ZEP resultierende Aufrechterhaltung eines hohen Gehaltes an Zx in der Thylakoidmembran deutet auf eine wichtige photoprotektive Funktion von Zx im Zusammenhang mit der Photoinhibition und der Reparatur von PSII im Starklicht hin. Spezies-spezifische Unterschiede in der Starklicht-Empfindlichkeit und somit unterschiedliche Anpassungsfähigkeiten der untersuchten Pflanzen an Starklicht konnten auf Unterschiede in der Blattdicke, der Menge an Xanthophyll-Zyklus Pigmenten (Vx, Antheraxanthin und Zx) und der qE-Kapazität zurückgeführt werden. Untersuchungen zur Lichtregulation der ZEP-Aktivität unter *in vitro* Bedingungen zeigten, dass die ZEP im dunkel- und lichtadaptierten Zustand eine ähnliche Aktivität besitzt, welche durch Zugabe von Reduktionsmitteln (wie z.B. Dithiothreitol) nicht stimuliert werden kann. Diese Befunde sprechen gegen eine Regulation der ZEP Aktivität durch Thiol-Modulation. Behandlung der ZEP mit verschiedenen ROS zeigte, dass die ZEP zeit- und konzentrationsabhängig durch Wasserstoffperoxid (H_2O_2) inaktiviert wird, jedoch nicht durch Singulettsauerstoff und Superoxid. Dies legt nahe, dass die unter *in vivo* Bedingungen zu beobachtende Starklicht-induzierte Inaktivierung der ZEP auf einer Oxidation der ZEP durch (H_2O_2) beruht.

3. Introduction

3.1 The chloroplast: structure and protein import

The chloroplast represents an identifier for photoautotrophic organisms. Being the only plastid containing the green pigment chlorophyll (Chl), it represents the site of light-harvesting and carbon-fixation reactions of photosynthesis (Jarvis & Robinson, 2004). The semi-autonomous organelle supposedly originated from cyanobacterial ancestors (Cavalier-Smith, 2000), since it contains its own genome (plastome) and is surrounded by a membrane bilayer system. The plastome encodes about 100 different proteins, mostly proteins of the photosynthetic electron transport chain (ETC) like the D1 protein, a core protein of photosystem II (PSII) (Jarvis & Robinson, 2004). However, the majority of plastidic proteins is encoded in the nucleus. These proteins are synthesized in the cytosol in a precursor state and are subsequently transported into the chloroplast. This transport is driven by a translocon at the outer and the inner envelope membrane of the chloroplast that is shortly called TOC/TIC transporter. In the chloroplast, the proteins are folded to their native state by different chaperons (Richter & Lamppa, 1998; Jackson-Constan et al.; 2001, Paila et al., 2015) and transported to their destination.

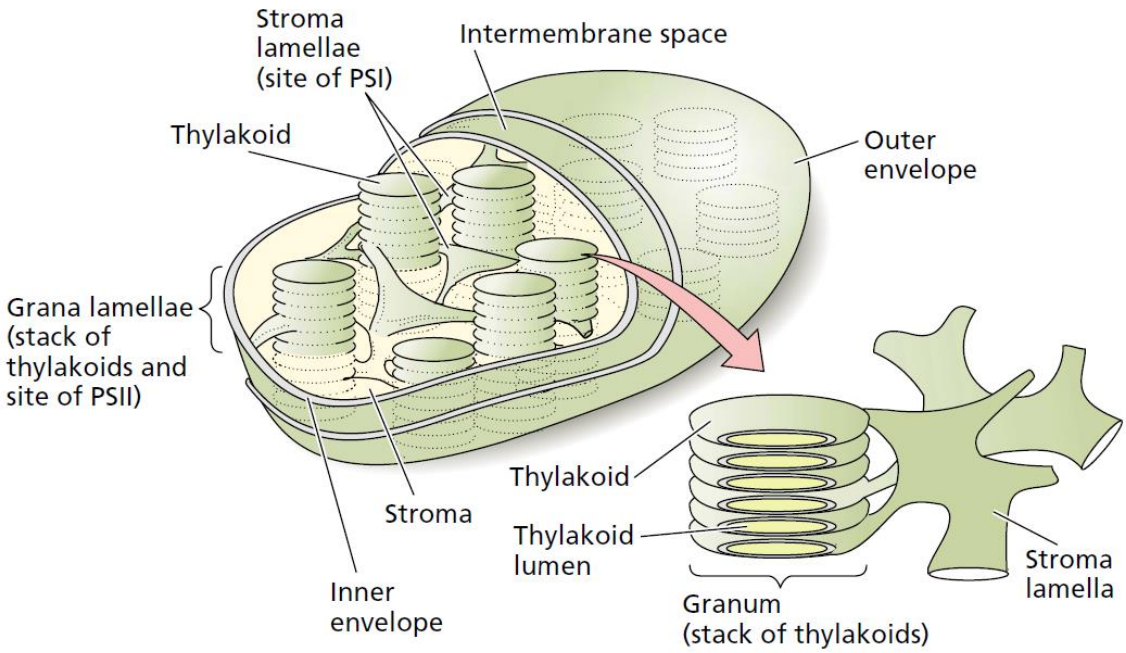

Figure 1: Schematic representation of a chloroplast (Taiz & Zeiger, 2010). (A) Depiction of a chloroplast and its thylakoid membrane system. (B) Detailed view of stacked grana lamella and unstacked stroma lamella of the thylakoid membrane.

The chloroplast is isolated from the cytosol by two membranes, the inner and the outer envelope membrane, that are a consequence to its evolutionary origin. These membranes

enclose the stroma which contains a second membrane system, the thylakoid membrane. The latter one forms a compact membrane network and separates the stroma from the thylakoid lumen. Thylakoids can be present as unstacked stroma lamellae and stacked grana lamellae (Fig. 1B). Stroma lamellae are single membrane bilayers that are completely exposed to the stroma. A granum is consisting of a grana core (= stacked thylakoid membranes) and the grana margins. The latter are highly curved thylakoid membranes at the lateral periphery which connect two membranes of the grana core (Armbruster et al., 2013). The protein complexes of the photosynthetic apparatus are embedded into the thylakoid membrane (Fig. 2). PSII, Photosystem I (PSI) and ATP synthase are heterogeneously distributed in the thylakoid membrane, with PSII being located in the grana lamellae and PSI and ATP synthase in the stroma lamellae and the stroma-exposed regions of the grana. In contrast, the cytochrome b_6f complex (Cyt b_6f) is homogenously distributed among grana and stroma lamellae (Allen & Forsberg, 2001; Danielsson et al., 2004). Earlier studies showed that growth light conditions affect the formation and organization of the thylakoid membrane, with increasing growth light intensities resulting in a decreased number of membrane layers per granum (Anderson, 1986; Wood et al., 2018). Moreover, the membrane structure can dynamically reorganize in the short-term in response to different light intensities. In the dark or in low light (LL) grana are tightly stacked, whereas the exposure to high light causes an unstacking and swelling of the thylakoid membranes (Kirchhoff et al., 2011). The formation and reorganization of thylakoid membranes also depend on their composition of lipids. The majority of plant membranes is built up by glycolipids. The two major lipids monogalactosyldiacylglycerol (MGDG) and digalactosyl diacylglycerol (DGDG) are making up 50-60 and 20-30 mol percent of the total lipids, respectively. The two minor lipids phosphatidylglycerol (PG), a glycerophospholipid, and sulfoquinovosyldiacylglycerol (SQDG), a glyceroglycolipid, represent 5-10 mol percent of total lipids, respectively (Welti et al., 2002; Schumann et al., 2017). MGDG is a bound lipid that forms curved thylakoid, whereas DGDG, a bulk lipid, stabilizes the thylakoid network (Yoshioko-Nishimura, 2016; Yamamoto, 2016). The fatty acids of these membrane lipids are highly unsaturated (= polyunsaturated fatty acids (PUFA)). The membrane fluidity depends on the presence of PUFA: a higher degree of unsaturation leads to an increased membrane fluidity which supports the interaction of various proteins. Also, the light intensity has an effect on the membrane fluidity: moderate high light (HL) leads to an increased membrane fluidity, whereas the membrane fluidity in extreme HL is decreased due to the irreversible aggregation of photosystem II (PSII) core subunits (Yamamoto, 2016).

3.2 The photosynthetic electron transport chain (ETC)

Photosynthesis can be divided into two processes that are spatially separated within the chloroplast. The light-dependent electron transport across the thylakoid membrane leads to the production of ATP and NADPH (light reaction). In the light-independent process ATP and NADPH are used for the fixation and reduction of CO_2 in the so-called Calvin-Benson-Bassham cycle (CBB, so-called dark reaction). This cycle is localized in the chloroplast stroma.

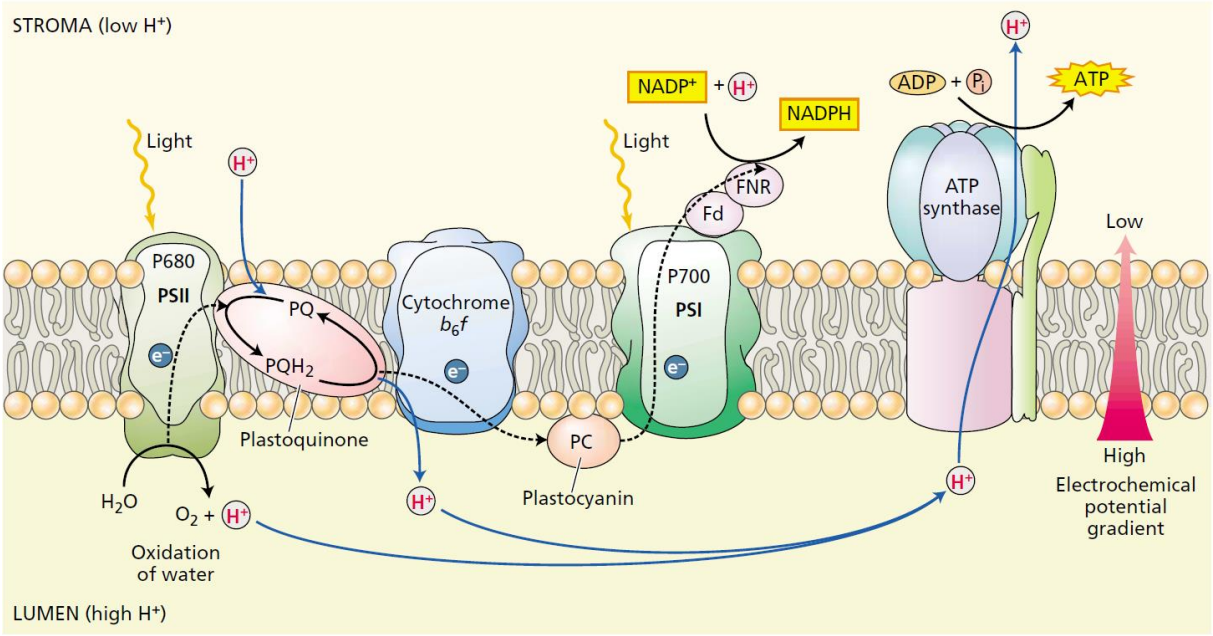

Figure 2: Schematic representation of the photosynthetic electron transport chain (Taiz & Zeiger, 2010). Image of the protein complexes that are embedded in the thylakoid membrane: photosystem II (PSII), cytochrome b_6f complex (Cyt b_6f), photosystem I (PSI) and ATP synthase. Moreover, the electron carriers are depicted: plastoquinone (PQ), plastohydroquinone (PQH_2), plastocyanin (PC), ferredoxin (Fd) and the ferredoxin-$NADP^+$ reductase (FNR). Black arrows display the electron transport over the photosynthetic electron transport chain. Blue arrows show the proton flow that is coupled to the electron transport.

The photosynthetic electron transport chain (ETC) generates an electron and proton transport across the thylakoid membrane which includes the three integral protein complexes PSII, PSI and Cyt b_6f as well as two mobile electron carriers, plastoquinone (PQ) and plastocyanin (PC) (Fig. 2). Charge separation in the reaction center (RC) P680 of PSII causes the oxidation of water (= photolysis) at the luminal side of the thylakoid membrane. The photolysis leads to the release of two protons (H^+) into the lumen and two electrons. These are transferred to the membrane-located electron carrier PQ along with two H^+ from the stroma so that PQ is reduced to plastohydroquinone (PQH_2), which transfers the electrons to Cyt b_6f. At Cyt b_6f, one electron is passed to the luminal electron carrier PC whereas the second electron is used for the re-

reduction of PQ at Cyt b_6f (Q-cycle). PC transfers the electron to the RC of PSI (P700) where it is forwarded to the stroma-localized ferredoxin (Fd) due to charge separation. In a final step, electrons are transported from Fd to ferredoxin-NADP-reductase (FNR) that reduces the final electron acceptor $NADP^+$ to NADPH (Fig.2). Through photolysis and the oxidation of PQH_2 at Cyt b_6f protons are released into the thylakoid lumen. This acidification leads to the formation of transthylakoid proton gradient (ΔpH). This proton motive force (*pmf*) displays the driving force for ATP synthesis (Choquet and Vallon, 2000; Nelson and Junge, 2015). The reflux of H^+ from the lumen to stroma induces the synthesis of ATP by ATP synthase (Fig. 2). The electron transfer from water (donor side of PSII) to $NADP^+$ (acceptor side of PSI) is defined as linear electron flow (LEF) and results in the generation of ATP and NADPH. Moreover, electrons can be recycled in the so-called cyclic electron flow (CEF): There, electrons are transferred from Fd (acceptor side of PSI) to PQ. This can be either regulated by the PROTON GRADIENT REGULATION proteins PGR5 and PGRL1 (DalCorso et al., 2008; Munekage et al., 2004) or by the NAD(P)H dehydrogenase-like (NDH) complex (Shikanai, 2007; Ifuku et al, 2011). The electrons can then be transported back to the donor side of PSI along Cyt b_6f. The CEF generates a ΔpH across the thylakoid membrane that is independent of the LEF and results in production of ATP, but not NADPH (Joliot and Johnson, 2011). Hence, it may regulate the ATP/NADPH-ratio depending on physiological demand (Kramer et al., 2004; Avenson , et al., 2005; Shikanai, 2007). Besides this regulatory function, the CEF contributes to the photoprotection of PSI (Suorsa et al, 2012).

3.3 Photosystem II (PSII) and light harvesting complex II (LHCII)

The protein super complex PSII is primarily located in the grana stacks of the thylakoid membrane. In its active state, PSII forms a homodimer, whereby each monomer consists of at least 25 subunits (Loll et al., 2005; Dekker and Boekema, 2005; Wei et al., 2016) with a total molecular mass of 350 kDa (Umena et al., 2011). The RC of each monomer is composed of the two homologous proteins D1 (PsbA) and D2 (PsbD) which bind 4 Chl *a* molecules (Broser et al., 2010; Umena et al., 2011). Two of these Chl *a* form the special Chl *a* pair P680 which is the primary electron donor and represents the site of charge separation. Moreover, a PSII RC core (Fig. 3B, including D1, D2, CP43, CP47 and Cyt b_{559}) monomer contains 35 Chl a, two pheophytins ($Pheo_{D1}$ and $Pheo_{D2}$), 11 β-carotenes, more than 20 lipids (MGDG, DGDG, SQDG and PG), two PQ (PQ_A and PQ_B), two heme irons, one non-heme iron, four manganese atoms, four calcium atoms and three Cl^- ions (Umena et. Al, 2011). Through charge separation, P680 transfers its electron to Pheo and forward to Q_A. The electron gap in P680 is directly filled by an electron that originates from photolysis at the oxygen evolving complex (OEC).

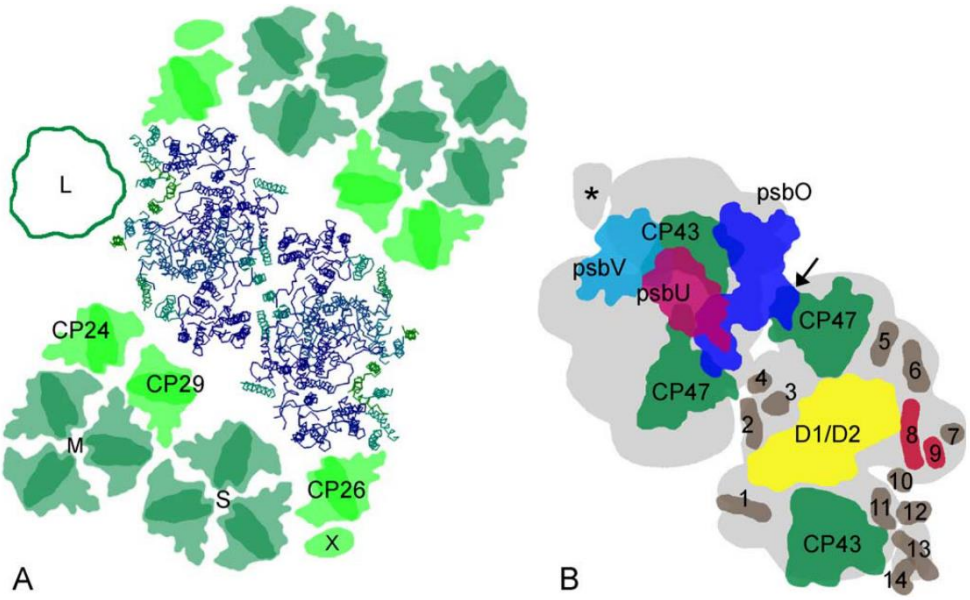

Figure 3: Schematic representation (top view) of the structure of a PSII-LHCII supercomplex from spinach (Dekker and Boekema, 2005). (A) PSII-LHCII supercomplex: transmembrane helices are depicted in blue. The minor antenna proteins CP24, CP26 and CP29 (light green) are present as monomers and are directly associated with the RC. They connect the RC with the LCHII trimers (dark green). Trimers can bind strongly (S), moderately (M) or loosely (L) to PSII core. (B) Detailed view of the proteins from the dimeric PSII RC. The left part shows the top view from the luminal side of the thylakoid membrane. The intrinsic membrane proteins are depicted on the right side.

.

The RC of PSII is surrounded by internal and external antenna proteins. The two internal antenna proteins CP47 (PsbB) and CP43 (PsbC) bind 16 and 14 Chl *a* molecules, respectively, as well as 11- β-carotenes (Umena et al., 2011). While D1 and D2 are the site of charge separation, CP47 and CP43 have light-harvesting functions: they absorb light energy and transfer this excitation energy to the RC. The external antenna proteins (light harvesting complex, LHC) can be classified as major and minor antenna proteins. The major antenna proteins Lhcb1, Lhcb2 and Lchb3 form trimers that consist in various combinations of these three proteins. They are typically present in an 8:3:1 stoichiometry (Jansson, 1994; Dekker and Boekema, 2005). In spinach, trimers were found to bind strongly (S), moderately (M) or loosely (L) to the PSII core (Fig. 3A) (Dekker and Boekema, 2005). In Arabidopsis, however, loosely bound LHCII trimers have not been detected (Yakushevska et al., 2001). In contrast, the minor antenna proteins Lchb4 (CP29), Lhcb5 (CP26) and Lhcb6 (CP24) are present as monomers and are directly associated with the PSII RC (Fig. 3A). Major and minor antenna proteins bind various molecules of Chl *a* and Chl *b* as well as different xanthophylls (Dekker and Boekema, 2005). Figure 4 shows a model for the structure of a LHCII monomer as well as

the localization of pigments within the monomer. Three transmembrane helices (A, B and C) and two short helices α-helices (D and E) at the luminal side of the thylakoid membrane form the protein backbone of Lhcb proteins (Liu et al., 2004). The pigment binding sites are denoted as V1, L1, L2 and N2. The Lut binding sites L1 and L2 are located at the two central helices A and B (Fig. 4) and are conserved in all Lhc complexes (Kühlbrandt et al., 1994). L1 is highly specific for binding Lut, whereas L2 is more variable (Morosinotto et al. 2003) and can be occupied by xanthophylls, like violaxanthin (Vx) or zeaxanthin (Zx), in the absence of Lut (Pogson et al., 1998; Croce and Weiss, 1999; Formaggio et al., 2001). In minor antenna proteins, L2 is predominantly occupied by Vx. The peripheral N1 site binds neoxanthin (Nx). A specific binding of Nx to the N1 site was only observed in LHCII complexes. The xanthophylls Vx or Zx can bind to the peripheral V1 site. Although V1 is inoperative in light harvesting, it matters for the photoprotective xanthophyll cycle since it supposedly provides a pool of convertible xanthophylls (Ruban et al., 1999; Caffari et al., 2001; Morosinotto et al., 2003). Moreover, 8 Chl *a* and 6 Chl *b* molecules are bound by each LHCII monomer (Liu et al., 2014). These Chl molecules are not only responsible for light harvesting and forwarding of excitation energy to the PSII RC, but they are also important for the stabilization of LCHII (Standfuss et al., 2005).

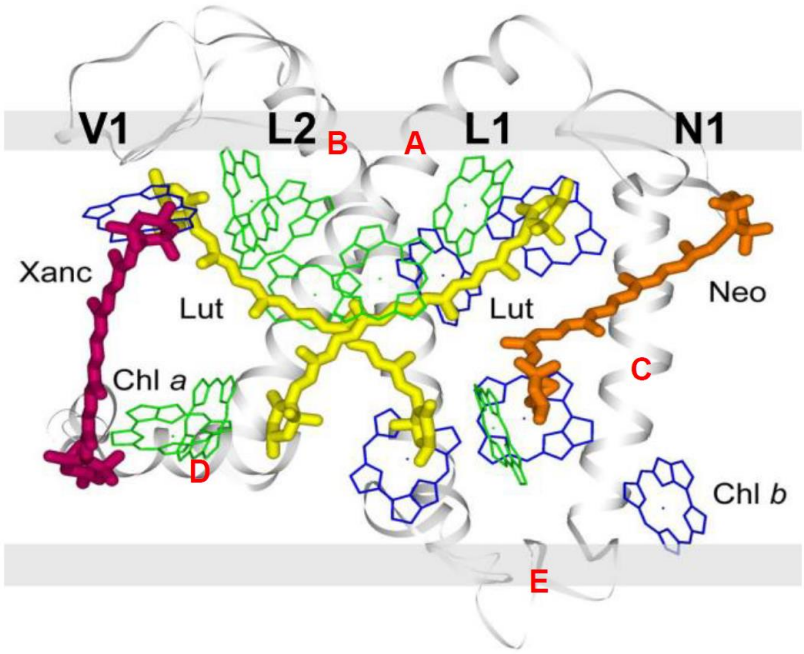

Figure 4: Model of a light harvesting complex (LHC) monomer of PSII. The protein backbone consists of three transmembrane helices (A, B, C) and two short α-helices that are allocating towards the lumen (D, E). Chls are shown in green (Chl *b*) and blue (Chl *a*), whereby only the tetrapyrrole rings are displayed. The LCHII monomer binds 4 xanthophylls: two central Lut (yellow) in the binding sites L1 and L2, one Nx (orange) in the N1 binding site and one xanthophyll cycle pigment (Xanc, magenta) in the V1 binding site.

3.4 Photosystem I (PSI) and light harvesting complex I (LCHI)

PSI is a large monomeric supercomplex with a molecular mass of about 600 kDa (Fig. 5). It is composed of 13 core proteins and four Lhca proteins (Qin et al., 2015) that form a half circle around the PSI core at the F-subunit side (Fig. 5) (Mazor et al., 2015). The PSI-LHCI supercomplex binds in total about 200 cofactors, including 155 Chl molecules (143 Chl *a* and 12 Chl *b*), 35 carotenoids (26 β-carotene, 5 Lut and 4 Vx), 10 lipids (6 PG, 3 MGDG and 1 DGDG), three Fe_2S_4 cluster and two phylloquinones (Amunts and Nelson, 2008; Qin et al., 2015). PSI-LHCI is exclusively localized in the grana margins and stroma lamallea (Albertsson, 2001) since it is hindered to enter the grana stacks caused by its bulky stromal protrusions (Amunts and Nelson 2008; Junge et al., 2009). The PSI RC is a heterodimer consisting of the proteins PsaA and PsaB (Mazor et al. 2015) and contains the special Chl *a* pair P700. P700 is the primary electron donor and $P700^+$ is re-reduced upon electron transport by accepting an electron from PC. Compared to $P680^+$ in PSII, $P700^+$ is only a weak oxidant and thus relatively harmless. Hence, $P700^+$ is an efficient quencher for excess excitation energy (Ort, 2001; Schöttler et al., 2011). The central function unit of PSI is related to the RC and three small extrinsic proteins (PsaC, PsaD and PsaE). PsaC, which binds the terminal iron-sulfur clusters FeS_A and FeS_B, PsaD and PsaE constitute the docking site of the electron acceptor Fd (Nelson and Junge, 2015). The minor proteins PsaF, PsaG, PsaH, PsaI, PsaJ, PsaK and PsaL surround the central function unit (Fig.5). All together form the PSI core that binds in total 98 Chl *a*, 22 β-carotenes, five lipids (three PG, one MGDG and one DGDG), three Fe_4S_4 clusters and two phylloquinones (Qin et al., 2015). The PSI core is surrounded by the peripheral antenna proteins Lhca1, Lhca2, Lhca3 and Lhca4. The LHC complex of PSI is conserved in size and is invariable. The antenna proteins form two types of heterodimers: Lhca1-Lhca4 and Lhca2-Lhca3 (Ben-Shem et al., 2003; Amunts et al., 2007; Amunts et al., 2010; Qin et al., 2015). Each Lhca monomer has three α-helices and one amphipathic helix in the lumen (Fig. 5) (Qin et al., 2015). Lhca proteins bind in total 45 Chl *a*, 12 Chl *b*, four β-carotene, five Lut, four Vx and five lipids (three PG and two MGDG) (Qin et al., 2015). The PSI-LHCI supercomplex is not only part of LEF, but is also involved in CEF, during which electrons deriving from Fd are further transferred to PQ. CEF is particularly active to compensate for an unbalanced ATP/NADPH ratio (Kramer et al., 2004; Avensone, 2005; Shikanai, 2007).

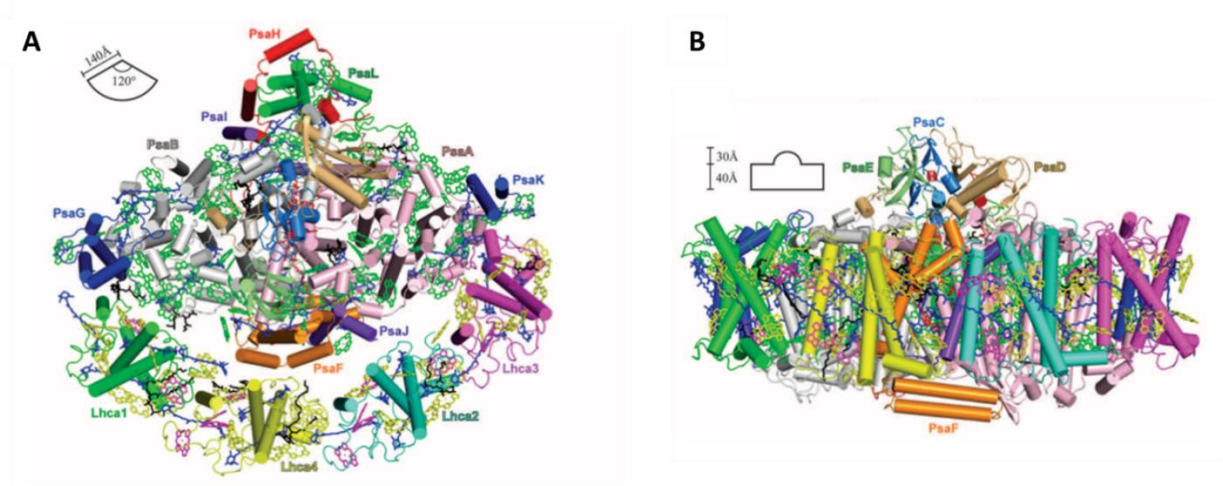

Figure 5: Structure of the PSI-LCHI supercomplex (Qin et al., 2015, modified). (A) View of the PSI-LHCI supercomplex from the stromal side. Lhca proteins (Lhca1:green; Lhca2: cyan; Lhca3: magenta; Lhca4: yellow) surround the PSI core (PsaA: pink; PsaB: gray; PsaC: light blue; PsaD: light brown; PsaE: light green; PsaF: orange; PsaG: dark blue; PsaH: red; PsaI and PsaJ: purple; PsaK: dark blue; PsaL: green) in a semilunar manner at the subunit PsaF. Chl *a* of PSI core are shown in green, Chl *a* and Chl *b* of LHCI is displayed in yellow and magenta, respectively, carotenoids are depicted in blue, and lipids are shown in black. (B) View of the PSI-LHCI core from the LHCI side. PsaC, PsaD and PsaE are exposed to the stroma. Color code as in (A).

3.5 Reactive oxygen species (ROS) and photo-protective mechanism

Since plants are sessile organisms, they have to cope with different light conditions over the course of the day. In general, the exposure to light leads to the excitation of Chl to singlet excited Chl ($^1Chl^*$) (Fig. 6). Under non-saturating light conditions, $^1Chl^*$ is mainly deactivated by photochemical reactions (Fig. 6). However, saturating light conditions lead to an accumulation of excess light energy in the antenna proteins of both photosystems. This energy cannot be fully processed by photochemical processes (Müller et al., 2001) so that excited Chl states accumulate in the antenna which favor the generation of reactive oxygen species (ROS) (Fig. 6). Changing the leaf orientation, decreasing the antenna size and movement of chloroplasts represent strategies to reduce the absorption of excess light energy and hence, the generation of ROS (Li et al., 2009). ROS are highly reactive and can oxidize proteins (especially from the photosynthetic apparatus), DNA and lipids (Müller et al., 2001) thereby damaging the chloroplast. However, ROS also function as signaling molecules (Mittler et al., 2004; Triantaphylidès and Havaux, 2009) and thus are involved in the communication between chloroplast and nucleus (Foyer and Noctor, 2009; Galvez-Valdivieso and Mullineaux, 2010).

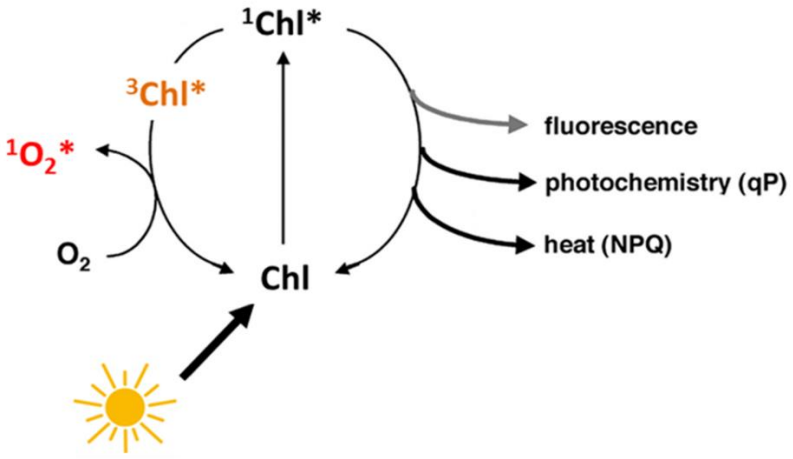

Figure 6: Means of energy release of excited chlorophyll molecules (Müller et al., 2001, modified). The absorption of light leads to the excitation of a Chl molecule. There are four possible ways for the Chl to return to the ground state: (1) emission of fluorescence, (2) photochemical quenching (qP), (3) non-photochemical quenching (NPQ) and (4) transition to persistent triplet Chl ($^3Chl^*$) and transfer of excitation energy on molecular oxygen (O_2).

The generation of ROS can occur at PSII and PSI. Excess light energy leads to an increase of the amount and of the lifetime of $^1Chl^*$. HL intensities, for instance, limit the rapid deactivation of $^1Chl^*$ in photosynthesis, which leads to an increased formation of excited triplet Chl ($^3Chl^*$). $^3Chl^*$ is a persistent Chl species that rapidly transfers excitation energy to molecular oxygen (O_2). This energy transfer leads to the formation of highly reactive singlet oxygen ($^1O_2^*$), a ROS species that was shown to be the major source for photo-oxidative damage to plants under *in vivo* conditions (Krieger-Liszkay, 2005; Triantaphylidès et al., 2008; Triantaphylidès and Havaux, 2009). The excess light energy at the level of $^3Chl^*$ and $^1O_2^*$ can be dissipated as heat (energy dissipation) by the two carotenoids Lut (in LHC proteins) and β-carotene (in the RC). Moreover, excess light energy can result in the so-called Mehler reaction at the acceptor side of PSI (Mehler, 1951; Ananyev et al., 1994). In that process, electrons from reduced Fd are transferred to O_2 which leads to the generation of superoxide-radicals ($\bullet O_2^-$). Superoxide can also be formed at PSII when electrons are transferred to O_2 (Pospíšil et al., 2004). $\bullet O_2^-$ can efficiently be detoxified by the so-called water-water cycle (Asada, 2000). In a first step, superoxide dismutase (SOD) converts two $\bullet O_2^-$ to hydrogen peroxide (H_2O_2) and O_2. Subsequently, ascorbate peroxidase (APX) detoxifies H_2O_2 by using ascorbate as an electron and H^+ donor. The two resulting water molecules can then be used for photolysis at PSII (Asada, 2000; Asada, 2006; Miyake, 2010). It is important to rapidly detoxify $\bullet O_2^-$ since the reduction of metal ions, such as Fe^{3+} and Cu^{2+}, by $\bullet O_2^-$ and the following reaction from the metal ions with H_2O_2 lead to the formation of highly reactive and toxic hydroxyl radicals (•OH). Besides SOD and APX, other enzymes, such as glutathione reductase (GR) (Asada, 2006) and peroxiredoxins (PRX) (Dietz, 2011) as well as non-enzymatic antioxidants like α-

tocopherol (Kobayashi and DellaPenna, 2008) and glutathione are involved in the scavenging of ROS and the repair of oxidative damage caused by ROS. Another mechanism to dissipate excess light energy as heat (energy dissipation) is termed non-photochemical quenching (NPQ) (Fig. 6).

3.6 Non-photochemical quenching (NPQ)

The dissipation of excess light energy as heat (energy dissipation) occurs in the antenna of PSII where excess excitation energy is quenched at the level of $^{1}Chl^{*}$ (Jahns and Holzwarth, 2012) so that the formation of $^{3}Chl^{*}$ and hence, the transfer of electrons to O_2 is reduced. NPQ is composed of several components: (1) pH-dependent quenching qE, (2) Zx-dependent quenching qZ, (3) state transition (qT), (4) the sustained and photoprotective antenna quenching component qH and (5) photoinhibition (qI) (Fig. 7) (Malnöe, 2018).

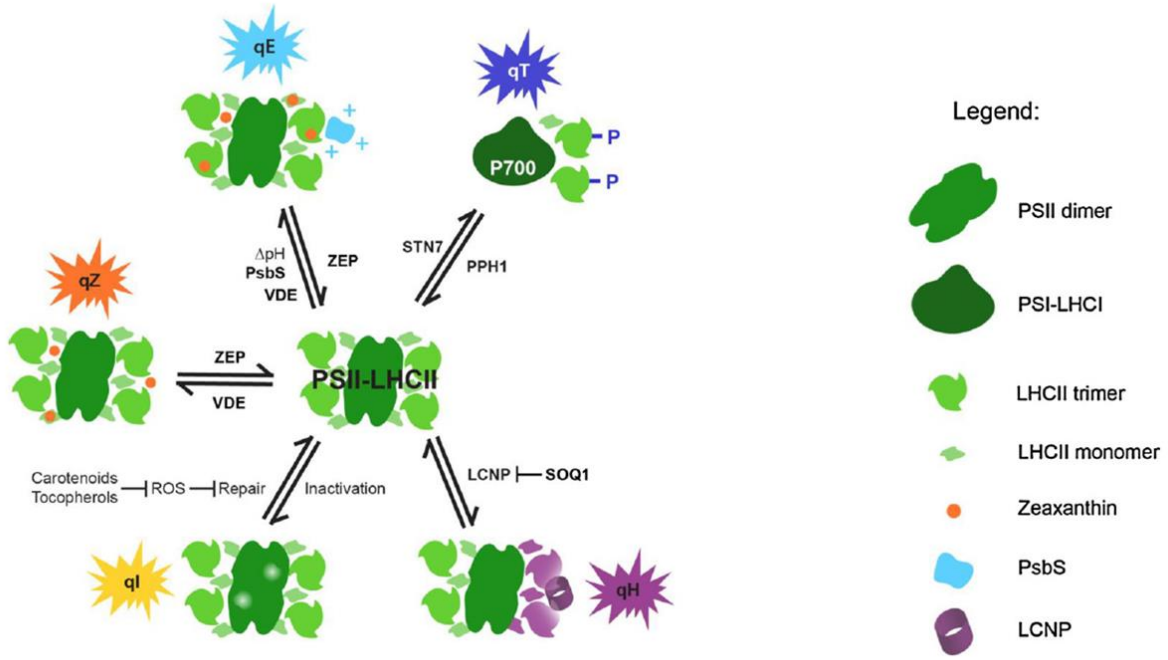

Figure 7: Schematic representation of the different NPQ components (Malnöe, 2018, modified). Top view of PSII-LHCII complexes and of PSI-LHCI complex. The reversible changes, which occur during the different NPQ states, are depicted. qE: pH-dependent quenching; qT: state transition; qH: sustained and photoprotective antenna quenching; qI: photoinhibition; qZ: Zx-dependent quenching. ΔpH: pH gradient formed upon photosynthetic electron transport; VDE: violaxanthin de-epoxidase; ZEP: zeaxanthin epoxidase; +: protonated PsbS residues; STN7: state transition7 kinase; PPH1: phosphatase involved in dephosphorylation of LHCII; -P: phosphorylated LHCII trimers; LCNP: plastid lipocalin; SOQ1: suppressor of quenching1 protein; ROS: reactive oxygen species; white points: damaged D1 protein in PSII reaction center.

Since NPQ is in direct competition with photosynthesis, it needs to be rapidly activated and inactivated in response to saturating and non-saturating light conditions, respectively. The balance of (1) reducing the formation of ROS under excess light conditions and (2) minimizing the inhibition of photosynthesis under non-saturating light conditions is very important to ensure that plants can use the absorbed light energy efficiently. If NPQ would constitutively be active under limiting light conditions, the light use efficiency would be drastically decreased which would have negative effects on plant fitness. Therefore, the components of NPQ are strictly regulated.

Under moderate light stress, qE represents the most dominant component of NPQ (Krause and Jahns, 2004). qE is strictly regulated by the pH of the thylakoid lumen, which represents a reliable indicator of the saturation of photosynthetic electron transport. This ensures that quenching only occurs when photosynthetic electron transport is not light-limited (Johnson et al., 2008). Photosynthetic electron transport leads to the acidification of the lumen. Once the lumen pH drops under a value of 6, the PsbS subunit of PSII, which functions as a sensor of the lumen pH (Li et al., 2000), is protonated. This protonation leads to a conformational change in the antenna of PSII that results in the detachment of trimeric LCHII complexes and hence, the switch of the antenna from a light harvesting to an energy dissipating state (Horton et al., 2008). Moreover, the xanthophyll cycle enzyme Vx de-epoxidase (VDE) is activated upon acidification of the thylakoid lumen and converts Vx to Zx via the intermediate antheraxanthin (Ax). Zx is a photoprotective pigment that is modulating and enhancing the quenching in LHCII (Demmig-Adams et al., 1990). Bound to antenna proteins, it is involved in the deactivation of $^{1}Chl^{*}$. When Zx is present as a free pigment in the thylakoid membrane, it detoxifies ROS and thus, resembles the function of tocopherol (Havaux et al., 2007). The activation and inactivation of qE occurs within seconds to minutes (Walters and Horton, 1991; Nilkens et al., 2010) and thus represents the most rapidly adjustable component of NPQ.

The Zx-dependent component qZ comprises processes that correlate with the de-epoxidation of Vx and the epoxidation of Zx. It is activated within 10-30 minutes (Nilkens et al., 2010) along with the conversion of Vx to Zx. qZ is independent from PsbS and not strictly regulated by pH. Once NPQ is established (by qE), qZ is contributing to NPQ even in the absence of a ΔpH. This allows a sustained dissipation of energy after long periods of HL. The relaxation of qZ occurs within 10 to 60 minutes in parallel with the reconversion of Zx to Vx (Nilkens et al., 2010; Kress and Jahns, 2017).

State transitions (qT) describe a redox-dependent reversible process in which LHCII trimers relocate between PSII and PSI for the purpose of regulating an imbalanced excitation of both photosystems (Rochaix, 2014; Nawrocki et al., 2016; Allen, 2017). This process is dependent on the phosphorylation state of LCHII trimers which is modified by the membrane-bound

STATE TRANSITION7 (STN7) kinase (Bellafiore et al., 2007). When the PQ pool is reduced (indicating an over-excitation of PSII compared to PSI), the STN7 kinase is activated and phosphorylates LHCII. This leads to the transition from the so-called state 1, where PSI is preferentially excited and LHCII is bound to PSII, to state 2, in that PSII is preferentially excited and LHCII is bound to PSI. In *Arabidopsis thaliana*, qT occurs under LL and ML (Tikannen et al., 2006) but its relative contribution to the entire NPQ is rather low (Nilkens et al., 2010). The activation and inactivation of qT occurs within 5 to 10 minutes (Walters and Horton, 1991; Nilkens et al., 2010).

The sustained and photoprotective antenna quenching component qH is localized at the peripheral antenna (LHCII) of PSII. The plastid Lipocalin (LCNP) is required directly (by forming NPQ sites) or indirectly (by modifying the LHCII environment) for qH (Malnöe et al., 2018). The SUPRESSOR OF QUENCHING1 (SOQ1) protein negatively suppresses qH by inhibiting LCNP (Fig. 7) to prevent qH induction under non-stress conditions. Consequently, knockout of SOQ1 in *A. thaliana* resulted in enhanced and sustained NPQ (Malnöe et al., 2018). Under stress conditions, such as cold and HL, qH is photoprotective since it reduces the lipid peroxidation levels. It has been proposed that LCNP protects the thylakoid membrane by enabling sustained NPQ in LHCII and thereby preventing the synthesis of $^1O_2^*$ under stress conditions (Malnöe et al., 2018).

Under long-lasting HL stress qI complements and partly supersedes the other NPQ components. It is dependent on the duration and intensity of illumination. Its activation proceeds after 30 minutes of HL (Nilkens et al., 2010; Jahns and Holzwarth, 2012). Processes that are included in the qI mechanism are (1) the damage of the D1 protein in PSII, (2) the degradation of D1 and (3) the *de novo* synthesis of D1 (Aro et al., 1993), and are often resumed as D1 turnover or PSII repair cycle. Photoinhibition can not only be understood simply as a damaging process but also as a protective mechanism, since the accumulation of excessive excitation energy in PSII is reduced during photoinhibition of PSII. The directed damage of D1 inactivates the PSII RC and thereby reduces the formation of ROS as well as the linear electron transport. If the sustained damage of the PSII RC would not be repaired by an efficient mechanism, the photosynthetic yield would constantly drop below 5% (Melis, 1999). Since the repair of the PSII RCs requires more than 30 minutes (depending on the extent of HL stress), qI represents the slowest inducible and reversible component of NPQ (Nilkens et al., 2010; Jahns and Holzwarth, 2012).

3.7 The D1 turnover

The D1 protein, combined with D2, forms the RC of PSII and thus is essential for the function of PSII and photosynthetic electron transport. Under HL, D1 is constitutively damaged, degraded and repaired (= D1 turnover). The rate of the D1 turnover depends on the light intensity as well as on the duration of illumination. It increases with increasing light stress conditions (Tyystjärvi and Aro, 1996). Under ML conditions, the degradation and the *de novo* synthesis of D1 are balanced. However, under severe HL stress, the amount of *de novo* synthesized D1 protein is lower compared to its degradation, which leads to photoinhibition (see paragraph 2.6) and net degradation of D1. The D1 turnover is a complex mechanism that can be divided into four phases: (1) monomerization of PSII, (2) proteolytic degradation of D1, (3) *de novo* synthesis of D1 protein and (4) dimerization of PSII (Fig. 8) (Kato et al., 2009; Yoshioko-Nishimura, 2016). The phases of the D1 turnover are spatially separated to ensure a high efficiency in PSII repair cycle (Koochak et al., 2019).

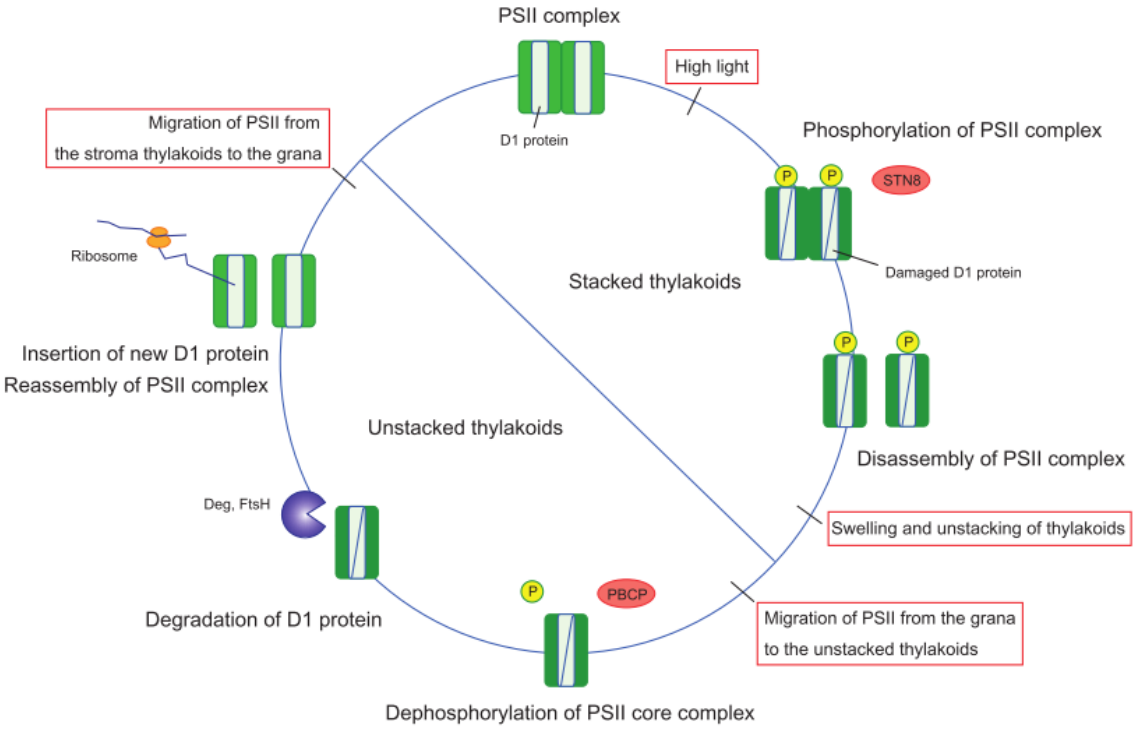

Figure 8: Schematic representation of the D1 turnover (Yoshioku-Nishimura,2016). The D1 turnover takes place in stacked and unstacked thylakoids. First, the damaged D1 protein is phosphorylated by STN8. The PSII dimer monomerizes so that the PSII monomer can migrate to the unstacked thylakoids. D1 is dephosphorylated by PBCP, which leads to its degradation by Deg and FtsH proteases. *De novo* synthesized D1 protein can directly be inserted to the PSII monomer which then reassembles to PSII complex and migrates to the stacked thylakoids in its active form.

The functional PSII-LHCII supercomplex is located in the grana core where it has the function of light harvesting and energy conversion. The PSII disassembly and the D1 degradation are located in the grana margins whereas the repair and reassembly of PSII occur in the stroma lamellae (Koochak et al., 2019). The monomerization of PSII is initiated by phosphorylation of damaged D1 protein by STATE TRANSITION8 (STN8) kinase. First, the trimeric and minor LHCs are released from PSII core. Then, the dimer monomerizes followed by the release of CP43. At the same time, thylakoid membranes are swelling and unstacking within minutes to support the migration of PSII from grana to unstacked thylakoids (grana margins and stroma lamellae) and hence enable proteases to degrade the D1 protein, since they are sterically hindered to enter the grana margins. In the grana margins, D1 is dephosphorylated by the PSII core phosphatase (PBCP), which initiates the degradation of D1 by proteases of the FtsH-family (filament temperature sensitive H) and of the Deg-family (Kato et al., 2012; Yoshioku-Nishimura, 2016). The D1 protein consist of five transmembrane helices (A, B, C, D and E) that form the AB-loop and the CD-loop (both exposed to the lumen) as well as the BC-loop and the DE-loop (both exposed to the stroma). The N-terminus is located in the stroma whereas the C-terminus is localized in the lumen. The FtsH proteases are ATP-dependent zinc metalloproteases that occur in different isoforms (1,2,5 and 8) which are located in the stroma. In *A. thaliana,* these proteases bind to the thylakoid membrane with two transmembrane helices forming a hexameric ring-shaped FtsH-complex that is composed of two type A (FtsH1 and 5) and four type B (FtsH2 and 8) subunits (Zaltsman et al., 2005). FtsH2 and 5 are 2-3 times and 4-5 times more abundant than FtsH8 and 1, respectively. The Deg proteases 1,5,8,2 and 7 (ATP-independent serine-proteases) are also involved in the D1 turnover. Deg1, 5 and 8 are localized in the lumen and degrade the CD-loop of D1 while the stromal localized Deg2 and Deg7 are responsible for the degradation of the DE-loop (Yoshioku-Nishimura, 2016). The *de novo* synthesis of the D1 protein takes place in parallel to the degradation of damaged D1. It is located on thylakoid-bound ribosomes where the elongation peptide is directly inserted into the thylakoid membrane. Subsequently, CP43 is attached to PSII, and after PSII reassembly, the functional PSII-LHCII supercomplex can migrate to the grana core. Under long-lasting light stress conditions, photoinhibition is higher compared to the D1 turnover capacity, which leads to irreversible damages of PSII and reduction of photochemical efficiency (Nath et al., 2013).

3.8 The xanthophyll cycle

The xanthophyll cycle is defined as the reversible and light-dependent conversion of Vx to Zx via the intermediate Ax that is present in all plants (Jahns et al., 2009). The xanthophyll cycle is one of the key players for the qE mechanism of NPQ (see paragraph 2.6), and essentially contributes to the reversible switch of the PSII antenna between a light harvesting state in LL and a dissipative state in HL (Jahns and Holzwarth, 2012). The two-stepped conversion of xanthophylls is catalyzed by the enzymes VDE and Zx epoxidase (ZEP) that are located at opposite sides of the thylakoid membrane (Fig. 9). The lumen-localized VDE converts Vx to Zx while ZEP is located in the stroma and catalyzes the back reaction from Zx to Vx (Fig. 9). Since VDE is encased in the thylakoid lumen, the xanthophyll cycle is distinctly restricted to the thylakoid membrane (Hager, 1969). The VDE is a water-soluble protein whose activity is strictly regulated by the lumen pH. In its inactive form, VDE is soluble in the lumen. Acidification of the lumen pH to values below 6.5 leads to the protonation of the VDE and by that to the binding of the enzyme to the thylakoid membrane (Gisselsson et al., 2004; Jahns et al., 2009), whereby VDE is converted into its active state. *In vitro* studies showed that VDE requires the water-soluble antioxidant ascorbate as co-factor whereby the utilization of ascorbate for Vx de-epoxidation is strongly pH-dependent (Bratt et al., 1995; Jahns et al., 2009). The highest VDE activity could be observed at pH values ≤ 5.8 (Fig. 9) (Jahns et al., 2009). Moreover, MGDG appears to play a key role for the activity of VDE, since VDE supposedly specifically interacts with MGDG enriched membrane regions (Latowski et al., 2002). VDE has the ability to target non-protein-bound Vx as well as protein-bound Vx, whereby protein-bound Vx needs to be released from the respective protein binding site prior to conversion. Early studies, in which Lhcb1 has been reconstituted with Vx at different binding sites, exhibited a rapid de-epoxidation of Vx bound to the V1 binding site, with kinetics that were similar to the conversion of non-protein-bound Vx (Jahns et al., 2001). The de-epoxidation of Vx bound to the L2 binding site occurs four times slower while Vx that was bound to the L1 binding site could not be converted at all under *in vitro* conditions (Jahns et al., 2001). As mentioned above (paragraph 2.6), Zx has a dual photoprotective function since it (1) dissipates excessive excitation energy by deactivating $^{1}Chl^{*}$, thereby preventing the formation of ROS when it is bound to antenna proteins and (2) it detoxifies already existing ROS when it is present in the lipid phase of the membrane (Havaux and Niyogi, 1999). Hence, Zx displays an important player for qE and qZ of NPQ. The photoprotective function of Zx is not required under non-saturating light conditions since the accumulation of Zx in LL could lead to an unfavorable dissipation of excitation energy instead of desired photochemical processes. Hence, Zx needs to be reconverted to Vx in LL and in the dark. Reconversion of Zx to Vx by ZEP occurs under all light conditions, but under saturating light conditions, VDE activity predominates ZEP activity, since Vx de-epoxidation proceeds about 5-10 times faster than Zx epoxidation (Jahns, 1995; Härtel et a., 1996; Marin

et al., 1996), so that Zx accumulates under HL conditions (Demmig-Adams et al., 1996; Jahns et al., 2009).

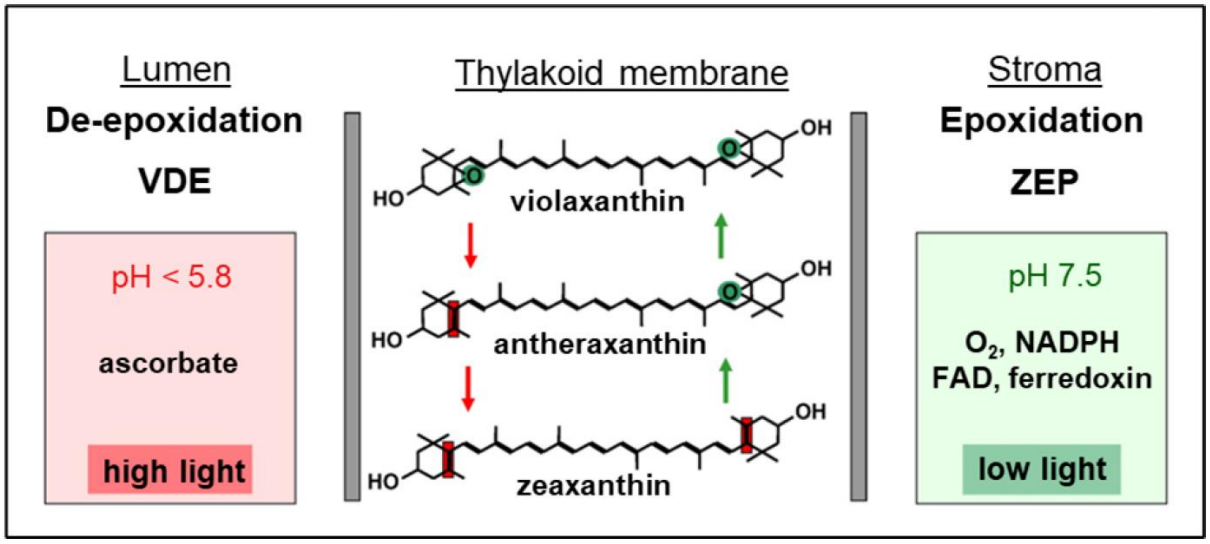

Figure 9: Schmetatic representation of the xanthophyll cycle reactions in higher plants (Jahns et al., 2009, modified). The two-stepped reaction takes place at the thylakoid membrane. The de-epoxidation from violaxanthin (Vx) to zeaxanthin (Zx) via the intermediate antheraxanthin (Ax) by Vx de-epoxidase (VDE) (red arrows) is located in the lumen. The epoxidation from Zx to Vx by Zx epoxidase (ZEP) (green arrows) takes place in the stroma. Required cofactors and stromal factors are depicted in the colored boxes.

Net epoxidation of Zx thus takes place predominantly under non-saturating light conditions and in the dark. ZEP requires O_2 and NADPH as co-substrates (Siefermann and Yamamoto, 1975; Bouvier et al., 1996). The reduction of NADPH levels in *nadk2* (to about 50% of wildtype (WT) levels) led to an accumulation of Zx in LL and in the dark, indicating that the NADPH concentration limits the rate of Zx epoxidation (Takahashi et al., 2006). *In vitro* studies with recombinant ZEP from pepper (*Capsicum annuum*) revealed that ZEP activity requires not only O_2 and NADPH, but also additional stromal factors including FAD, Fd, MGDG and DGDG as well as an optimum pH value of about 7.5 (Fig. 9) (Bouvier et al., 1996).

3.9 Zeaxanthin epoxidase (ZEP)

ZEP is a plant protein that belongs to the family of lipocalin proteins (Bugos et al., 1998) with monooxygenase activity (Büch et al., 1995). Due to its ability to convert Zx to Vx, ZEP is an important player in two physiological processes: (1) the photoprotective xanthophyll cycle and (2) the carotenoid biosynthesis and by that also in the synthesis of the stress hormone abscisic acid (ABA). ZEP is composed of three structural conserved domains: (1) a N-terminal transit sequence (cTP) that is required for the import into the chloroplast (Xiong et al., 2002), (2) a large central lipocalin/monooxygenase domain with NAD- and FAD-binding motifs that are supposedly essential for protein activity (Marin et al., 1996; Barrero et al., 2005) and (3) a C-terminal FHA-domain (forkhead associated domain, Fig. 10) (Xiong et al., 2002). FHA domains are small protein modules forming special β-sheet structures that serve as phosphopeptide binding sites and are involved in regulatory processes like signal transduction, DNA repair and transcription (Durocher and Jackson, 2002). FHA modules have been found in eukaryotes in various proteins like kinases, phosphatases, transcription factors, RNA-binding proteins as well as metabolic enzymes. Moreover, FHA domains were also found in some bacterial proteins (Durocher and Jackson, 2002). In addition to these three structural conserved domains, a C-terminal ADP-binding domain has been proposed for ZEP as well (Marin et al., 1996).

ZEP is encoded in Arabidopsis by the ABA1 gene on chromosome 5 (At5g67030.1/2). It is alternatively spliced so that two individual gene products emerge, AtZEP1 and AtZEP2, which are identical in the first 610 amino acids (Fig.10). AtZEP2 owns a premature stop codon with the result that it contains an incomplete C-terminal FHA-domain (Marin et al., 1996; Seo and Koshiba, 2002). Hence, AtZEP2 (61 kDa) is shortened compared to AtZEP1 (67 kDa). So far, AtZEP2 was not shown to accumulate to detectable amounts on the protein level in *A. thaliana*.

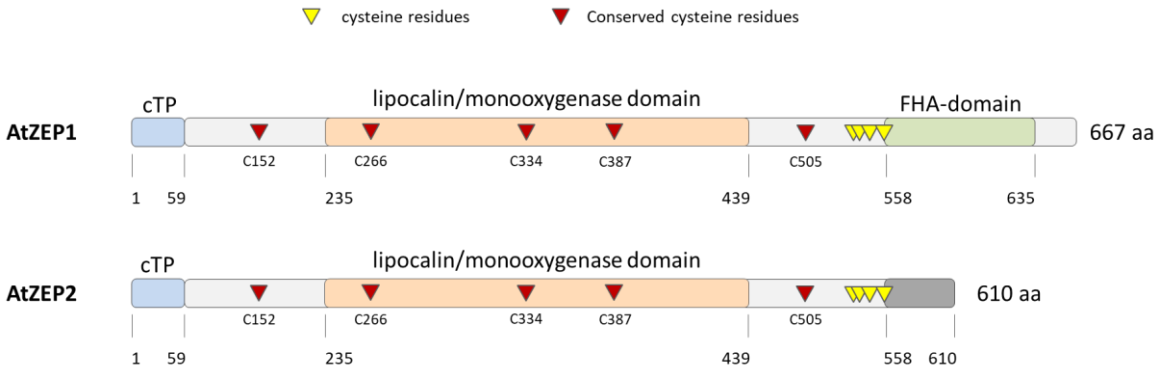

Figure 10: Schematic representation of AtZEP1 and AtZEP2 isoforms (after Barrero et al., 2005). In Arabidopsis, two AtZEP isoforms exist: AtZEP1 (At5g67030.1) and AtZEP2 (At5g67030.2). Since AtZEP2 possesses a premature stop codon, it contains an incomplete FHA-domain and hence, is shortened (610 aa, 61 kDa) compared to AtZEP1 (667 aa, 67 kDa). cTP: chloroplast transit peptide.

AtZEP1 is present in the chloroplast where it was shown to be distributed among the thylakoid membrane, the envelope membrane and the stroma (Schwarz et al., 2015). The thylakoid membrane-bound and stromal ZEP are present in similar high levels (45-50 %), whereas the envelope membrane-bound ZEP represents only < 5 % of the total ZEP amount (Schwarz et al., 2015). This distribution is unchanged in dark-adapted and light-adapted plants (Schwarz et al., 2015). While the thylakoid membrane-bound ZEP is assumed to be involved in the xanthophyll cycle, envelope membrane-bound ZEP is supposedly participating to the carotenoid and ABA synthesis (Schwarz et al., 2015). The function of stromal-located ZEP is still unknown. Schwarz et al. (2015) assumed that the stromal ZEP constitutes a pool of inactive ZEP that can be activated under defined conditions. In *Nicotiana benthamiana*, ZEP is encoded by the ABA2 gene and no splicing variants are known in this species. ZEP deficient mutants in *A. thaliana* and *N. benthamiana* are named *aba1* and *aba2*, respectively. Analysis of the localization of the corresponding point mutations in the *ABA1* gene in different *A. thaliana aba1* mutants revealed that most mutations are located within or near the Lipocalin/Monooxygenase domain (Barrero et al., 2005), which supports the importance of this domain for enzyme activity. ZEP activity in *aba1* and *aba2* mutants is partially or fully inhibited so that Zx accumulates to high levels while Vx and more importantly the endogenous ABA content is decreased. The latter is likely responsible for the impairment of vegetative growth and leave morphology in *aba1*/*aba2* mutants (Rock and Zeevart, 1991). Moreover, the reduced ABA content leads to a higher rate of water loss, reduced seed dormancy and salt-tolerant germination in *aba1* and *aba2* mutants (Korneef et al., 1982; Barrero et al., 2005). In contrast, overexpression of ZEP in *A. thaliana* leads to an increased amount of ABA under non-stressed conditions (Park et al., 2008). The role of ZEP in photoprotection has been examined in *npq2* (non-photochemical quenching = *aba1-6*) mutants. Under light limiting growth conditions, these mutants exhibited a decreased PSII quantum yield efficiency as well as a faster induction of NPQ compared to wild type (Niyogi et al., 1998; Dall'Osto et al., 2005; Kalituho et al., 2007). This supports the view that increased levels of Zx negatively affect photosynthetic efficiency.

The regulation of ZEP on the molecular level is largely unknown. Similar to the regulation of VDE, the regulation of ZEP occurs at the post-transcriptional level (North et al., 2005; Jahns et al. 2009). It could be shown that epoxidation of Zx is inhibited under long-lasting HL exposure (Reinhold et al., 2008). Moreover, a correlation between the relaxation of the qI component of NPQ and Zx epoxidation has been described (Jahns and Miehe, 1996; Verhoeven et al., 1996; Kress and Jahns, 2017). The retarded conversion of Zx to Vx due to HL-induced downregulation of ZEP supports the photoprotective function of Zx during and after HL-stress and suggests, that the preservation of high Zx levels may represent a kind memory for photo-oxidative stress (Jahns and Holzwarth, 2012). In line with this hypothesis, Zx was shown to accumulate in evergreen plants during the overwintering period in parallel with a

continuous downregulation of PSII activity (Öquist and Huner, 2003; Zarter et al., 2006). This increased Zx accumulation supposedly displays a high demand to protect PSII from photooxidative damage. The basic molecular mechanism of ZEP activation and inactivation remains elusive. It has been proposed that either phosphorylation of ZEP (Kim et al. 2017; Xu et al. 1999) or ROS-induced modifications (Reinhold et al., 2008) might be responsible for ZEP inactivation in response to HL. Studies with knockout mutants of the two thylakoid kinases state transition7 and 8 (STN7 and STN8) revealed that the phosphorylation of PSII proteins had no impact on the short-term downregulation of Zx epoxidation (Reinhold et al., 2008). Moreover, mutants with deficient NADPH-dependent thioredoxin (TRX) reductase C (NTRC) accumulate Zx and show an increased NPQ capacity (Naranjo et al., 2016), which points to a possible regulation of ZEP. Indeed, alignment of the amino acid sequences of ZEP from *A. thaliana* and other land plants revealed that out of nine cysteine (Cys) residues in *A. thaliana,* five Cys are highly conserved (Naranjo et al., 2016; Da et al., 2018), supporting the possibility that ZEP is functionally regulated by the TRX system. *In vitro* assays with recombinant ZEP displayed an affinity of ZEP to form aggregates under non-reducing conditions along with the formation of intermolecular disulfide bonds (Da et al., 2018). These findings indicate that ZEP could be a target of thiol-dependent regulation (Naranjo et al., 2016).

3.10 Redox regulatory system of the chloroplast

The maintenance of the chloroplast metabolism under fluctuating light conditions is important to avoid damage of the photosynthetic apparatus. The thiol-dependent redox regulation in the chloroplast enables a rapid adaption of chloroplast function to the dark/light transition and hence, preserves a redox balance between the light reactions (LEF and CEF) and stromal carbon metabolism. The activity of proteins as well as the conformation and the stability can be modulated by the reversible formation of disulfide bonds between the thiol groups of two Cys residues (thiol switch) (Buchanan, 2016). In the chloroplast, thiol switches are catalyzed by two distinct redox regulatory systems: (1) Fd-TRX system and (2) NTRC system (Fig. 11). The mutually working systems constitute the redox regulatory system of the chloroplast (Pérez-Ruiz et al., 2017) which represents a crucial regulator of photosynthesis and chloroplast metabolism as well as of ROS detoxification. While the Fd-TRX system is light-dependent, the NTRC system is active in the dark as well as in LL.

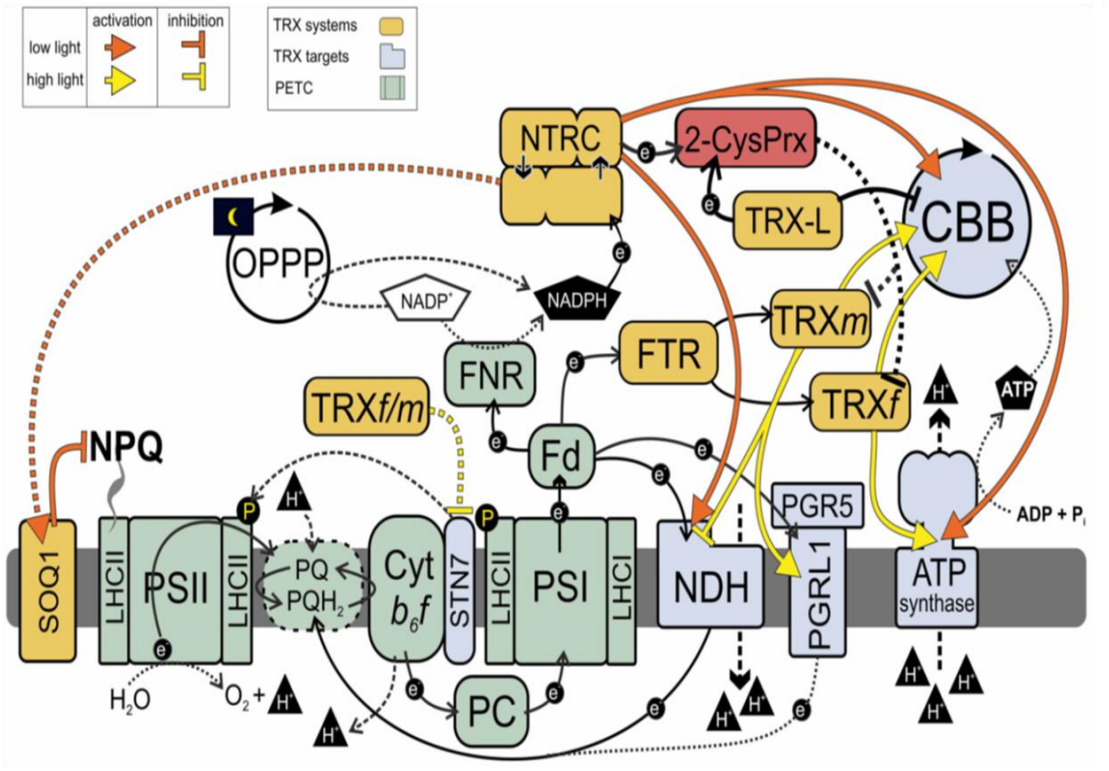

Figure 11: Model of the redox regulatory system of the chloroplast (Nikkanen and Rintamäki, 2019). Under low light (LL) and in the dark, the NADPH-dependent thioredoxin reductase C (NTRC) activates the Calvin-Benson-Bassham (CBB) cycle, the ATP synthase as well as the NAD(P)H dehydrogenase-like (NDH) complex. NTRC is possibly involved in the downregulation of NPQ by SUPPRESSOR OF QUENCHING1 (SOQ1). The required NADPH derives from linear electron transport (LET, in light) as well as from the oxidative pentose phosphate pathway (OPPP, in the dark). Under high light (HL), thioredoxins (TRXs) are involved in the activation of the CBB cycle, the ATP synthase and PROTON GRADIENT REGULATION protein PGRL1. Moreover, TRXs inhibit the NDH complex and potentially also the STATE TRANSITION7 kinase (STN7). 2-cys peroxiredoxin (2-CysPrx) is reduced by NTRC and TRXs and is involved in the oxidation of TRX m and TRX f.

The Fd-TRX system consists of three components: (1) Fd, (2) TRX and (3) Fd-dependent TRX reductase (FTR). Fd functions as primary electron donor since it is reduced upon LEF in light. Oxidation of Fd by FTR leads to the subsequent reduction of TRX by FTR. TRXs are a group of small oxidoreductases (~ 12 kDA), that control the structure and function of proteins by the cleavage of disulfide bonds. They represent transmitter of redox energy since they can induce thiol switches in target proteins in the reduced state. These target proteins are thus termed thiol switch proteins due to their ability to form inter- and intramolecular disulfide bonds. Within the chloroplast, five types of TRX have been found in the stroma, termed TRX f, m, x, y and z, consisting of (1) two f-type TRX isoforms (TRX f1 and f2), four m-type TRX isoforms (TRX m1, m2, m3 and m4), (3) one x-type TRX isoform (TRX x), (4) two y-type TRX isoforms (TRX y1 and y2) and (5) one z-type TRX isoform (TRX z) (Okegawa and Motohashi, 2015). The TRX m isoforms represent the by far most abundant type (about 70% of all TRX, Okegawa and Motohashi, 2015). TRX f and TRX m are known for a long time to regulate key enzymes that

are involved in photosynthetic carbon assimilation (Jacquot et al., 1978: Wolosiuk et al., 1979), including light-activated enzymes of the CBB cycle (Okegawa and Motohashi, 2015). Moreover, TRX m is important for the regulation of protein import (Bartsch et al., 2008; Kovcás-Bogdán et al., 2010) as well as the chlorophyll metabolism (Bartsch et al., 2008; Ikegami et al., 2007; Richter et al., 2013). TRX x and TRX y presumably participate in cellular responses to oxidative stress (Collin et al., 2003; Collin et al, 2004) and sulfur metabolism, whereas TRX z has been suggested to be involved in the control of plastid transcription (Arsova et al., 2010).

The NTRC system consists of a single enzymatic component termed NTRC. It is constituted of a C-terminal fused TRX domain and N-terminal reductase (NTR) domain and is functional as a homodimer. Thereby, the active site of the TRX domain from one subunit of NTRC can be reduced by the NTR domain of the other subunit (Naranjo et al., 2016). The TRX subunit can then reduce (and hence activate) target proteins. NTRC uses NADPH as primary electron source. Since NAPDH also derives from oxidative pentose phosphate pathway (OPPP) in darkness (Fig. 11), the activity can be uncoupled from the light-dependent LEF (Pérez-Ruiz et al., 2017).

Pérez-Ruiz et al. (2017) and Liebthal et al. (2018) suggested that the Fd-TRX system and the NTRC system are interconnected at two different levels: the redox input (electron supply) and the redox transmission. The electron transfer from reduced Fd to $NADP^+$, catalyzed by FNR, links both systems at the redox input level, whereas they are connected via the redox balance of 2-cys peroxiredoxin (2-CysPrx), a chloroplast thiol peroxidase, at the transmission level (Fig. 11). 2-CysPrx acts as a sensor of ROS (especially H_2O_2) as well as a scavenger of ROS and therefore, is involved in the antioxidative defense of the chloroplast. Depending on the environmental conditions as well as on the metabolic status, 2-CysPrx can be present as a reduced, oxidized or over-oxidized form and thus, is assumed to function as a redox sensor (Liebthal et al., 2018). Although both TRXs and NTRC can re-reduce 2-CysPrx, TRXs reduce 2-CysPrx less efficient than NTRC. Regarding ZEP regulation, studies with TRX m triple mutants (trxm1,2,4) revealed that ZEP activity is reduced under low illumination in these mutants, which results in an accumulation of Zx (Da et al., 2018). In addition, TRX m1, TRX m2 and TRX m4 have been shown to interact directly with the ZEP protein, and it was suggested that TRX m isoforms might be involved in the post-translational regulation of either the stability or the activity of ZEP (Da et al., 2018). Although studies with the *ntrc* mutant did not provide direct evidence that ZEP is a target of NTRC under low and medium light intensities, *in vitro* experiments with purified recombinant ZEP revealed that purified NTRC effectively reduces intermolecular disulfide bonds of ZEP (Naranjo at al., 2018). Moreover, *ntrc* mutants accumulated higher amounts of Ax and Zx than the wild type and showed not only a higher NPQ during illumination, but also a more slowly relaxing component of NPQ (Nikkanen

et al., 2019). This again supports the view, that ZEP activity is directly or indirectly regulated by NTRC. However, despite all these findings, the role of the redox-regulatory system on ZEP activity remains elusive.

3.11 Long-term acclimation to different growth conditions

Since plants are sessile organisms, they have to cope with different light conditions ranging from LL and HL to fluctuating light conditions. Therefore, plants must be able to acclimate properly to different and variable light conditions in the short-term and in the long-term. As pointed out above in detail, the regulation of photosynthetic light utilization, including photoprotective mechanisms, represents an important short-term acclimation. However, to assure a high competitiveness under field conditions, efficient long-term acclimation to different growth light conditions is mandatory. Numerous studies identified typical characteristics of plants in response to different growth light intensities. Acclimation to increasing growth light intensities have been shown to occur at the level of leaf morphology, thylakoid membrane structure, pigment composition as well as at the level of regulation of metabolic processes. Compared to LL, HL grown plants have thicker leaves consisting of more cell layers as well as larger cells (Björkman and Holmgren, 1963; Ludlow and Wilson, 1971; Wild and Wolf, 1980; Weston et al., 2000). Moreover, the number of chloroplasts per cell is known to be increased in HL-grown plants (Anderson et al, 1973; Anderson, 1986). At the level of thylakoid membrane organization, HL was shown to induce a reduction of grana stacking in comparison with LL (Anderson et al., 1973; Lichtenthaler at el., 1981). Growth light specific features have further been identified at the pigment level. HL grown plants or sun leaves are known to have an increased Chl a/b ratio (Boardman, 1977; Wild, 1980; Lichtenthaler et al., 1981; Bailey et al., 2004) and elevated levels of β-carotene and xanthophyll cycle pigments (Anderson, 1986; Bailey et al., 2004, Schumann et al., 2017) when compared with LL grown plants or shade leaves. Moreover, HL plants are characterized by an increased PSII/PSI ratio and a smaller PSII antenna size (Schoettler and Toth, 2014; Albanese et al., 2016). As expected, HL-grown plants further exhibit higher electron transport and CO_2 assimilation rates as well as higher light compensation points (Björkman and Holmgren, 1963; Ludlow and Wilson, 1971; Boradman, 1977; Wild, 1980). At the level of photoprotective mechanisms, long-term HL acclimated plants were shown to have a generally higher NPQ capacity, mainly due to an increased capacity of qE quenching (Brugnoli et al., 1994; Demmig-Adams and Adams, 1996; Park et al., 1996; Ballottari et al., 2007; Mishra et al., 2012), which is accompanied by higher levels of Zx and an increased PsbS content (Schumann et al., 2017).

4. Aims of the Work

The xanthophyll cycle essentially contributes to photoprotection in all plants (Jahns et al., 2009). While the regulation of VDE activity is well understood, the regulation of ZEP activity still remains elusive. Previous work has shown that ZEP activity is light-regulated. Down-regulation of ZEP activity in response to HL stress in parallel with inactivation of PSII has been described in *A. thaliana* plants (Reinhold et al., 2008). Moreover, reduced ZEP activity was further described for mutants affected in plastidic redox regulation (Naranjo et al., 2016; Da et al., 2017), suggesting a possible down-regulation of ZEP activity in darkness. To gain more insight into the light-regulation of ZEP activity and the underlying molecular mechanisms, the impact of HL on ZEP activity in context with photoinhibition of PSII was characterized in detail in different plant species (Arabidopsis, tobacco, pea and spinach). To understand species-specific differences in HL sensitivity, the four species were characterized at different levels with respect to their acclimation properties to different growth light intensities, and with respect to the regulation of ZEP activity and PSII activity. In addition, comparative analysis of ZEP activity in the dark- and light-acclimated state was studied *in vitro* with isolated thylakoids, to clarify a possible redox-regulation of ZEP activity. Finally, the same *in vitro* approach was used to investigate a possible inactivation of ZEP by different ROS species.

5. Hypotheses

1) Manuscript 1 describes the effect of long-term HL exposure on ZEP activity and ZEP content in four species: *N. benthamiana*, *A. thaliana*, *P. sativum* and *S. oleraceae*. During photoinhibition of PSII, ZEP activity was inhibited as well, and ZEP protein was degraded along with the D1 protein in all species. In presence of streptomycin (SM), an inhibitor of chloroplast protein biosynthesis, ZEP and PSII activity were more strongly inhibited in parallel, which was accompanied by a severe degradation of D1 and ZEP. These data suggest that photoinhibition of PSII and ZEP activity as well as degradation of D1 and ZEP protein are closely correlated and implies that the retention of high amounts of Zx due to the inactivation ZEP is essentially important for photoprotection during the PSII repair cycle. The observation that inactivation and degradation of ZEP during photoinhibition was found in all four studied species supports the view, that this is a general response of land plants to photoinhibitory HL conditions. Moreover, the tested species showed different sensitivities to HL with Arabidopsis and tobacco being more HL-sensitive compared to pea and spinach. Comparative analysis of a number of parameters in the four species implied that the presence of stromal ZEP, the leaf morphology, thylakoid membrane dynamics, the VAZ pool size as well as the Chl (*a*+*b*) content per leaf area might be critical determinants of HL sensitivity.
2) Manuscript 2 characterizes the long-term acclimation of *N. benthamiana*, *A. thaliana*, *P. sativum* and *S. oleraceae* plants to different growth light conditions (LL = about 20 µmol photon m^{-2} s^{-1}, NL = about 100 µmol photon m^{-2} s^{-1} and HL = about 500 µmol photon m^{-2} s^{-1}). All species were capable of acclimating to different growth light conditions and showed typical responses to increasing growth light such as (1) increasing leaf thickness, (2) reducing the grana width, (3) increasing the Chl *a*/*b* ratio and the amount of Chl (*a*+*b*) per leaf area, (4) increasing light saturation of photosynthetic electron transport, (5) increasing NPQ and qE capacity as well as (6) reducing the HL sensitivity of PSII and ZEP activity. The higher light sensitivity of tobacco and Arabidopsis plants (reported in manuscript 1) was even more pronounced in LL-acclimated plants, but rather attenuated in HL-acclimated tobacco and Arabidopsis plants, compared to pea and spinach. However, the correlation of PSII and ZEP activity (also reported in manuscript 1) was maintained in all plant species and under all growth light conditions. Comparison of the HL sensitivities of all species and under all growth light conditions identified (1) the leaf thickness, (2) the VAZ pool size and (3) the qE capacity as critical determinants of proper acclimation to HL intensities.
3) Manuscript 3 investigates the molecular basis of the light regulation of ZEP activity under *in vitro* conditions using thylakoids from *S. oleraceae*. A comparison of ZEP activity in the

dark- and light-acclimated state revealed that ZEP is fully active in the dark acclimated state. Moreover, the addition of the reductants DTT and TCEP did not result in a stimulating effect in either state, indicating that ZEP activity is not prone to thiol modification. This argues against a modulation of ZEP activity by the thioredoxin system. Moreover, this work revealed that ZEP activity is irreversibly affected by H_2O_2, in a time- and concentration-dependent manner, with the second step of Zx epoxidation (Ax to Vx) being more affected than the first step (Zx to Ax). However, singlet oxygen and superoxide did not seem to inactivate ZEP. This implies that inactivation of ZEP activity und HL conditions might be related to direct modification of ZEP by H_2O_2.

6. Manuscript 1

The zeaxanthin epoxidase is degraded along with the D1 protein during photoinhibition of photosystem II

Plant Direct, Vol. 3, No. 11, pp. 1-13

November 2019

DOI: 10.1002/pld3.185

Contributions:

P.J. conceived the project. P.J. and S.B. designed the experiments; S.B. performed most of the experiments including the short-term light induction experiments, protein analysis, pigment analysis, fluorescence measurements, thylakoid preparation and statistical analysis; N.S. contributed to the experiments with Arabidopsis plants; M.M. performed the electron microscopy; P.J. wrote the article with contributions of all authors.

Received: 16 October 2019 | Accepted: 4 November 2019

DOI: 10.1002/pld3.185

ORIGINAL RESEARCH

The zeaxanthin epoxidase is degraded along with the D1 protein during photoinhibition of photosystem II

Stephanie Bethmann[1] | Michael Melzer[2] | Nadine Schwarz[1] | Peter Jahns[1]

[1]Plant Biochemistry, Heinrich-Heine-University Düsseldorf, Düsseldorf, Germany

[2]Leibniz Institute of Plant Genetics and Crop Plant Research (IPK), Gatersleben, Germany

Correspondence
Peter Jahns, Plant Biochemistry, Heinrich-Heine-University Düsseldorf, Universitätsstr.1, 0-40225 0üsseldorf; Physiology and Cell Biology, Düsseldorf, Germany.
Email: pjahns@hhu.de

Funding information
Deutsche Forschungsgemeinschaft, Grant/Award Number: JA 665/12-1 and GRK 1525

Abstract

The xanthophyll zeaxanthin is synthesized in chloroplasts upon high light exposure of plants and serves central photoprotective functions. The reconversion of zeaxanthin to violaxanthin is catalyzed by the zeaxanthin epoxidase (ZEP). ZEP shows highest activity after short and moderate high light periods, but becomes gradually down-regulated in response to increasing high light stress along with down-regulation of photosystem II (PSII) activity. ZEP activity and ZEP protein levels were studied in response to high light stress in four plant species: *Arabidopsis thaliana*, *Pisum sativum*, *Nicotiana benthamiana* and *Spinacia oleracea*. In all species, ZEP protein was degraded during photoinhibition of PSII in parallel with the D1 protein of PSII. In the presence of streptomycin, an inhibitor of chloroplast protein synthesis, photoinhibition of PSII and ZEP activity as well as degradation of D1 and ZEP protein was strongly increased, indicating a close correlation of ZEP regulation with PSII photoinhibition and repair. The concomitant high light-induced inactivation/degradation of ZEP and D1 prevents the reconversion of zeaxanthin during photoinhibition and repair of PSII. This regulation of ZEP activity supports a coordinated degradation of D1 and ZEP during photoinhibition/repair of PSII and an essential photoprotective function of zeaxanthin during the PSII repair cycle.

KEYWORDS

D1 turnover, photoinhibition, photosystem II, xanthophyll cycle, zeaxanthin, zeaxanthin epoxidase

1 | INTRODUCTION

The xanthophyll zeaxanthin (Zx) serves central photoprotective functions in land plants (Jahns & Holzwarth, 2012). It is involved in non-photochemical quenching (NPQ) of excess light energy in photosystem II (PSII) and additionally acts as an antioxidant in the thylakoid membrane (Havaux, Dall'Osto, & Bassi, 2007; Havaux & Niyogi, 1999). Zx is formed in the de-epoxidation reactions of the xanthophyll cycle (Jahns, Latowski, & Strzalka, 2009; Yamamoto, Nakayama, & Chichester, 1962) from violaxanthin (Vx). This reaction takes place in the thylakoid membrane and is catalyzed by the Vx de-epoxidase (VDE) which is localized in the thylakoid lumen. VDE activity is strictly regulated by the thylakoid lumen pH and the VDE is activated at pH values < 6.0 (Hager, 1969; Pfündel &

Dilley, 1993) along with the pH-dependent qE component of NPQ (Briantais, Vernotte, & Picaud, 1979; Takizawa, Cruz, Kanazawa, & Kramer, 2007). This pH-regulation ensures that Zx formation and NPQ induction occur only at light intensities that saturate the photosynthetic electron transport. The reconversion of Zx to Vx is catalyzed by the Zx epoxidase (ZEP) which is localized in the chloroplast stroma (Schwarz et al., 2015) and has a pH optimum of about 7.5 (Siefermann & Yamamoto, 1975). The exact regulation of ZEP activity, however, remains elusive.

NPQ comprises a number of different mechanisms, which have been identified mainly on basis of their different relaxation kinetics, and which have been termed qE, qT, qZ, and qI (Nilkens et al., 2010; Quick & Stitt, 1989; Walters & Horton, 1991). Zx is supposed to be directly or indirectly involved in most NPQ processes, including qE, qZ, and qI (Kress & Jahns, 2017; Nilkens et al., 2010). The pH-regulated, so-called energy-dependent quenching qE is the most flexible NPQ component, related to its rapid regulation (within 1–2 min) in response to light-dependent changes in the lumen pH. Under a wide range of natural conditions, qE represents the dominating NPQ component. Activation of qE is mediated by the PsbS protein, which acts as sensor of the lumen pH and induces conformational changes in the antenna of PSII through interaction with LHCII proteins (Correa-Galvis, Poschmann, Melzer, Stühler, & Jahns, 2016; Sacharz, Giovagnetti, Ungerer, Mastroianni, & Ruban, 2017). Induction of the maximum qE capacity further requires the presence of Zx. Two general models for the role of Zx in qE have been developed during the past years: A direct role of Zx in qE is favored by Fleming and co-workers (Ahn et al., 2008; Avenson et al., 2008; Holt et al., 2005), while an indirect allosteric role has been proposed by Horton, Ruban and co-workers (Horton, Ruban, & Wentworth, 2000; Kana et al., 2016; Ruban & Horton, 1999). Since current models of qE quenching locate the quenching process to the internal binding sites L1 and L2, a direct function of Zx likely requires binding of Zx at these sites, whereas an indirect allosteric role might also be based on Zx binding at the periphery of antenna proteins. Recent work hypothesized binding of Zx to the periphery of antenna complexes (Xu, Tian, Kloz, & Croce, 2015) supporting rather an indirect role of Zx in qE. The qZ component of NPQ is activated/deactivated in the time range of 10–30 min and has been correlated with the dynamics of Zx synthesis/epoxidation (Dall'Osto, Caffarri, & Bassi, 2005; Nilkens et al., 2010). This component represents a sustained, pH-independent (once Zx has been synthesized) form of quenching and is likely identical with the Zx-dependent phase of photoinhibition described earlier (Jahns & Miehe, 1996; Leitsch, Schnettger, Critchley, & Krause, 1994; Thiele, Krause, & Winter, 1998). For the qZ component of NPQ, a direct function of Zx has been proposed for the monomeric antenna protein Lhcb5 (Dall'Osto et al., 2005). The photoinhibitory qI quenching is the slowest inducible and relaxing NPQ component, which becomes activated after prolonged illumination of plants at high light intensities. Photoinhibition involves the light-induced damage of the PSII reaction center, which is accompanied by phosphorylation and proteolytic cleavage of the 01 protein (Aro, Virgin, & Andersson, 1993; Ohad, Kyle, & Arntzen, 1984). Recovery from photoinhibition requires degradation and re-synthesis of D1. This repair cycle likely occurs in the stroma exposed region of the thylakoid membrane (Jarvi, Suorsa, & Aro, 2015) and involves degradation of the D1 protein by FtsH and Deg proteases (Kato, Miura, Ido, Ifuku, & Sakamoto, 2009; Kato, Sun, Zhang, & Sakamoto, 2012). The possible role of Zx in qI is unknown. Recent analyses of the dynamics of NPQ and xanthophyll conversion, however, brought evidence that Zx has no direct function in qZ and qI (Kress & Jahns, 2017).

Earlier work indicated that Zx epoxidation is kinetically correlated with recovery from photoinhibition (Jahns & Miehe, 1996; Verhoeven, Adams, & 0emmig-Adams, 1996) and stepwise down-regulated with decreasing PSII activity under high light stress (Kress & Jahns, 2017; Reinhold, Niczyporuk, Beran, & Jahns, 2008). The molecular basis of this down-regulation of ZEP activity is unclear. Recent studies provided evidence that ZEP activity is susceptible to redox regulation. Arabidopsis *ntrc* mutants, which are defective in NA0PH thioredoxin reductase C (NTRC), accumulate higher levels of Zx than wild-type plants upon illumination at non-saturating light intensities (Naranjo et al., 2016). Although no redox modification of the ZEP was detectable in that work, reduction of sulfhydryl group of the ZEP protein by either NTRC or via thioredoxins (Trx) may be involved in the regulation of ZEP activity. The latter idea was strongly supported by recent analyses of Arabidopsis plants with silenced Trx m proteins (Da et al., 2017). Like *ntrc* mutants, also *trxm* mutants accumulate higher levels of Zx than wild-type plants upon illumination at non-saturating light intensities. Moreover, this work provided evidence for a redox modification of ZEP and a direct interaction of Trx m and ZEP (Da et al., 2017). These data underline, that the ZEP protein becomes (at least partially) inactive in darkness along with the oxidation of Trx, and requires light activation through the Trx system for full activity. The high light-induced down-regulation of ZEP activity might thus be based on redox regulation.

To investigate the comparative down-regulation of PSII and ZEP activity and changes in the protein level of D1 and ZEP, we studied the inactivation of ZEP during photoinhibition in Arabidopsis, pea, tobacco, and spinach. Our data suggest a concomitant degradation of D1 and ZEP protein after severe light stress, indicating an important role of Zx in photoprotection of PSII during high light (HL)-induced D1 turnover.

2 | MATERIAL AND METHODS

2.1 | Plant material and growth conditions

Arabidopsis (*Arabidopsis thaliana*, ecotype Col-0), pea (*Pisum sativum*, cv. Kleine Rheinländerin), and spinach (*Spinacia oleracea*, cv. Polka) plants were grown in a greenhouse under short-day conditions (8-hr light/ 16-hr darkness) at light intensities of about 100 µmol photons m^{-2} s^{-1}. Tobacco (*Nicotiana benthamiana*) plants were grown in a greenhouse under long-day conditions (16 hr light/8 hr darkness) at light intensities of about 150 µmol photons m^{-2} s^{-1}. About 6–8 weeks old plants were used for all species, except for pea plants,

which were harvested after 2–3 weeks. For all experiments, plants at the end of dark phase were used as a control.

2.2 | Isolation of intact chloroplasts and thylakoid membranes

A total of 10-20 g leaf material was harvested from dark-adapted plants, washed with water and stored for 1-2 hr at 4°C in the dark. Chloroplast isolation was carried out according to (Kley, Heil, Muck, Svatos, & Boland 2010). In short, leaf material was homogenized in isolation medium (1 mM $MgCl_2$,1 mM $MnCl_2$, 10 mM $NaHCO_3$, 300 mM sorbitol, 20 mM HEPES/ KOH, pH 7.6, 5 mM EGTA, 5 mM EOTA) and filtered through 4 layers of gauze and 1 layer of nylon mesh (40 µm). After centrifugation (10 min, 2,000 *g*) through a 50% percoll cushion, the resulting pellet, which contained intact chloroplasts, was resuspended in isolation medium. For isolation of thylakoid membranes, intact chloroplasts were osmotically shocked by 1 min incubation in 5 mM $MgCl_2$. After centrifugation for 5 min at 4,000 *g*, the pelleted thylakoid membranes were resuspended in a medium containing 5 mM $MgCl_2$, 5 mM NaCl, 2 mM KH_2PO_4, 40 mM HEPES/NaOH pH 7.6, and 0.33 M sorbitol.

2.3 | Infiltration with streptomycin

For infiltration with streptomycin (SM), leaf disks (1 cm diameter) were placed on a solution containing 3 mM SM and incubated for 1 hr in a desiccator. Control samples were infiltrated with H_2O under the same conditions.

2.4 | Determination of PSII activity

Leaf disks were placed on water and exposed to HL (1,000 or 2,000 µmol photons m^{-2} s^{-1}) on a temperature-controlled cuvette (20°C or 4°C) for up to 8 hr. After HL treatment, samples were transferred to LL (10–20 µmol photons m^{-2} s^{-1}) for up to 16 hr. At indicated times, leaf disks were incubated for 5 min in darkness and the Fv/Fm ratio was determined with a Joliot-type spectrophotometer (JTS-10, BioLogic). Subsequently, leaf disks were frozen in liquid N_2 and stored for pigment extraction at -20°C. n addition, three leaf disks were frozen and stored at -20°C for protein extraction.

2.5 | Protein extraction and immunoblot analyses

Proteins of leaf samples were extracted with protein extraction buffer (1.6% SDS (w/v), 1 M urea, 50 mM Tris/HCl pH 7.6) by mortaring in an Eppendorf vial (1,000 rpm, Heidolph RZR 2051). For chloroplast and thylakoid samples, 10 µl were mixed with 30 µl protein extraction buffer. Subsequently, protein extracts were incubated at 70°C for 20 min and non-soluble material was pelleted by 20 min centrifugation at 13 000 *g*. Protein concentrations were determined with the Bio-Rad® 0C Protein Assay (Bio-Rad) according to the manufacturers protocol.

For immunoblot analysis, proteins were separated by S0S-PAGE according to (Laemmli, 1970) and subsequently transferred to a PVDF membrane (FluoroTrans®W PV0F 0.2 µm, Pall Life Sciences) in a semi-dry blot chamber (Power Blotter, Thermo Scientific), applying the 3 buffer system as described (Kyhse-Andersen, 1984). Incubation with the primary antibody was carried out either for 1 hr at room temperature (RT) or overnight at 4°C, incubation with the secondary anti-mouse- gG antibody (Sigma-Aldrich) for 1 hr at RT. The secondary antibody was visualized by chemiluminescence (PicoLucent™ Plus-HRP; GBiosciences) and detected with the LAS-4000 mini (GE Healthcare). The following polyclonal primary antibodies were used; anti-AtZEP and anti-NtZEP (commissioned work, Pineda Antibody), anti-Lhcb2 (AS01003), anti-01 (AS05084) and anti-RbcL (AS03037) (Agrisera Antibodies).

2.6 | Pigment analyses

For pigment analyses, frozen leaf material was carefully mortared in an Eppendorf vial (100 rpm, Heidolph RZT 2051) upon addition of acetone. After short centrifugation (5 min, 17,000 *g*), extracts were filtered (0.2 µm pore size) and then used for reversed-phase HPLC according to (Färber, Young, Ruban, Horton, & Jahns, 1997).

2.7 | Light and transmission electron microscopy

Leaf disks were placed on water and exposed to HL (2,000 µmol photons m^{-2} s^{-1}) on a temperature-controlled cuvette (4°C) for 8 hr. For structural analysis, the central part of leaf disks (1 cm diameter) of dark acclimated state and 8 hr of HL exposure were cut into 2 mm^2 pieces. For each plant species and each treatment, 3-4 leaf disks were used for combined conventional and microwave-assisted fixation, substitution, resin embedding, sectioning, and microscopical analysis as described (Schumann, Paul, Melzer, Dörmann, & Jahns, 2017).

2.8 | Statistical analysis

Statistical analyses of pigment composition and light utilization parameters were performed using R studio (version 1.1.463). ANOVA was used to test significant differences among genotypes. Variance homogeneity was tested by Levenes's test. The post hoc test (Tukey HSD) was performed for multiple comparison analysis. Statistical analyses of immunoblot staining intensities were done with Student's *t* test using Microsoft Office Excel 2010–2016 (Microsoft Corporation). Significant differences ($p < .05$) were marked by different letters.

3 | RESULTS

3.1 | Spinach and pea chloroplasts do not contain stroma-localized ZEP protein

Recent work has shown that ZEP protein in Arabidopsis chloroplasts is distributed between the thylakoid membrane (45%–50% of the total ZEP protein), the chloroplast stroma (45%–50%) and the envelope membrane (<10%) (Schwarz et al., 2015). The small fraction of ZEP protein associated with the envelope membrane is supposed to be involved in general carotenoid biosynthesis, while the thylakoid membrane-bound fraction functions in the xanthophyll cycle (Schwarz et al., 2015). In contrast, the function of stroma-localized ZEP protein is unknown. We investigated the existence of stroma-localized ZEP protein in pea, spinach, and tobacco chloroplasts by comparing the protein content of intact chloroplasts with that of isolated thylakoid membranes. As shown in Figure 1, ZEP content of thylakoid membranes was clearly reduced to about 50% in comparison to ZEP content of chloroplasts in Arabidopsis and tobacco plants, supporting the existence of stroma-localized ZEP protein in these two species. However, similar amounts of ZEP were found for thylakoid membranes and intact chloroplasts in pea and spinach (Figure 1), indicating that no stroma-localized fraction of ZEP exists in these species. Obviously, the distribution of ZEP protein between the thylakoid membrane and the chloroplast stroma is not obligatory in chloroplasts of land plants. Moreover, the intensity of the bands detected for ZEP in chloroplasts was similar among the four species. Provided that the affinity of the antibodies to the ZEP protein is similar in each species, this indicates similar total levels of ZEP in chloroplasts of each species.

3.2 | ZEP activity is inhibited by high light intensities

The HL sensitivity of PSII and ZEP activity in the four species was studied on basis of changes in the maximum PSII efficiency as derived from the Fv/Fm ratio (for PSII activity) and the de-epoxidation state (DEPS) of the xanthophyll cycle pigments (for ZEP activity).

The response of plants to moderate HL stress (30 min at 1,000 µmol photons m^{-2} s^{-1} and 20°C) and severe HL stress (8 hr at 2,000 µmol photons m^{-2} s^{-1} and 4°C) was determined for leaves infiltrated either with H_2O (Figure 2) or 3 mM streptomycin (SM) (Figure 3), an inhibitor of protein synthesis in chloroplasts.

Moderate HL stress (30 min at a light intensity of 1,000 µmol photons m^{-2} s^{-1} and at 20°C) induced a reduction of Fv/Fm to values in the range from 85% to 95% of the dark Fv/Fm ratio (Figure 2a). Pea and spinach plants showed the lowest reduction of the PSII quantum yield (to about 95%) and a complete recovery during subsequent LL (20–30 µmol photons m^{-2} s^{-1}) exposure for 4 hr. n contrast, Arabidopsis and tobacco plants exhibited a more pronounced reduction of Fv/Fm (to about 85%) and the recovery in LL was incomplete (Figure 2a). In parallel, DEPS of the xanthophyll cycle pigments Zx, antheraxanthin (Ax), and violaxanthin (Vx), calculated as (Zx + 0.5Ax)/(Vx + Ax+Zx) x 100, increased during the HL period to values of 35%–55% and decreased to values between 5% and 15% at the end of the LL phase (Figure 2b). While the increase of 0EPS in HL is related to the conversion of Vx to Zx by VDE, the decrease of DEPS in LL reflects ZEP activity. Comparing the differences among the four plants species, pea plants showed highest and spinach plants lowest DEPS at the end of the HL phase, while DEPS at the end of the LL phase was similar in all species. This indicates similar ZEP activities in all species after short-term HL treatment.

More severe HL stress (8 hr at a light intensity of 2,000 µmol photons m^{-2} s^{-1} and at 4°C) induced a strong reduction of Fv/Fm to values ranging from 15% in Arabidopsis to about 30% in pea and about 45% in spinach (Figure 2c). In tobacco plants, however, Fv was completely abolished, resulting in Fv/Fm values of nearly 0 at the end of the HL treatment. 0uring 16 hr recovery at LL and 20°C, the Fv/Fm values recovered almost completely in pea, spinach and Arabidopsis, while in tobacco plants an increase to only 30% was determined. Under the same conditions, DEPS increased during HL exposure to values between about 60% (tobacco) and 80% (pea and spinach) (Figure 2d). Compared to the moderate light treatment (Figure 2b) the decrease of DEPS in the subsequent LL period was retarded, resulting in DEPS values of 25%-30% (pea and spinach) and 45%-55% (Arabidopsis and tobacco) at the end of 16 hr LL exposure. Hence, severe HL stress

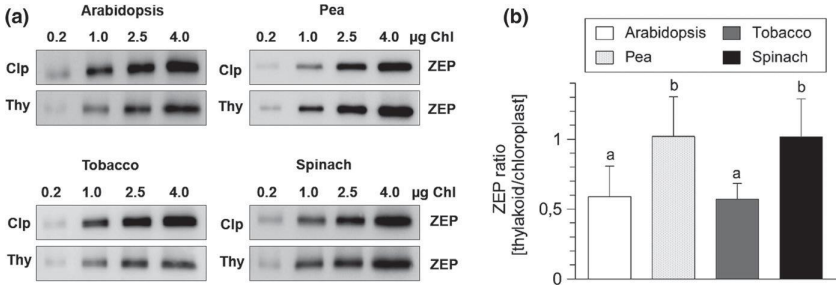

FIGURE 1 Abundance of ZEP protein in chloroplasts and thylakoid membranes. ntact chloroplasts and thylakoid membranes were isolated from dark-adapted leaves. Proteins equivalent to the same Chl content of the corresponding chloroplast and thylakoid preparations were separated by S0S-PAGE and ZEP abundance was assessed by immunoblotting. (a), Representative blots from 4 biological replicates. (b), Quantification of the ratio of ZEP content in thylakoids relative to chloroplasts. Mean values (± *SD*) of at least 2 technical replicates for each of 4 biological replicates (n = 8) are shown. Significant differences (Tukey HSD, $p < .05$) among the different species are indicated

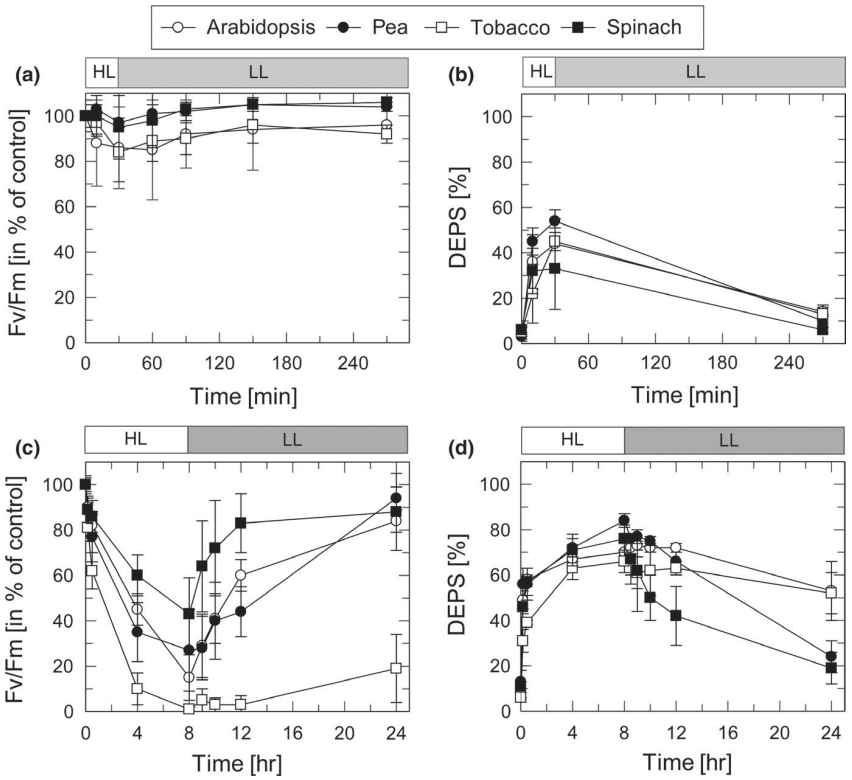

FIGURE 2 Dynamics of PSII and ZEP activity during and after HL exposure. Detached leaves from dark-adapted plants were infiltrated with H_2O and floated on water in a temperature-controlled cuvette. Leaves were exposed to high light (HL) for 30 min at 1,000 µmol photons m^{-2} s^{-1} and 20°C (a,b) or for 8 hr at 2,000 µmol photons m^{-2} s^{-1} and 4°C (c,d). Subsequently, leaves were transferred to low light (LL, 10–20 µmol photons m^{-2} s^{-1}) at 20°C for 4 hr (a,b) or 16 hr (c,d). PS activity was derived from measurements of the Fv/Fm ratio (a,c) and ZEP activity from HPLC analysis of the de-epoxidation state (DEPS) of the xanthophyll cycle pigments (b,d). 0EPS [%] = (Zx + 0.5Ax)/(Vx + Ax +Zx) x 100. 0ata represent mean values ± *SD* from 8 (a,c) or 4 (b,d) independent measurements

resulted in down-regulation of ZEP activity, which was more pronounced in Arabidopsis and tobacco as compared to pea and spinach. Overall, these data support the correlation of HL-induced inactivation of PS and ZEP in all species, with tobacco and Arabidopsis plants being more sensitive to HL than pea and spinach plants.

3.3 | ZEP activity is inhibited in the presence of streptomycin

To evaluate the impact of the inhibition of the D1 turnover on HL-induced changes in PSII and ZEP activity, leaves were incubated prior to HL exposure with SM. Under moderate HL stress (30 min at a light intensity of 1,000 µmol photons m^{-2} s^{-1} at 20°C), PS activity was not affected by SM treatment as obvious from the similar dynamics of PSII activity in the presence (Figure 3a) and in the absence (Figure 2a) of SM. Interestingly, however, ZEP activity was slightly reduced in the presence of SM (20%–25% DEPS at the end of the LL phase, Figure3b, compared to 5%–15% in the absence of SM, Figure 2b). Only in spinach plants, no inhibitory effect of SM was detectable.

Under severe HL stress (8 hr at a light intensity of 2,000 µmol photons m^{-2} s^{-1} at 4°C), the PS activity was nearly completely abolished in all plant species after HL treatment, except for spinach plants, which retained a residual activity of about 30% at the end of HL exposure (Figure 3c). While PS activity in spinach recovered to values of about 60% during subsequent exposure for 16 hr to LL, no increase of the Fv/Fm ratio was detectable for the other species. This reflects the efficient suppression of recovery of photoinhibited PSII due to inhibition of D1 synthesis by SM. Hence, the differences among the species in the sensitivity of PSII activity toward HL were no longer visible in the presence of SM. The incomplete inactivation of PSII after HL treatment, as well as the partial recovery of PSII activity during subsequent LL exposure, in the presence of SM in spinach leaves is likely related to an incomplete uptake of SM in chloroplasts of this species.

Strikingly, inhibition of PS recovery was accompanied by complete inhibition of ZEP activity (Figure 3d). While synthesis of Zx–and thus the increase of 0EPS–during the HL period was not affected by SM (cf. Figure 2d), no decrease of DEPS was detectable during the entire subsequent 16 LL exposure (Figure 3d). Only spinach plants showed a slight decrease of DEPS from about 80% to 60% during the first 4 hr of recovery, in line with the incomplete inactivation of PSII by SM in this species (Figure 3c 9***). These data indicate that ZEP activity is efficiently inhibited in the presence of SM. To test, whether SM is a direct inhibitor of ZEP, SM was added to thylakoids membranes, isolated from pre-illuminated plants (30 min, 1,000 µmol photons m^{-2} s^{-1}). In none of the species any significant effect of SM on ZEP activity was detectable (Figure S1), suggesting that the strong inhibitory effect on SM in HL treated leaves is due to an indirect function of SM, likely related to the suppression of the PSII repair cycle.

3.4 | ZEP protein is degraded in parallel with the D1 protein

The impact of HL (2,000 µmol photons m^{-2} s^{-1} at 4°C) on the degradation of D1 and ZEP protein was determined by immunoblot

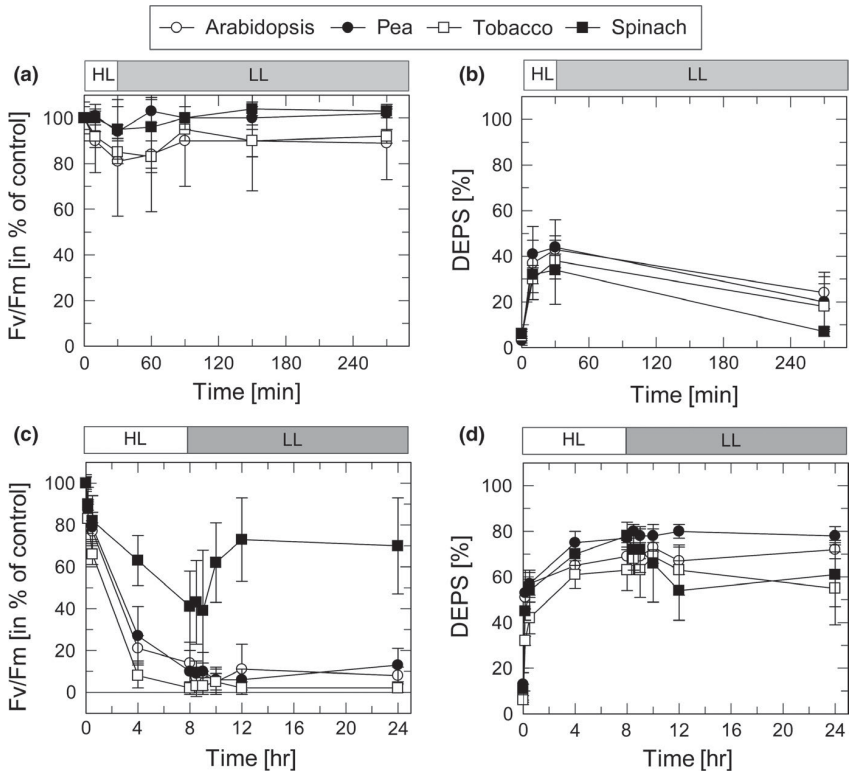

FIGURE 3 Impact of streptomycin HL-induced inactivation of PSII and ZEP. Detached leaves from dark-adapted plants were infiltrated with 3 mM SM and floated on water in a temperature-controlled cuvette. Leaves were exposed to high light (HL) for 30 min at 1,000 µmol photons m^{-2} s^{-1} and 20°C (a,b) or for 8 hr at 2,000 µmol photons m^{-2} s^{-1} and 4°C (c,d). Subsequently, leaves were transferred to low light (LL, 10–20 µmol photons m^{-2} s^{-1}) at 20°C for 4 hr (a,b) or 16 hr (c,d). PSII activity was derived from measurements of the Fv/Fm ratio (a,c) and ZEP activity from HPLC analysis of the de-epoxidation state (DEPS) of the xanthophyll cycle pigments (b,d). DEPS [%] = (Zx + 0.5Ax)/(Vx + Ax +Zx) x 100. 0ata represent mean values ± *SD* from 8 (a,c) or 4 (b,d) independent measurements

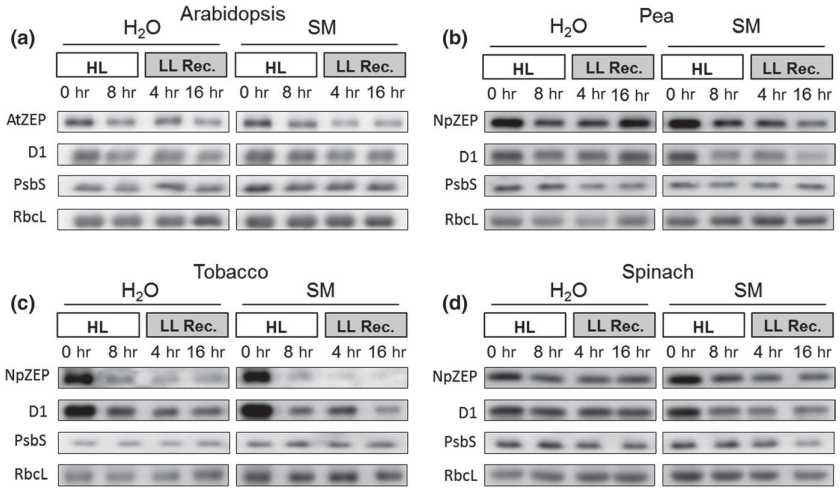

FIGURE 4 High light-induced changes of the 01 and ZEP protein content. 0etached leaves of Arabidopsis (a), pea (b), spinach (c) and tobacco (d) plants were vacuum-infiltrated with H_2O or 3 mM SM, as indicated in each panel. Leaves were exposed to HL for 8 hr at 2,000 µmol photons m^{-2} s^{-1} and 4°C and then transferred to LL (10–20 µmol photons m^{-2} s^{-1}) for 16 hr. Total leaf protein extracts equivalent to 5 µg protein were separated by S0S-PAGE. The abundance of ZEP and 01 protein, as well as of the large subunit of RubisCO (RbcL) was assessed by immunoblotting with specific antibodies. Representative blots from at least 3 biological replicates are shown

analysis of leaf proteins extracted before and after 8 hr Hl treatment and during a subsequent recovery in LL (20 µmol photons m^{-2} s^{-1} at 20°C) (Figure 4). The PS subunit PsbS and the large subunit of RubisCO (RbcL) were used as control proteins for thylakoid membrane proteins and stromal proteins, respectively. In absence of SM, moderate degradation of both D1 and ZEP protein was detectable in all plants (Figure 4, Figure S2). The most pronounced degradation of ZEP and D1 was found in tobacco plants, in accordance with the most pronounced HL sensitivity of PSII in this species (cf. Figures 2 and 3). The amount of PsbS or RbcL did not change under these conditions (Figure 4, Figure S2). n the presence of SM, D1 and ZEP degradation was enhanced in all species. Again, the most pronounced degradation was detected for tobacco plants (Figure 4d), while less pronounced degradation occurred in

spinach plants (Figure 4b,c). The latter coincides with the highest resistance against HL determined for spinach (Figures 2 and 3). Again, the amount of PsbS and RbcL remained unchanged (Figure 4, Figure S2). The more pronounced degradation of ZEP together with D1 in the presence of SM suggests that ZEP degradation is directly coupled to D1 turnover. Hence, these data support the view that ZEP and D1 proteins degradation occurs in parallel in response to HL-induced damage of PSII.

3.5 | Species-specific differences in HL sensitivity correlate with different VAZ pool sizes rather than with different light utilization capacities

Different HL sensitivities among the species could originate from different capacities of photosynthetic light utilization. Chl fluorescence analyses were applied to determine the light dependence of electron transfer and energy dissipation. The light dependence of the redox state of Q_A and P700 was derived from the parameters qL and $Y_{(ND)}$, respectively, as determined with the 0UAL PAM 101 fluorometer. For qL, Arabidopsis and pea plants showed a similar light response (50% reduction of Q_A at about 90 and 110 µmol photons $m^{-2}s^{-1}$, respectively), whereas spinach leaves exhibited half reduction of Q_A at significantly higher light intensities (about 170 µmol photons m^{-2} s^{-1} higher light intensities), and pea showed intermediate values (about 140 µmol photons m^{-2} s^{-1}) (Figure S3a, Table 1).

Similar trends were observable for the light response of the redox state of P700 (Figure S3b, Table 1). In this case, however, only spinach leaves required significantly higher light intensities for half-maximal P700 oxidation (about 200 µmol photons m^{-2} s^{-1}), whereas all other species showed similar values in the range from about 100–130 µmol photons m^{-2} s^{-1}). Hence, the four species exhibit different light responses of the redox state of the electron transport chain, with spinach plants requiring the highest light intensities for reduction of Q_A and P700 oxidation. This became also evident from the light response of energy dissipation (Figure S3c, Table 1).

For NPQ induction, the light response was shifted to significantly higher light intensities in spinach leaves (half-maximal NPQ at about 200 µmol photons m^{-2} s^{-1}), as compared to the other species (about 80–120 µmol photons m^{-2} s^{-1}). Moreover, spinach exhibited the highest maximum NPQ capacity among all species (Figure S3c, Table 1). These specific characteristics of spinach leaves might contribute to the lower HL sensitivity of this species compared to Arabidopsis and tobacco. However, the very similar light response determined for pea and tobacco plants (Figure S3, Table 1), which both showed pronounced differences in HL sensitivity, indicates that the light dependence of light utilization is not directly correlated with the overall HL sensitivity. Notably, also the maximum NPQ capacity, which was constituted predominantly by qE under these experimental conditions (Table 1), did not correlate with the susceptibility to photoinhibition. Therefore, photosynthetic light utilization is unlikely to be the critical determinant for different HL sensitivities of the four species.

We further analyzed the pigment content to obtain information about possible differences in the photosystem composition. The Chl a/b ratio, which can be used as an estimate for differences in the PSII antenna size, was lower in spinach plants as compared to all other species (Table 2). Although the difference was statistically not significant due to the high standard deviation, this indicates a slightly smaller PSII antenna size in spinach plants. Since pea plants showed a different HL response than Arabidopsis and tobacco, but a similar Chl a/b ratio, the PSII antenna size is likely not responsible for an altered sensitivity towards HL stress. However, the two species with lowest HL susceptibility (pea and spinach) exhibited a 2–3-fold larger pool size of the xanthophyll cycle pigments Vx, Ax, and Zx (VAZ pool size, Table 2) and a higher convertibility of VAZ pigments during HL (DEPS, Figures 2 and 3, Table 2). These characteristics result in a much higher Zx content of pea and spinach plants compared to tobacco and Arabidopsis, which might explain the higher HL sensitivity of the latter two species. The VAZ pool size and 0EPS might thus be critical determinants for the HL sensitivity of the species.

3.6 | Leaf morphology and thylakoid membrane organization

Leaf morphology and thylakoid membrane organization was studied by light and electron microscopy to identify possible specific morphological characteristics that might be related to the more pronounced HL sensitivity of Arabidopsis and tobacco plants. Leaf thickness varied among the species between 200 and 300 µm, with pea plants showing the thinnest leaves and spinach the thickest ones (Figure 5a,d), and thus without specific structural properties of HL sensitive species. However, the two species with higher HL resistance, pea and spinach, were particularly characterized by smaller parenchyma cells (about 50 vs. 100 µm in Arabidopsis and tobacco) and more layers of parenchyma cells (Figure 5a,d). Thus, differences in leaf morphology might contribute to HL sensitivity. All species showed comparable chloroplast size and thylakoid membrane structures in the dark acclimated state, but pea chloroplasts were more round-shaped compared to the oval-shaped chloroplast of the other species (Figure 5b,e). However, whereas the amount of Chl per chloroplast was similar in all species, the two less HL sensitive species, pea and spinach, contained about 50% higher amount of Chl per leaf area (Table 2), which is in line with the increased number of parenchyma cells in these two species (Figure 5a,d). Please note, that this increase was only significant for spinach, due to the rather high standard deviation found in pea. Nevertheless, the Chl content per leaf area might thus also be a critical determinant for the HL sensitivity of the species. After 8 hr of HL exposure, leaf thickness was unchanged in all species except for tobacco plants, which exhibited a reduction of leaf thickness by about 30% (Figure 5d). This striking feature of tobacco leaves likely reflects the pronounced HL sensitivity of this species. Moreover, HL exposure induced structural changes of thylakoid membranes, particularly related to the stacking of membranes (Figure 5e,f). However, no general common response

TABLE 1 Light dependence of light utilization parameters derived from light response curves measured with the 0UAL-PAM 100 fluorimeter

Parameter		Arabidopsis	Pea	Tobacco	Spinach
qL	LI_{50}	93 ± 23[a]	141 18[bc]	109 ± 26[ab]	174 16[c]
$Y_{(ND)}$	LI_{50}	100 ± 13[a]	117 ± 53[a]	127 ± 23[a]	197 ± 26[b]
NPQ	max	2.60 ± 0.32[a]	3.18 0.44[b]	3.44 0.26[bc]	3.83 ± 0.23[c]
	LI_{50}	107 ± 12[a]	76 ± 55[a]	116 ± 31[a]	223 45[b]
qE	max	2.08 ± 0.35[a]	2.73 0.43[b]	2.98 ± 0.26[bc]	3.40 0.24[c]

Note: Maximum values (max) or the light intensities at which half-maximal values of the respective parameter were reached (LI_{50}) are listed. Data represent mean values ± *SD* of 8 independent experiments. Superscript letters indicate significant differences (Tukey HSD, $p < .05$) among the different species.

Abbreviations: NPQ, total non-photochemical quenching; qE, pH-dependent component of NPQ; qL, fraction of oxidized Q_A; $Y_{(ND)}$, fraction of oxidized P700.

TABLE 2 Pigment composition

Parameter	Arabidopsis	Pea	Tobacco	Spinach
Nx	28 ± 3[ab]	31 ± 3[a]	25 4[b]	32 ± 1[a]
Lut	92 ± 1[a]	119 14[b]	89 ± 16[a]	91 14[a]
VAZ	32 ± 3[a]	95 ± 19[b]	37 ± 13[a]	74 7[b]
Chl a/b	2.92 ± 0.35[a]	3.10 ± 0.57[a]	3.09 ± 0.26[a]	2.66 0.42[a]
$DEPS_{max}$	70 4[ab]	84 3[c]	66 ± 5[a]	76 ± 6[bc]
Chl (a + b)/Clp	0.40 0.10[a]	0.56 ± 0.11[a]	0.59 ± 0.08[a]	0.55 ± 0.02[a]
nmol Chl (a + b)/cm^2 leaf area	28 4[a]	38 ± 13[ab]	25 4[a]	41 11[b]

Note: The xanthophyll content (Lut, lutein; Nx, neoxanthin; VAZ, sum of xanthophyll cycle pigments) is given in relation to 1,000 Chl (a + b). The maximal de-epoxidation state of the VAZ pigments ($DEPS_{max}$) was derived from pigment analyses after 8 hr of illumination at 2,000 µmol photons m^{-2} s^{-1} (cf. Figure 2d). The data represent mean values ± *SD* with $n > 20$ for Nx, Lut, VAZ and Chl a/b; $n = 8$ for $DEPS_{max}$ and $n = 4$ for Chl (a + b) per Chloroplast (Clp) and nmol Chl (a + b) per leaf area. Superscript letters indicate significant differences (Tukey HSD, $p < .05$) among the different species.

in relation to different HL sensitivity was detectable among the four species, but the two HL sensitive species (Arabidopsis and tobacco) tended to better preserve the grana structure of thylakoid membrane than the less HL sensitive ones (pea and spinach). Particularly pea chloroplasts showed a pronounced disordering of thylakoid membrane stacking, while grana stacks were rather increased in spinach chloroplast. Thus, HL-induced reorganization of the thylakoid membrane might thus also contribute to the resistance against HL stress.

4 | DISCUSSION

4.1 | Regulation of ZEP activity

Zeaxanthin epoxidase activity is known to be down-regulated upon increasing photoinhibition of PSII activity and hence photo-oxidative stress in chloroplasts (Reinhold et al., 2008). Accordingly, ZEP activity was nearly completely inhibited in tobacco or strongly down-regulated in the other species after 8 hr Hl treatment at 4°C, in parallel with PSII inactivation (Figures 2 and 3). Changes in ZEP protein amounts in response to HL stress have not been assessed so far. The HL-induced degradation of ZEP shown in the present work thus indicates an irreversible HL-induced damage of ZEP (analogous to D1). The HL-induced down-regulation of ZEP activity ensures that high levels of Zx are retained in response to prolonged HL stress to allow for efficient reactivation (or retention) of energy dissipation and thus photoprotection after intermediate LL phases. Hence, the inactivation of ZEP is understood as long-term memory of photo-oxidative stress (Jahns & Holzwarth, 2012). This regulatory principle also applies to in vivo conditions, since winter acclimation of evergreen plants was shown to be accompanied by retention of high Zx levels along with inactivation of PS efficiency (Adams & 0emmig-Adams, 1995; Adams, 0emmig-Adams, Rosenstiel, Brightwell, & Ebbert, 2002; Adams, 0emmig-Adams, & Verhoeven, 1995; Öquist & Huner, 2003). These characteristics support an essential photoprotective function of Zx during photoinhibition of PSII. Notably, such a memory function of Zx also applies to short-term down-regulation of PSII efficiency in context with the pH-regulated qE mechanism (Horton, Wentworth, & Ruban, 2005), which is also modulated by Zx. As the de-activation of qE by the lumen pH is much faster than the reconversion of Zx to Vx, Zx is retained also in the short-term,

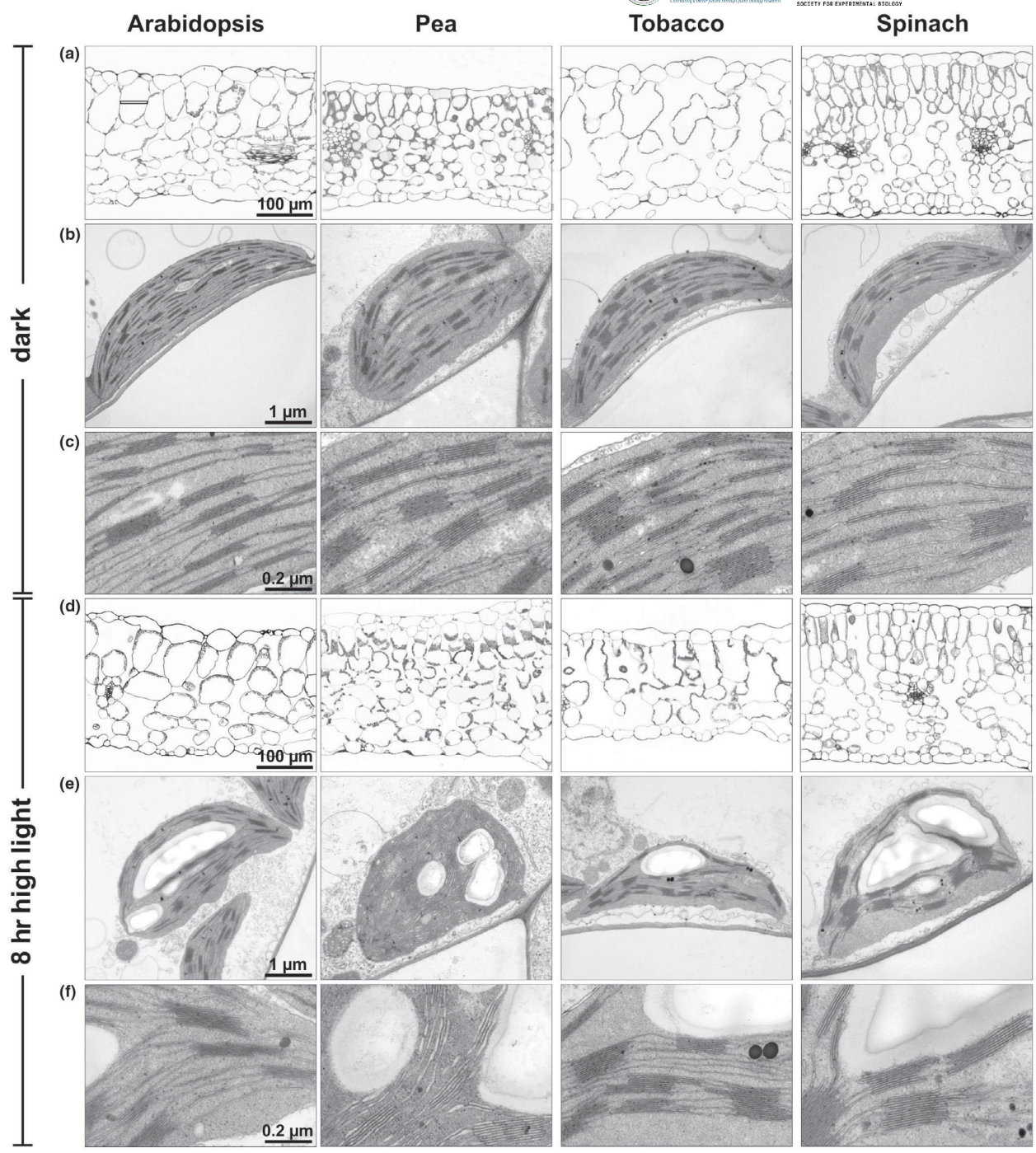

FIGURE 5 Leaf morphology and thylakoid membrane organization. (a,d) Light microscopic images of leaf cross-sections. (b,e) Electron microscopic images of chloroplasts. (c,f) Thylakoid membrane organization. (a-c) Dark acclimated leaves. (d-f) Leaves after 8 hr of HL exposure. Representative images of at least 4 biological replicates are shown

which ensures rapid reactivation of maximal qE capacity under rapidly fluctuating HL conditions.

The regulation of ZEP activity is thus central for photoprotection and operates at different time scales. However, the molecular basis of ZEP regulation is not fully understood. Recent work showed that ZEP activity is regulated in the short-term by Trx (Da et al., 2017) and NTRC (Naranjo et al., 2016), implying an essential function of redox-sensitive sulfhydryl groups of ZEP protein in regulation. On basis of the proposed redox regulation, it can be assumed that ZEP has low or no activity in the dark, and is fully activated under illumination through Trx mediated reduction of specific sulfhydryl groups. In contrast, the molecular basis of HL-induced down-regulation of

ZEP activity is unclear. Related to the proposed redox regulation of ZEP activity, however, it is tempting to speculate that ZEP is inactivated by reactive oxygen species (ROS), which possibly irreversibly oxidize redox-sensitive cysteine residues.

4.2 | Degradation of ZEP protein

The observed HL-induced degradation of ZEP protein indicates that it is irreversibly damaged upon high photo-oxidative stress, possibly due to oxidation by ROS. Restoration of ZEP activity might thus require the degradation of inactive protein and import of newly synthesized protein. These characteristics resemble the general features of the well-known HL-induced D1 turnover. The very close correlation of the down-regulation of PSII and ZEP activity and the parallel degradation of D1 and ZEP suggests a coordinated regulation of ZEP activity/degradation related to PSII inactivation/D1 degradation, which might involve an interaction of PSII and ZEP. ZEP is localized at the stroma side of the membrane and should have access to the stroma exposed regions of the membrane only, but not to the inner part of the grana region, where functional PSII is located. Since damaged PSII centers are supposed to migrate to the stroma exposed regions of the membrane, it is conceivable that ZEP can interact particularly with damaged PSII. However, on basis of non-denaturing blue native gel electrophoresis, no co-migration of ZEP and PSII was detectable in thylakoids from HL treated plants (Schwarz et al., 2015), suggesting that either no interaction or only a weak interaction of the two proteins exists. Nevertheless, an interaction of damaged PSII and ZEP might explain, why inactivation and degradation of ZEP protein is enhanced in the presence of SM. Since ZEP is encoded in the nucleus, ZEP synthesis should not be influenced directly by SM, suggesting that accelerated ZEP degradation in the presence of SM is rather related to the inhibited D1 turnover and thus PSII repair. Consequently, ZEP degradation might be triggered by the accumulation of non-functional PSII, and hence under conditions when PSII repair cannot keep pace with PSII damage, either due to enhanced rates of PSII inhibition or due to reduced rates of PSII repair. The sensing of accumulation of non-functional PSII by ZEP does not necessarily require an interaction of damaged PSII and ZEP but could also be related to a, so far unknown, factor involved in PSII repair or reassembly. Interestingly, ZEP activity was found to be affected by SM even under moderate HL stress, independent of an additional inhibitory effect on PSII activity. Since SM had no direct effect on ZEP activity, this supports the view, that the accumulation of a putative signaling factor can also be triggered independent of pronounced inactivation of PSII in the presence of SM. Consequently, inactivation (and likely also degradation) of ZEP seems to be not directly related to inactivation of PSII but rather to a functional PSII repair mechanism.

Irrespective of such a putative trigger factor, the down-regulation/degradation of ZEP upon accumulation of damaged PSII implies an essential function of Zx for photoprotection during the PSII repair cycle. Such a function is supported by the characteristics of the Arabidopsis xanthophyll cycle mutants *npq1* and *npq2* (Niyogi, Grossman, & Björkman, 1998), which revealed an increased HL sensitivity of Zx deficient *npq1* (Havaux & Niyogi, 1999; Kalituho, Rech, & Jahns, 2007; Sarvikas, Hakala, Pätsikkä, Tyystjärvi, & Tyystjärvi, 2006) and a less pronounced HL sensitivity of Zx accumulating *npq2* (Dall'Osto et al., 2005; Kalituho et al., 2007) compared to wild-type plants. Zx is known to be present in the thylakoid membrane either in association with antenna proteins or as non-protein bound molecule in the lipid phase of the membrane. Since no binding of the Zx to the PSII reaction center has been reported so far, it is thus likely that non-protein bound Zx serves as photoprotective xanthophyll during PSII repair. Such a function might be the basis for the shown qE-independent function of Zx (Havaux & Niyogi, 1999). This view is further supported by well-known increase of the VAZ pool size during long-term HL acclimation of plants (Bailey, Horton, & Walters, 2004; 0emmig-Adams, Cohu, Muller, & Adams, 2012; Mishra et al., 2012; Schumann et al., 2017). Since long-term acclimation to HL also involves the reduction of the PSII antenna size and thus of xanthophyll binding sites, it is very likely that a significant fraction of the additionally accumulated VAZ pigments is not bound to antenna proteins. Recent work challenged the view that formed Zx rebinds to the Vx binding sites of the PSII antenna proteins (Xu et al., 2015). Thus it can be speculated, that Zx is generally located at the surface of antenna proteins and by that may contribute to protection of the PSII reaction center.

4.3 | Species-specific differences in HL sensitivity

Plants of Arabidopsis and tobacco turned out to be more sensitive to HL than of pea and spinach. To determine putative specific physiological and morphological parameters of HL sensitivity, a comparative analysis of two more HL sensitive and two less HL sensitive species has been carried out. Based on our results, we suggest the following parameters to be crucial for the determination of HL sensitivity: (a) The presence of stroma-localized ZEP, (b) Leaf morphology and thylakoid membrane dynamics, (c) The pigment composition (VAZ pool size and Chl content per leaf area).

The function of the stroma-localized ZEP protein determined in Arabidopsis (Schwarz et al., 2015) (Figure 1) is unclear. nterestingly, a stroma-localized fraction of ZEP was also found in tobacco chloroplasts, but not in the two less HL sensitive species, pea and spinach (Figure 1). Since the total amount of ZEP protein was found to be similar in all species (Figure 1), we conclude that the stroma-localized fraction does not represent an additional pool of ZEP protein, but that binding of a fraction of ZEP to the thylakoid membrane is restricted. The ZEP protein binds to the stroma exposed region of thylakoid membrane and interacts with the membrane through hydrophobic interactions (Schaller, Wilhelm, Strzatka, & Goss, 2012; Schwarz et al., 2015). Species-specific differences in the binding efficiency of ZEP protein to the thylakoid membrane might be due to differences in the properties of either the thylakoid membrane or the ZEP protein. Since the predicted amino acid sequences of the

ZEP proteins in the different species show a high degree of identity, it seems unlikely that specific properties of the ZEP protein are responsible for the binding efficiency to the thylakoid membrane. It is unknown, however, which part of the protein is involved in binding to the membrane. It is further unclear, whether binding of ZEP requires a specific interaction with other proteins. In such a case, limited number of interactions partners present in the membrane might restrict ZEP binding to the membrane. Alternatively, different membrane properties could limit ZEP binding. For steric reasons, ZEP protein has only access to the stroma exposed regions of the membrane but not to the grana partitions. Thus, the relative portion of stroma exposed membranes might restrict ZEP binding as well. On basis of the EM analysis of thylakoid membrane organization (Figure 5), however, no obvious differences in thylakoid membrane organization were detectable among the different species under non-stressed conditions. It is thus most likely, that other membrane characteristics are responsible for the reduced binding of ZEP protein and hence the occurrence of a stroma-localized fraction of ZEP in Arabidopsis and tobacco.

At the level of leaf morphology, particularly the parenchyma cell size and the number of layers of parenchyma cells correlated with the HL sensitivity. The two species with higher HL resistance, pea and spinach, were particularly characterized by about 50% smaller parenchyma cells (about 50 µm in pea and spinach vs. 100 µm in Arabidopsis and tobacco) leading to more layers of parenchyma cells. The resulting light gradient within the leaf due to shading and light scattering might reduce light absorption in chloroplasts of inner layers of cells and hence induce reduced inactivation of PSII relative to the total number of chloroplasts. Earlier work further showed that a lower Chl content per leaf area is accompanied by higher susceptibility to photoinhibition (Patsikka, Kairavuo, Sersen, Aro, & Tyystjärvi, 2002). Therefore, the lower Chl content per leaf area found here for Arabidopsis and tobacco plants (Table 2) could contribute to the higher HL sensitivity of these two species. Moreover, recent work showed that structural rearrangement of the thylakoid membrane is accompanied with light-induced activation of qE (Schumann et al., 2017) and further regulates the balance between linear and cyclic electron transfer (Wood et al., 2018). Therefore, structural reorganization of membrane stacking is likely important for the activation of photoprotective mechanisms. The less pronounced thylakoid membrane reorganization in Arabidopsis and tobacco chloroplast in response to HL exposure compared to pea and spinach (Figure 5) might thus further determine the more pronounced HL sensitivity in these two species.

One of the most striking species-specific feature of the two more HL resistant species, pea and spinach, is the strongly increased VAZ pool size (Table 2) compared to Arabidopsis and tobacco. The increased VAZ pool size has important consequences related to photoprotective properties. The large VAZ pool size provides a large fraction of non-protein bound Zx in the lipid phase of the thylakoid membrane, which might contribute significantly to the protection of damaged PSII monomers during the PSII repair cycle in non-appressed regions of the membrane, either due to ROS de-activation in the lipid phase of the membrane or by promoting energy dissipation upon interaction with PSII reaction centers. ROS de-activation might be of particular importance, because earlier work showed that D1 protein synthesis and hence repair of PSII is vulnerable to ROS (Kojima et al., 2007; Nishiyama et al., 2001), while contribution to energy dissipation would require an interaction of Zx with PSII, either at specific binding sites or at the surface of PSII reactions center or antenna proteins. Moreover, non-protein bound Zx is supposed to affect the membrane properties with respect to fluidity and/or stability, similar to tocopherols (Havaux, 1998), and changes in the membrane fluidity are supposed to be involved in the PSII repair cycle (Goral et al., 2010; Yoshioka-Nishimura, 2016). The less flexible thylakoid membrane structure in response to HL (Figure 5) observed in the two species with a small VAZ pool size, Arabidopsis and tobacco, thus strongly supports such a role of Zx. Since an increase of the VAZ pool size is a typical long-term HL acclimation response of plants (Bailey et al., 2004; 0emmig-Adams et al., 2012; Mishra et al., 2012; Schumann et al., 2017), we propose that this parameter is an important factor determining the different HL sensitivities of the studied plant species.

ACKNOWLEDG MENTS

This work was supported by the Deutsche Forschungsgemeinschaft (JA 665/12-1 and GRK 1525 to PJ). We thank Marion Benecke and Kirsten Hoffie (IPK Gatersleben) for technical assistance with sample preparation for microscopy.

CONFLICT OF INTEREST

The authors declare no conflict of interest.

AUTHOR CONTRIBUTIONS

P.J. conceived the project. P.J. and S.B. designed the experiments; S.B. performed most of the experiments; N.S. contributed to the experiments with Arabidopsis plants; M.M. performed the electron microscopy; P.J. wrote the article with contributions of all authors.

REFERENCES

Adams, W. W., & 0emmig-Adams, B. (1995). The xanthophyll cycle and sustained thermal energy dissipation activity in *Vinca minor* and *Euonymus kiautschovicus* in winter. *Plant, Cell and Environment*, *18*, 117-127. https://doi.org/10.1111/j.1365-3040.1995.tb00345.x

Adams , W. W., 0emmig-Adams, B., Rosenstiel, T. N., Brightwell, A. K., & Ebbert, V. (2002). Photosynthesis and photoprotection in overwintering plants. *Plant Biology*, *4*, 545-557. https://doi.org/10.1055/s-2002-35434

Adams, W. W., 0emmig-Adams, B., Verhoeven, A. S., Barker, 0. H. (1995). 'Photoinhibition' during winter stress: Involvement of sustained xanthophyll cycle-dependent energy dissipation. *Australian Journal of Plant Physiology*, *22*, 261–276.

Ahn, T. K., Avenson, T. J., Ballottari, M., Cheng, Y.-C., Niyogi, K. K., Bassi, R., & Fleming, G. R. (2008). Architecture of a charge-transfer state regulating light harvesting in a plant antenna protein. *Science*, *320*, 794-797. https://doi.org/10.1126/science.1154800

Aro, E.-M., Virgin, ., & Andersson, B. (1993). Photoinhibition of photosystem II. Inactivation, protein damage and turnover. *Biochimica Et Biophysica Acta*, *1143*, 113-134.

Avenson, T. J., Ahn, T. K., Zigmantas, 0., Niyogi, K. K., Li, Z., Ballottari, M., … Fleming, G. R. (2008). Zeaxanthin radical cation formation in minor light-harvesting complexes of higher plant antenna. *Journal of Biological Chemistry*, *283*, 3550-3558. https://doi.org/10.1074/jbc.M705645200

Bailey, S., Horton, P., & Walters, R. G. (2004). Acclimation of Arabidopsis thaliana to the light environment: The relationship between photosynthetic function and chloroplast composition. *Planta*, *218*, 793–802. https://doi.org/10.1007/s00425-003-1158-5

Briantais, J.-M., Vernotte, C., Picaud, M., Krause, G. H. (1979). A quantitative study of the slow decline of chlorophyll *a* fluorescence in isolated chloroplasts. *Biochimica Et Biophysica Acta*, *548*, 128–138.

Correa-Galvis, V., Poschmann, G., Melzer, M., Stühler, K., & Jahns, P. (2016). PsbS interactions involved in the activation of energy dissipation in *Arabidopsis*. *Nature Plants*, *2*, 15225. https://doi.org/10.1038/nplants.2015.225

0a, Q., Sun, T., Wang, M., Jin, H., Li, M., Feng, 0., . Liu, B. (2017). M-type thioredoxins are involved in the xanthophyll cycle and proton motive force to alter NPQ under low-light conditions in Arabidopsis. *Plant Cell Reports*, *37*(2), 279–291. https://doi.org/10.1007/s00299-017-2229-6

0all'Osto, L., Caffarri, S., & Bassi, R. (2005). A mechanism of nonphotochemical energy dissipation, independent from PsbS, revealed by a conformational change in the antenna protein CP26. *The Plant Cell*, *17*, 1217-1232. https://doi.org/10.1105/tpc.104.030601

0emmig-Adams, B., Cohu, C. M., Muller, O., & Adams, W. W. (2012). Modulation of photosynthetic energy conversion efficiency in nature: From seconds to seasons. *Photosynthesis Research*, *113*, 75–88. https://doi.org/10.1007/s11120-012-9761-6

Farber, A., Young, A. J., Ruban, A. V., Horton, P., & Jahns, P. (1997). Dynamics of xanthophyll-cycle activity in different antenna subcomplexes in the photosynthetic membranes of higher plants: The relationship between zeaxanthin conversion and nonphotochemical fluorescence quenching. *Plant Physiology*, *115*, 1609–1618. https://doi.org/10.1104/pp.115.4.1609

Goral, T. K., Johnson, M. P., Brain, A. P. R., Kirchhoff, H., Ruban, A. V., & Mullineaux, C. W. (2010). Visualizing the mobility and distribution of chlorophyll proteins in higher plant thylakoid membranes: Effects of photoinhibition and protein phosphorylation. *The Plant Journal*, *62*, 948-959. https://doi.org/10.1111/j.1365-313X.2010.04207.x

Hager, A. (1969). Light dependent decrease of the pH-value in a chloroplast compartment causing the enzymatic interconversion of violaxanthin to zeaxanthin; relations to photophosphorylation. *Planta*, *89*, 224-243.

Havaux, M. (1998). Carotenoids as membrane stabilizers in chloroplasts. *Trends in Plant Science*, *3*, 147-151. https://doi.org/10.1016/S1360-1385(98)01200-X

Havaux, M., Dall'Osto, L., & Bassi, R. (2007). Zeaxanthin has enhanced antioxidant capacity with respect to all other xanthophylls in Arabidopsis leaves and functions independent of binding to PS antennae(1[C][W]). *Plant Physiology*, *145*, 1506–1520. https://doi.org/10.1104/pp.107.108480

Havaux, M., & Niyogi, K. K. (1999). The violaxanthin cycle protects plants from photooxidative damage by more than one mechanism. *Proceedings of the National Academy of Sciences of the United States of America*, *96*, 8762–8767. https://doi.org/10.1073/pnas.96.15.8762

Holt, N. E., Zigmantas, D., Valkunas, L., Li, X. P., Niyogi, K. K., & Fleming, G. R. (2005). Carotenoid cation formation and the regulation of photosynthetic light harvesting. *Science*, *307*, 433-436. https://doi.org/10.1126/science.1105833

Horton, P., Ruban, A. V., & Wentworth, M. (2000). Allosteric regulation of the light-harvesting system of photosystem II. *Philosophical Transactions of the Royal Society of London Series B-Biological Sciences*, *355*, 1361–1370. https://doi.org/10.1098/rstb.2000.0698

Horton, P., Wentworth, M., & Ruban, A. (2005). Control of the light harvesting function of chloroplast membranes: The LHCII-aggregation model for non-photochemical quenching. *Febs Letters*, *579*, 4201-4206. https://doi.org/10.1016/j.febslet.2005.07.003

Jahns, P., & Holzwarth, A. R. (2012). The role of the xanthophyll cycle and of lutein in photoprotection of photosystem II. *Biochimica Et Biophysica Acta-Bioenergetics*, *1817*, 182–193. https://doi.org/10.1016/j.bbabio.2011.04.012

Jahns, P., Latowski, D., & Strzalka, K. (2009). Mechanism and regulation of the violaxanthin cycle: The role of antenna proteins and membrane lipids. *Biochimica Et Biophysica Acta-Bioenergetics*, *1787*, 3-14. https://doi.org/10.1016/j.bbabio.2008.09.013

Jahns, P., & Miehe, B. (1996). Kinetic correlation of recovery from photoinhibition and zeaxanthin epoxidation. *Planta*, *198*, 202–210. https://doi.org/10.1007/BF00206245

Jarvi, S., Suorsa, M., & Aro, E.-M. (2015). Photosystem repair in plant chloroplasts - Regulation, assisting proteins and shared components with photosystem II biogenesis. *Biochimica Et Biophysica Acta-Bioenergetics*, *1847*, 900–909. https://doi.org/10.1016/j.bbabio.2015.01.006

Kalituho, L., Rech, J., & Jahns, P. (2007). The role of specific xanthophylls in light utilization. *Planta*, *225*, 423-439.

Kana, R., Kotabova, E., Kopecna, J., Trsková, E., Belgio, E., Sobotka, R., & Ruban, A. V. (2016). Violaxanthin inhibits nonphotochemical quenching in light-harvesting antenna of Chromera velia. *FEBS Letters*, *590*, 1076–1085.

Kato, Y., Miura, E., do, K., fuku, K., & Sakamoto, W. (2009). The variegated mutants lacking chloroplastic FtsHs are defective in D1 degradation and accumulate reactive oxygen species. *Plant Physiology*, *151*, 1790-1801. https://doi.org/10.1104/pp.109.146589

Kato, Y., Sun, X., Zhang, L., & Sakamoto, W. (2012). Cooperative 01 degradation in the photosystem II repair mediated by chloroplastic proteases in arabidopsis. *Plant Physiology*, *159*, 1428-1439. https://doi.org/10.1104/pp.112.199042

Kley, J., Heil, M., Muck, A., Svatos, A., & Boland, W. (2010). solating intact chloroplasts from small Arabidopsis samples for proteomic studies. *Analytical Biochemistry*, *398*, 198–202.

Kojima, K., Oshita, M., Nanjo, Y., Kasai, K., Tozawa, Y., Hayashi, H., & Nishiyama, Y. (2007). Oxidation of elongation factor G inhibits the synthesis of the D1 protein of photosystem II. *Molecular Microbiology*, *65*, 936-947. https://doi.org/10.1111/j.1365-2958.2007.05836.x

Kress, E., & Jahns, P. (2017). The dynamics of energy dissipation and xanthophyll conversion in arabidopsis indicate an indirect photoprotective role of zeaxanthin in slowly inducible and relaxing components of non-photochemical quenching of excitation energy. *Frontiers in Plant Science*, *8*, 2094. https://doi.org/10.3389/fpls.2017.02094

Kyhse-Andersen, J. (1984). Electroblotting of multiple gels - A simple apparatus without buffer tank for rapid transfer of proteins from polyacrylamide to nitrocellulose. *Journal of Biochemical and Biophysical Methods*, *10*, 203–209.

Laemmli, U. K. (1970). Cleavage of structural proteins during the assembly of the head of bacteriophage T4. *Nature*, *227*, 680–685. https://doi.org/10.1038/227680a0

Leitsch, J., Schnettger, B., Critchley, C., & Krause, G. H. (1994). Two mechanisms of recovery from photoinhibition in vivo: Reactivation of photosystem II related and unrelated to D1 protein turnover. *Planta*, *194*, 15–21. https://doi.org/10.1007/BF00201029

Mishra, Y., Johansson Jänkänpää, H., Kiss, A. Z., Funk, C., Schröder, W. P., & Jansson, S. (2012). Arabidopsis plants grown in the field and climate chambers significantly differ in leaf morphology and photosystem components. *BMC Plant Biology*, *12*, 6. https://doi.org/10.1186/1471-2229-12-6

Naranjo, B., Mignee, C., Krieger-Liszkay, A. Hornero-Mendez, 0., Gallardo-Guerrero, L., Cejudo, F. J., & Lindahl, M. (2016). The chloroplast NA0PH thioredoxin reductase C, NTRC, controls

non-photochemical quenching of light energy and photosynthetic electron transport in Arabidopsis. *Plant Cell and Environment*, *39*, 804-822.

Nilkens, M., Kress, E., Lambrev, P., Miloslavina, Y., Müller, M., Holzwarth, A. R., & Jahns, P. (2010). dentification of a slowly inducible zeaxanthin-dependent component of non-photochemical quenching of chlorophyll fluorescence generated under steady state conditions in *Arabidopsis*. *Biochimica Et Biophysica Acta*, *1797*, 466-475. https://doi.org/10.1016/j.bbabio.2010.01.001

Nishiyama, Y., Yamamoto, H., Allakhverdiev, S. ., naba, M., Yokota, A., & Murata, N. (2001). Oxidative stress inhibits the repair of photodamage to the photosynthetic machinery. *The EMBO Journal*, *20*, 5587–5594. https://doi.org/10.1093/emboj/20.20.5587

Niyogi, K. K., Grossman, A. R., & Björkman, O. (1998). Arabidopsis mutants define a central role for the xanthophyll cycle in the regulation of photosynthetic energy conversion. *The Plant Cell*, *10*.

Ohad, ., Kyle, 0. J., & Arntzen, C. J. (1984). Membrane-protein damage and repair - removal and replacement of inactivated 32-kilodalton polypeptides in chloroplast membranes. *Journal of Cell Biology*, *99*, 481-485. https://doi.org/10.1083/jcb.99.2.481

Öquist, G., & Huner, N. P. A. (2003). Photosynthesis of overwintering evergreen plants. *Annual Review of Plant Biology*, *54*, 329–355.

Pätsikkä, E., Kairavuo, M., Sersen, F., Aro, E.-M., & Tyystjärvi, E. (2002). Excess copper predisposes photosystem II to photoinhibition in vivo by outcompeting iron and causing decrease in leaf chlorophyll. *Plant Physiology*, *129*, 1359-1367. https://doi.org/10.1104/pp.004788

Pfündel, E. E., & 0illey, R. A. (1993). The pH dependence of violaxanthin deepoxidation in isolated pea chloroplasts. *Plant Physiology*, *101*, 65-71. https://doi.org/10.1104/pp.101.1.65

Quick, W. P., & Stitt, M. (1989). An examination of factors contributing to non-photochemical quenching of chlorophyll fluorescence in barley leaves. *Biochimica Et Biophysica Acta*, *977*, 287–296.

Reinhold, C., Niczyporuk, S., Beran, K. C., & Jahns, P. (2008). Short-term down-regulation of zeaxanthin epoxidation in *Arabidopsis thaliana* in response to photo-oxidative stress conditions. *Biochimica Et Biophysica Acta (BBA) - Bioenergetics*, *1777*, 462-469. https://doi.org/10.1016/j.bbabio.2008.03.002

Ruban, A. V., & Horton, P. (1999). The xanthophyll cycle modulates the kinetics of nonphotochemical energy dissipation in isolated light-harvesting complexes, intact chloroplasts, and leaves of spinach. *Plant Physiology*, *119*, 531-542. https://doi.org/10.1104/pp.119.2.531

Sacharz, J., Giovagnetti, V., Ungerer, P., Mastroianni, G., & Ruban, A. V. (2017). The xanthophyll cycle affects reversible interactions between PsbS and light-harvesting complex II to control non-photochemical quenching. *Nature Plants*, *3*, 16225. https://doi.org/10.1038/nplants.2016.225

Sarvikas, P., Hakala, M., Pätsikkä, E., Tyystjärvi, T., & Tyystjärvi, E. (2006). Action spectrum of photoinhibition in leaves of wild type and npq1-2 and npq4-1 mutants of Arabidopsis thaliana. *Plant and Cell Physiology*, *47*, 391-400. https://doi.org/10.1093/pcp/pcj006

Schaller, S., Wilhelm, C., Strzatka, K., & Goss, R. (2012). nvestigating the interaction between the violaxanthin cycle enzyme zeaxanthin epoxidase and the thylakoid membrane. *Journal of Photochemistry and Photobiology B-Biology*, *114*, 119–125. https://doi.org/10.1016/j.jphotobiol.2012.05.019

Schumann, T., Paul, S., Melzer, M., Dörmann, P., & Jahns, P. (2017). Plant growth under natural light conditions provides highly flexible short-term acclimation properties toward high light stress. *Frontiers in Plant Science*, *8*, 681. https://doi.org/10.3389/fpls.2017.00681

Schwarz, N., Armbruster, U., ven, T., Brückle, L., Melzer, M., Feussner, I., & Jahns, P. (2015). Tissue-specific accumulation and regulation of zeaxanthin epoxidase in arabidopsis reflect the multiple functions of the enzyme in plastids. *Plant and Cell Physiology*, *56*, 346-357. https://doi.org/10.1093/pcp/pcu167

Siefermann, 0., & Yamamoto, H. Y. (1975). Properties of NA0PH and oxygen-dependent zeaxanthin epoxidation in isolated chloroplasts. *Archives of Biochemistry and Biophysics*, *171*, 70–77.

Takizawa, K., Cruz, J. A., Kanazawa, A., & Kramer, 0. M. (2007). The thylakoid proton motive force in vivo. Quantitative, non-invasive probes, energetics, and regulatory consequences of light-induced pmf. *Biochimica Et Biophysica Acta-Bioenergetics*, *1767*, 1233-1244. https://doi.org/10.1016/j.bbabio.2007.07.006

Thiele, A., Krause, G. H., & Winter, K. (1998). *In situ* study of photoinhibition of photosynthesis and xanthophyll cycle activity in plants growing in natural gaps of the tropical forest. *Australian Journal of Plant Physiology*, *25*, 189–195. https://doi.org/10.1071/PP97119

Verhoeven, A. S., Adams, W. W. ., & 0emmig-Adams, B. (1996). Close relationship between the state of the xanthophyll cycle pigments and photosystem II efficiency during recovery from winter stress. *Physiologia Plantarum*, *96*, 567–576.

Walters, R. G., & Horton, P. (1991). Resolution of components of non-photochemical chlorophyll fluorescence quenching in barley leaves. *Photosynthesis Research*, *27*, 121–133.

Wood, W. H. J., MacGregor-Chatwin, C., Barnett, S. F. H., Mayneord, G. E., Huang, X., Hobbs, J. K., … Johnson, M. P. (2018). Dynamic thylakoid stacking regulates the balance between linear and cyclic photosynthetic electron transfer. *Nature Plants*, *4*, 116–127. https://doi.org/10.1038/s41477-017-0092-7

Xu, P., Tian, L., Kloz, M., & Croce, R. (2015). Molecular insights into Zeaxanthin-dependent quenching in higher plants. *Scientific Reports*, *5*(1), 13679. https://doi.org/10.1038/srep13679

Yamamoto, H. Y., Nakayama, T. O. M., & Chichester, C. O. (1962). Studies on the light and dark interconversions of leaf xanthophylls. *Archives of Biochemistry and Biophysics*, *97*, 168–173.

Yoshioka-Nishimura, M. (2016). Close relationships between the psii repair cycle and thylakoid membrane dynamics. *Plant and Cell Physiology*, *57*, 1115–1122. https://doi.org/10.1093/pcp/pcw050

SUPPORTING INFORMATION

Additional supporting information may be found online in the Supporting Information section.

How to cite this article: Bethmann S, Melzer M, Schwarz N, Jahns P. The zeaxanthin epoxidase is degraded along with the D1 protein during photoinhibition of photosystem II. *Plant Direct*. 2019;3:1–13. https://doi.org/10.1002/pld3.185

Figure S1

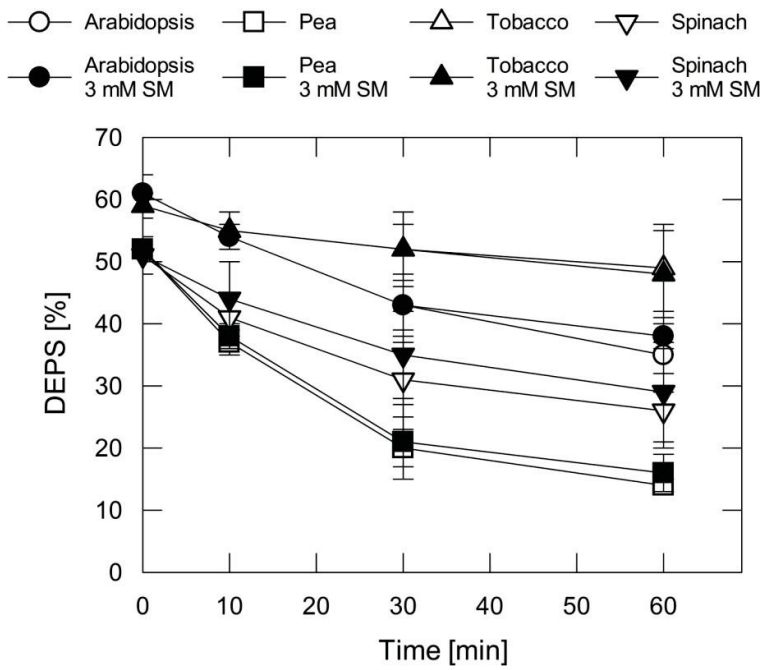

Figure S1. Impact of streptomycin on ZEP activity in isolated thylakoids. Thylakoid membranes were isolated from dark-adapted leaves pre-illuminated for 2 h at 1000 µmol photons m^{-2} s^{-1}. Thylakoid membranes equivalent to 100 µg Chl were suspended in epoxidation medium and gently stirred at room temperature and in the dark for up to 60 min. When indicated, 3 mM streptomycin (SM) was added. At indicated time, aliquots equivalent to 20 µg Chl were removed, and the de-epoxidation state (DEPS = (Zx+0.5Ax)/(Vx+Ax+Zx) x 100) of the xanthophyll cycle pigments was determined by HPLC analysis. Data represent mean values ± SD from 3 independent measurements.

Figure S2

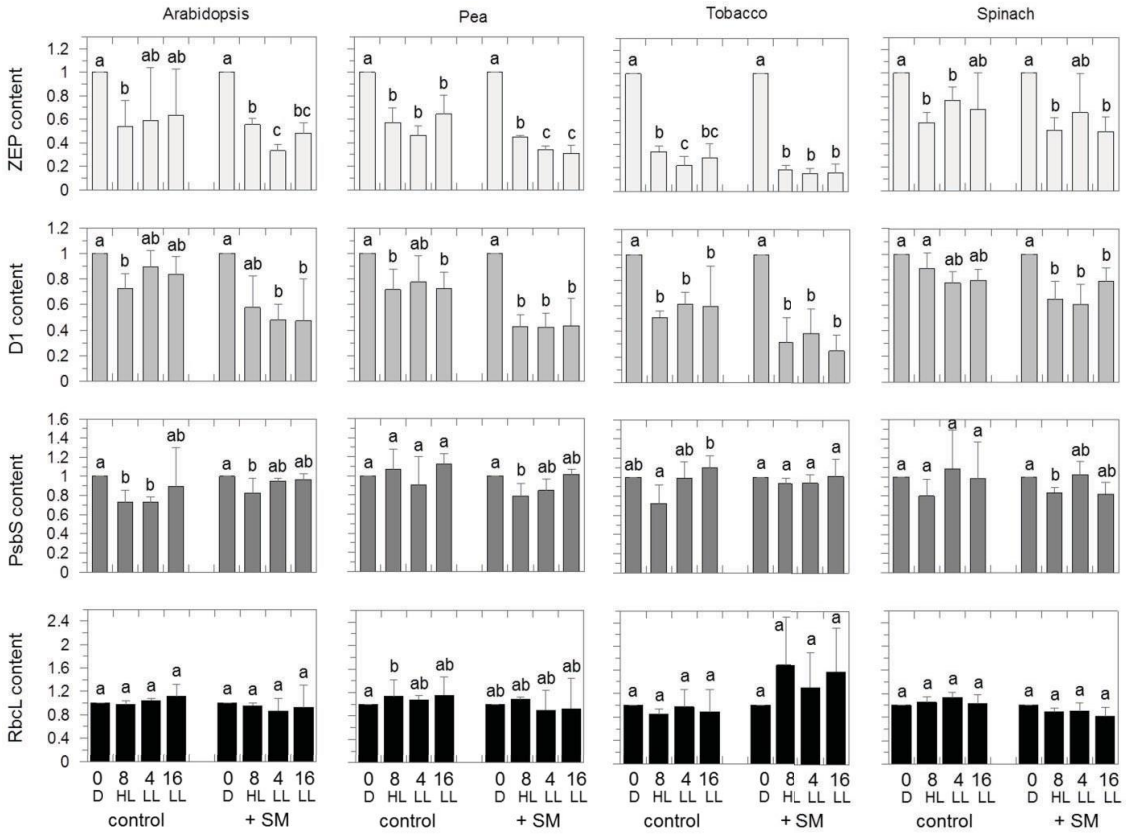

Figure S2. Quantification of HL-induced changes of the protein content. The relative abundance of ZEP, D1, RbcL and PsbS was estimated from immunoblot analyses with specific antibodies (representative blots are shown in Fig. 4). Signal quantification was carried out using the program ImageStudioLite. The signal intensities within each experiment (dark control (0, D); end of 8 hl HL (8, HL), and after additional LL recovery for 4 h (12, LL) and 12 h (24, LL)) are shown in relation to the control samples before onset of HL illumination (0, D), which were normalized to 1 in each case. Mean values (± SD) derived from 3 independent experiments (n = 3) are shown. Significant HL-induced differences in the abundance of the respective proteins (student's t-test, $p < 0.05$) are indicated for each species.

Figure S3

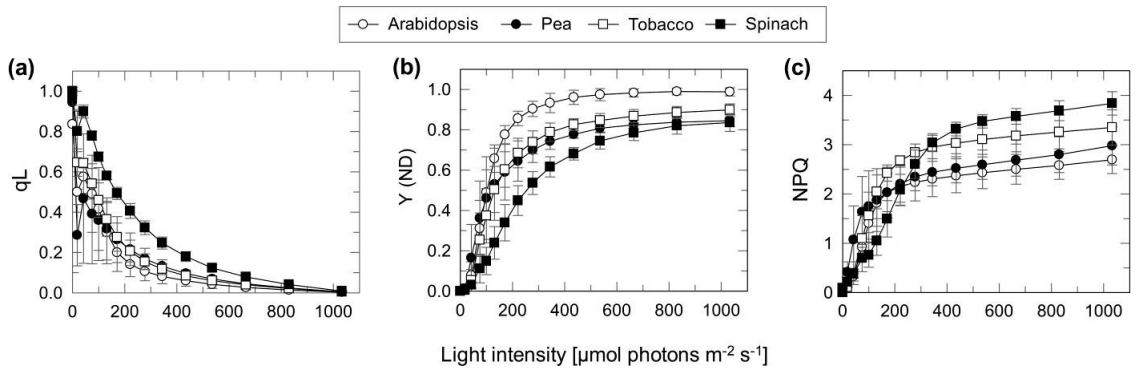

Figure S3. Light dependence of light utilization. The light response of the redox state of the plastoquinone pool (a), of the redox state of the PSI donor side (b) and of energy dissipation (c) was determined with the DUAL PAM 101 fluorometer. Before each measurement, plants were dark-acclimated for 2 h. Light response curves were measured from the lowest to the highest light intensity and leaves were acclimated to each light intensity for 2 min. Mean values ± SD of 4 independent measurements are shown.

7. Manuscript 2

The impact of light-acclimation on the regulation of zeaxanthin epoxidase in different plant species

Stephanie Bethmann, Ann-Kathrin Haas, Michael Melzer, Peter Jahns

Status: to be submitted

Contributions:

S.B., M.M. and P.J. designed the research; S.B. and A.K.H. performed the experiments; S.B. and A.K.H performed the short-term light induction experiments; A.K.H. performed the chlorophyll fluorescence measurements and protein analysis; S.B. and A.K.H. contributed to pigment analysis and statistical analysis; S.B. and M.M. analyzed data; S.B. and P.J. wrote the original draft; S.B., A.K.H, M.M. and P.J. reviewed and edited the manuscript.

The impact of long-term acclimation to different growth light intensities on the regulation of zeaxanthin epoxidase in different plant species

Stephanie Bethmann[1], Ann-Kathrin Haas[1], Michael Melzer[2] and Peter Jahns[1*]

[1]Photosynthesis and Stress Physiology of Plants, Heinrich-Heine-University Düsseldorf, 40225 Düsseldorf, Germany
[2]Leibniz Institute of Plant Genetics and Crop Plant Research (IPK), Gatersleben, Germany

*Corresponding author: E-mail, pjahns@hhu.de; Fax, +49-211-8113706

Abstract

Proper short- and long-term acclimation to different growth light intensities is essential for the survival and competitiveness of plants in the field. In particular, long-lasting or fluctuating high light conditions are challenging for plants due to the high level of photo-oxidative stress emerging from such conditions along with formation of ROS. High light exposure is known to induce the down-regulation and photoinhibition of photosystem II (PSII) activity to reduce ROS formation. The xanthophyll zeaxanthin (Zx) has been shown to serve central photoprotective functions in these processes. We have shown in recent work with different plant species (Arabidopsis, tobacco, spinach and pea) that photoinhibition of PSII and degradation of the PSII reaction center protein D1 is accompanied by the inactivation and degradation of zeaxanthin epoxidase (ZEP). ZEP catalyzes the reconversion of Zx to violaxanthin. Hence, inhibition of ZEP results in the retention of high Zx levels in the thylakoid membrane, supporting an important photoprotective function of Zx along with photoinhibition and repair of PSII. Different high light sensitivity of the above-mentioned species correlated with differential down-regulation of both PSII and ZEP activity. Here, we investigated the acclimation properties of these species to different growth light intensities with respect to the ability to adjust photoprotective strategies. We show that the species differ in the phenotypic plasticity in response to short- and long-term high light conditions at different morphological and physiological levels. However, the close co-regulation of PSII and ZEP activity remains a common feature in all species and under all conditions.

Keywords: Licht acclimation, Photo-oxidative stress, Photoprotection, Reactive oxygen species, Xanthophyll cycle, Zeaxanthin epoxidase

Introduction

Light energy is not only the ultimate energy source of photosynthetic organisms, but carries also a high damaging potential. Whenever the amount of absorbed light energy exceeds the levels that can be utilized for photosynthesis, the probability of the formation of reactive oxygen species (ROS) and thus the risk of photo-oxidative damage increases (Moller et al. 2007; Niyogi 1999). Therefore, photosynthetic organisms must be able not only to utilize efficiently low light intensities, but also to avoid photo-oxidative damage at high light intensities. Hence, proper short- and long-term acclimation to different light intensities is essential for the competitiveness of plants in the field.

Acclimation to rapidly changing light intensities particularly involves the regulation of photoprotective energy dissipation mechanisms, known as non-photochemical quenching (NPQ) of excitation energy. In the short-term (few minutes), the pH-dependent quenching mechanism of NPQ, qE, serves as important regulator providing the capacity to rapidly switch the antenna of photosystem II between a light-harvesting (at low light, LL) to a dissipative (at high light, HL) state (Horton et al. 1996; Ruban et al. 2012). The thylakoid lumen pH, which is a direct measure of the saturation of photosynthetic electron transport, acts as key regulator of qE and activates both the PsbS protein and zeaxanthin (Zx) synthesis at pH < 6.0. Since the quenching of excitation energy via the qE mechanism is in direct competition to photosynthesis, it is essential to deactivate qE rapidly upon a shift form high to low light. In particular the reconversion of Zx to violaxanthin (Vx) is known to limit the kinetics of the deactivation of qE (Ruban and Horton 1999; Ruban and Johnson 2010). Consequently, over-expression of ZEP has been successfully applied to accelerate qE relaxation under fluctuating light in tobacco (Kromdijk et al. 2016) and Arabidopsis (Garcia-Molina and Leister 2020) plants. Long-lasting HL stress is known to induce photoinhibition of PSII (Krause 1988; Powles 1984). Photoinhibition is based on the irreversible damage of the PSII reaction center protein D1. Recovery from photoinhibition requires the degradation of damaged D1 followed by the resynthesis of D1 and reassembly of functional PSII (Aro et al. 1993). Photoinhibition of PSII and degradation of D1 has recently been shown to be accompanied by down-regulation of ZEP activity and degradation of ZEP protein, respectively (Bethmann et al. 2019). The physiological importance of down-regulation of ZEP activity alongside with photoinhibition is to maintain high levels of Zx in response to long-lasting HL stress, supporting an important photoprotective role of Zx during photoinhibition of PSII (Bethmann et al. 2019). The parallel degradation of D1 and ZEP further indicates that Zx is particularly required during the PSII repair cycle (Bethmann et al. 2019). These characteristics support an important role of Zx for short-term acclimation of plants to HL at time scales from minutes to hours.

Long-term (days to weeks) acclimation to different growth light conditions occurs at a wide range of levels and particularly involves adjustments of leaf architecture, the chloroplast structure, and the regulation of photosynthetic light utilization (Anderson 1986; Boardman 1977; Schoettler and Toth 2014; Schumann et al. 2017). Typical acclimation responses to increasing growth light intensities include e.g. increased leaf thickness, reduced width of grana stacks, higher chlorophyll (Chl) a/b ratios, higher CO_2 assimilation rates and higher photoprotective capacity (Boardman 1977; Brugnoli et al. 1994; Lichtenthaler et al. 1981; Park et al. 1996; Schumann et al. 2017). With respect to photoprotection, plant acclimation to increasing growth light intensities is accompanied by an increasing NPQ capacity (Bailey

et al. 2001; Schumann et al. 2017), in particular the capacity of qE quenching. An increase of the qE capacity during long-term acclimation to HL conditions is accompanied by a reduction of photoinhibition of photosynthesis, supporting the photoprotective function of this NPQ mechanism. The qE capacity is predominantly regulated by the amount of the PsbS protein (Li et al. 2000; Li et al. 2002) and the amount of Zx (Kalituho et al. 2007; Nilkens et al. 2010; Niyogi et al. 1998). Long-term acclimation of Arabidopsis to HL has been shown to be accompanied by increased amounts of PsbS protein (Schumann et al. 2017). The amount of Zx that can be generated in the thylakoid membrane is mainly determined by the total pool size of the xanthophyll cycle pigments (VAZ pool = sum of violaxanthin (Vx), antheraxanthin (Ax) and Zx). Indeed, an increase of the VAZ pool size in response to increasing growth light intensities has also been shown in several studies (Bailey et al. 2004; Demmig-Adams et al. 2012; Mishra et al. 2012; Schumann et al. 2017). In contrast to the PsbS protein, however, the photoprotective role of Zx is not only limited to the qE mechanism of NPQ. Zx also contributes to the more slowly (min to hours) developing and relaxing components of NPQ, qZ and qI (Nilkens et al. 2010) and further acts as antioxidant in the thylakoid membrane (Havaux et al. 2007; Havaux and Niyogi 1999). These additional functions are particularly important for photoprotection under long-term HL stress conditions, under which pronounced photoinhibition of photosynthesis and hence PSII occur. Hence, an increase of the VAZ pool size in response to increasing HL stress during growth provides the basis for the accumulation of higher amounts of Zx under photoinhibitory light conditions. Moreover, the long-term retention of high levels of Zx under photoinhibitory conditions is further ensured by the down-regulation of ZEP activity alongside with long-lasting photoinhibition (Bethmann et al. 2019; Reinhold et al. 2008). This down-regulated of ZEP activity is likely also the basis for the long-term retention of Zx under *in vivo* conditions described for evergreen plants under severe winter stress conditions (Adams et al. 2002; Adams et al. 1995; Adams et al. 2004; Öquist and Huner 2003).

The varying capacities of different species to cope with HL stress is determined by complex traits deriving from different morphological and physiological properties, including photosynthetic light utilization and photoprotective capacities. In a recent comparative study on four different species (*Arabidopsis thaliana, Nicotiana benthamiana, Pisum sativum, Spinacia oleracea)*, we have shown that Arabidopsis and tobacco plants are more sensitive to short-term HL stress than pea and spinach plants (Bethmann et al. 2019). These different HL sensitivities were found to be not simply related to different properties of photosynthetic light utilization. Instead, this work provided evidence that the VAZ pool size and thus the amount of Zx formed in HL might be a critical determinant for different HL sensitivity (Bethmann et al. 2019). To gain further insights into the importance of the VAZ pool and of the regulation of the xanthophyll cycle for the HL sensitivity, we characterized the long-term acclimation of the four plant species to three different growth light conditions: low light (LL, about 20 µmol photons m^{-2} s^{-1}), normal light (NL, about 100 µmol photons m^{-2} s^{-1}) and high light (HL, about 500 µmol photons m^{-2} s^{-1}).

Material and methods

Plant material

For this work Arabidopsis (*Arabidopsis thaliana*, ecotype Col-0), spinach (*Spinacia oleraceae*), pea (*Pisum sativum*, cv. Kleine Rheinländerin) and tobacco (*Nicotiana benthamiana*) plants were used. The

germination of Arabidopsis, spinach and pea plants proceeded under short-day conditions (8 h light/ 16 h dark) in the greenhouse at light intensities of 100 µmol photons $m^{-2}s^{-1}$ and at temperatures between 20 and 25 °C. Tobacco plants germinated under long-day conditions (16 h light/ 8 h dark) in the greenhouse at light intensities of 100 µmol photons $m^{-2}s^{-1}$ and at temperatures between 20 and 25°C. Pea plants were transferred to LL (~ 20 µmol photons $m^{-2}s^{-1}$), NL (~ 100 µmol photons $m^{-2}s^{-1}$) and HL (~ 500 µmol photons $m^{-2}s^{-1}$) directly after germination while Arabidopsis, spinach and tobacco seedlings were transferred to these light conditions 2-3 weeks after germination. LL plants and NL plants from tobacco were grown at long-day conditions at temperatures between 20 and 25°C, while Arabidopsis, spinach and pea NL plants and HL plants were grown at short-day conditions at temperatures between 20 and 25°C. 2-3 weeks old pea plants and 6-8 weeks old Arabidopsis, spinach and tobacco plants were used for the experiments. Plants were dark-adapted overnight prior to the experiments.

Determination of PSII activity

Leaf disks (1 cm diameter) were placed on water on a temperature-controlled cuvette (20 °C) and exposed to HL (2000 µmol photons $m^{-2}s^{-1}$) for up to 8 h. Subsequent to HL treatment, leaf disks were transferred to LL (~ 10-20 µmol photons $m^{-2}s^{-1}$) for another 16 h. At specific times, leaf disks were incubated in darkness for 5 min and the F_v/F_m-ratio was determined with a Dual-PAM 100 (Heinz Walz GmbH, Effeltrich, Germany). Leaf disks were frozen in liquid N_2 and stored at -20°C for pigment and protein extraction, respectively.

Light and transmission electron microscopy

Leaf disks (1 cm diameter) were placed on water on a temperature-controlled cuvette (20°C) and exposed to HL (2000 µmol photons $m^{-2}s^{-1}$) for up to 8 h. The central part of the leaf disks was cut into 2 mm^2 pieces for structural analysis. The combined conventional and microwave-assisted fixation, substitution, resin embedding, sectioning and microscopical analysis as described in (Schumann et al. 2017) was performed using 3-4 leaf disks for each plant species and each treatment.

Light response curves

The Chl fluorescence was measured with the DUAL-PAM 100 fluorimeter (Heinz Walz GmbH, Effeltrich, Germany). Leaf disks were illuminated at light intensities from 28 µmol photons $m^{-2}s^{-1}$ to 1209 µmol photons $m^{-2}s^{-1}$ whereby the light intensity has been increased at intervals of 2 min. Saturation pulses (400 ms, 6,000 µmol photons $m^{-2}s^{-1}$) were applied at intervals of 2 min to determine NPQ as (F_m/F_m' – 1) (Krause and Jahns 2004). qL has been determined as $(F_m' - F)/(F_m' – F'_0) \times F'_0/F$ according to (Kramer et al. 2004).

Protein extraction and immunoblot analyses

For protein extraction, 3 leaf disks were ground in an Eppendorf vial (1,000 rpm, Heidolph RZR 2051) with protein extraction buffer (1.6 % SDS (w/v), 50 mM Tris/HCl, pH 7.6). Protein extracts were incubated at 70 °C for 20 min and subsequently non-soluble material was pelleted by centrifugation at 13,000 g

for 20 min. Protein concentrations were determined using the Bio-Rad® DC Protein Assay (Bio-Rad) according to the instruction manual.

For immunoblot analysis, proteins were initially separated by SDS-PAGE after (Laemmli 1970). Thereafter, the transfer of the proteins onto a PVDF membrane (FluoroTrans®W PVDF 0.2 µm, Pall Life Sciences) in a semi-dry blot chamber (Power Blotter, Thermo Scientific) was executed applying the 3-buffer system as described by (Kyhse-Andersen 1984). The primary antibody was incubated either overnight at 4°C or for 1 h at room temperature (RT). The incubation of the secondary anti-rabbit-IgG antibody (Sigma-Aldrich) occurred for 1 h at RT. The visualization of the secondary antibody by chemiluminescence (Millipore Corporation, Billerica, USA) was carried out with the LAS-4000 mini (GE Healthcare). The following polyclonal primary antibodies were used: anti-AtZEP and anti-NpZEP (commissioned work, Pineda Antibody), anti-D1 (AS05084) and anti-RbcL (AS03037) (Agrisera Antibodies).

Pigment analyses

The xanthophyll content was determined by HPLC analysis of the pigment content according to (Färber et al. 1997). Frozen leaf disks were ground in an Eppendorf vial (1,000 rpm, Heidolph RZT 2051) upon addition of 100 % acetone. Samples were centrifuged for 5 min at 17,000 g (4°C). The pigment extracts were filtered (0.2 µm pore size) and finally used for reversed-phase HPLC according to (Färber et al. 1997).

Statistical analyses

All statistical analyses of this work were performed using R studio (version 1.2.1335, Boston, USA). ANOVA was used to determine significant differences among genotypes. Variance homogeneity was tested by a Levene test. Multiple comparison analysis was performed by using the post hoc test (Tukey HSD). Significant differences ($p < 0.05$) were marked by different letters.

Results

Leaf morphology and thylakoid membrane organization

The morphology of leaves and chloroplasts was determined by light and electron microscopy. Light microscopic analysis of leaf cross-sections (supplementary Fig. S1) revealed that the four species showed different light acclimation responses at the level of leaf thickness (Fig. 1). When comparing LL and NL plants (Fig. 1A), only leaves from spinach and tobacco plants showed significantly thicker leaves in the NL acclimated state, while Arabidopsis and pea plants developed only slightly, but not significantly thicker leaves in the NL acclimated state. When comparing NL and HL plants, significantly increased leaf thickness in HL plants was determined for Arabidopsis and spinach plants, but not for pea and tobacco plants. For tobacco plants, even a significant reduction of leaf thickness close to the value of LL plants was observed (Fig. 1A).

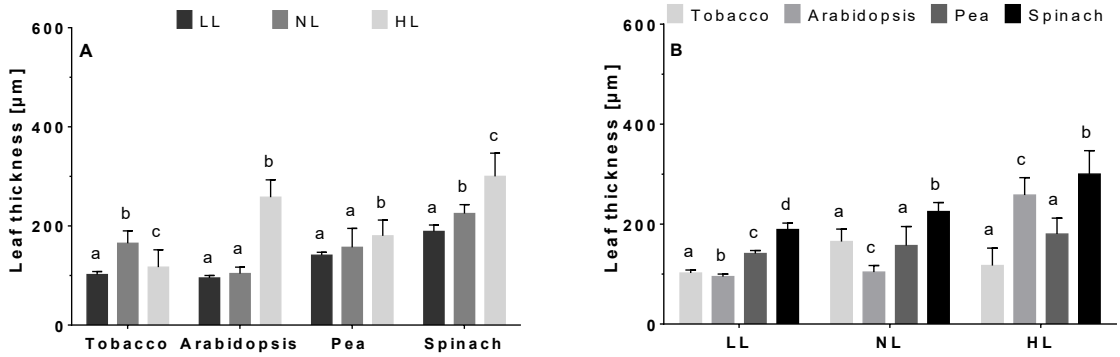

Figure 1. Changes in leaf thickness. Leaf thickness was determined from light microscopic images of leaf cross-sections. **A**, Comparison of growth conditions. **B**. Comparison of species. Data represent mean values ± SD from 13-64 images. Letters indicate significant differences (One-Way Anova $p < 0.05$).

When comparing the leaf thickness of different species (Fig. 1B), significant differences were found for each acclimation state. For LL plants, Arabidopsis and tobacco showed the lowest leaf thickness, whereas spinach developed the thickest leaves, and pea showed intermediate values. For NL plants, thickest leaves were again found for pea, intermediate values for pea and tobacco, and again thinnest leaves for Arabidopsis. In the HL acclimated state, Arabidopsis plants developed thicker leaves than pea and tobacco, while thickest leaves were again detectable for spinach leaves. In conclusion, all species showed in general the typical increase acclimation response at the level of leaf thickness with increasing leaf thickness upon acclimation to higher light intensities (except for the HL acclimated tobacco plants), but each species showed individual relative changes.

Chloroplast and thylakoid membrane structure

The structure of chloroplasts did not reveal a clear general trend of changes in response to different growth light intensities, and did not show pronounced differences among the species (Fig. 2A-D). In tobacco and Arabidopsis plants, the height of chloroplasts reached maximum values in NL grown plants, whereas pea plants showed decreasing chloroplast height and spinach plants increasing chloroplast

height with increasing growth light intensities (Fig. 2A). Comparing the chloroplast height among the different species, similar values were determined for all species in LL grown plants. Under NL and HL conditions, pea chloroplast showed the lowest height, whereas tobacco and spinach exhibited the highest chloroplasts. (Fig. 2B). For the width of chloroplasts, no clear trend was detectable in response to different growth light intensities (Fig. 2C). Tobacco and pea plants showed narrowest chloroplasts under LL conditions. Arabidopsis under NL conditions, and no significant differences in response to the growth light intensity was found for spinach. When comparing the chloroplast width of the different species, no pronounced differences were detectable for NL and HL plants, whereas clearly narrower chloroplasts were visible in LL grown plants from tobacco and pea plants, when compared to Arabidopsis and spinach (Fig. 2D).

With respect to thylakoid membrane structure, no clear general trend for changes in the height of grana stacks in response to different growth light intensities were detectable (Fig. 2E). Comparison of the different species, however, revealed that pea plants contain the highest grana stacks under all growth light conditions, whereas lowest height of grana were determined for Arabidopsis plants, and intermediate values for spinach and tobacco plants (Fig. 2F). In contrast, grana width showed a clear trend of reduction of the grana width with increasing growth light intensities (Fig. 2G). Moreover, grana width was smaller in spinach and tobacco plants under all growth light conditions when compared to Arabidopsis and pea, although significant differences were not given in all cases due to the quite large standard deviations (Fig. 2H). Hence, the width of grana is the only morphological parameter at the level of chloroplasts which showed a clear trend of acclimation response to different growth light intensities in all species.

Light utilization properties

The properties of photosynthetic light utilization were analyzed by light response curves measured with a DUAL PAM 101 fluorometer. The reduction of the plastoquinone (PQ) pool (qL) and P700 (Y(ND)) was used as indicator of saturation of photosynthetic electron transport and the NPQ as a measure of energy dissipation (Table 1).

The light dependence of these parameters was evaluated by the light intensity LI_{50}, at which the half-maximum value of each parameter was reached. The LI_{50} values thus represent a measure for the half-saturation of electron transport (qL and Y(ND)) and energy dissipation (NPQ). As expected, an increase of the LI_{50} values were found for all species with increasing growth light intensity, supporting the acclimation of photosynthetic light utilization in response to growth light conditions. Reduction of the PQ pool required (significantly) higher light intensities in HL acclimated plants of Arabidopsis and tobacco than in NL plants, whereas LL plants showed only slightly lower LI_{50} values than NL plants (Table 1). In contrast, pea and spinach plants showed a pronounced increase of LI_{50} values for qL in NL plants compared to LL plants, whereas LI_{50} values of HL acclimated plants were only slightly increased compared to NL plants.

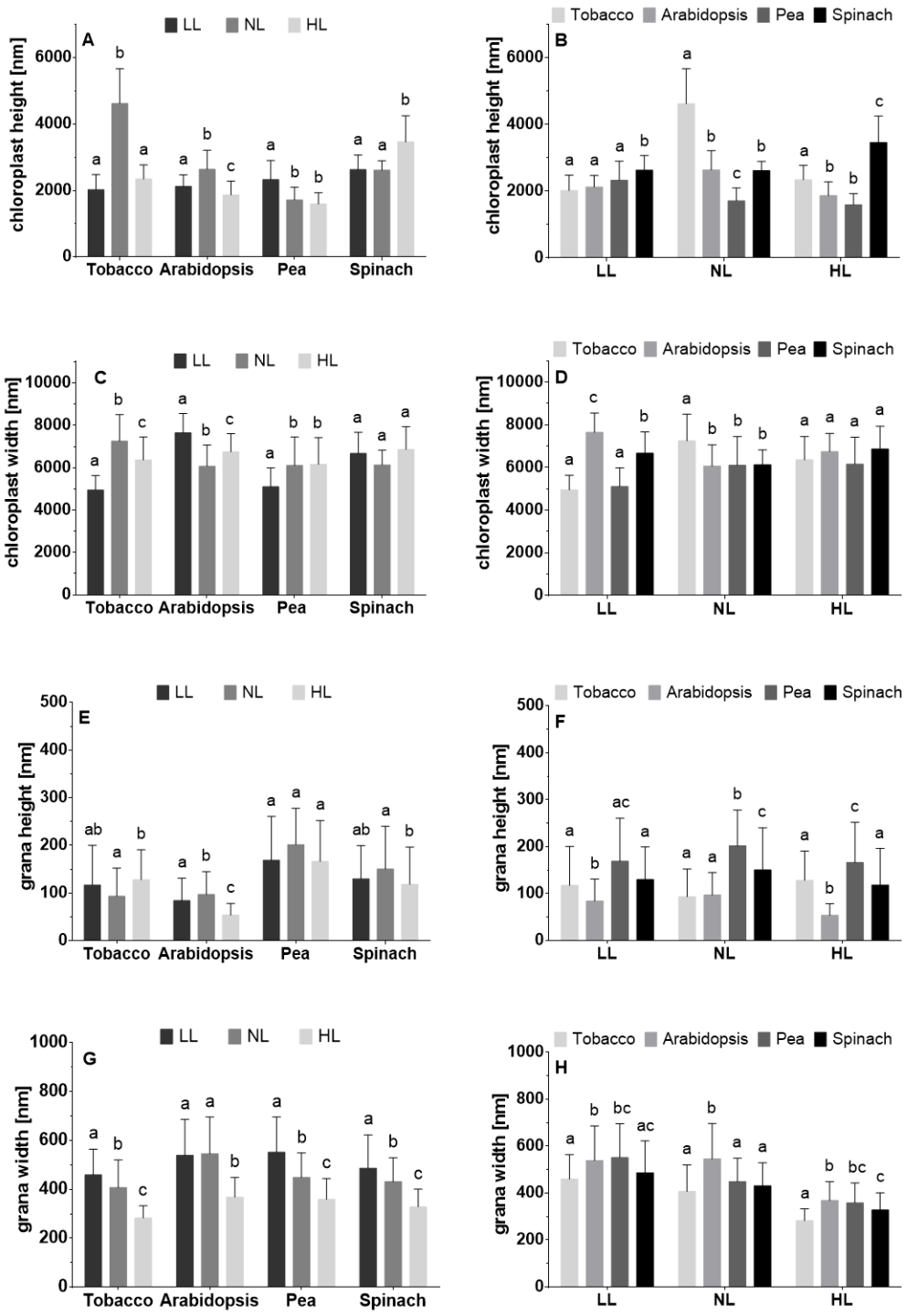

Figure 2. Chloroplast and thylakoid membrane structure. Chloroplast size (**A-D**) and grana size (**E-H**) were quantified from electron microscopic images. Panels on the left-hand side (A,C,E,G) show comparison of the growth conditions for each species, panels on the right-hand side (B,D,F,H) show differences among the species for each growth condition. Data represent mean values ± SD from 6-35 images. Letters indicate significant differences (One-Way Anova, $p < 0.05$).

The same general trend was observable for the LI_{50} values of Y(ND) and NPQ, except for the very low value for HL acclimated spinach plants (Table 1). Obviously, NL plants of Arabidopsis and tobacco plants show at the level of light utilization rather properties of LL plants, while NL plants from pea and spinach plants are more similar to HL plants. Moreover, the LI_{50} values for Y(ND) and NPQ were in most cases very similar in each species, but always higher than the LI_{50} values for qL, indicating that reduction of the PSII acceptor side occurs at lower light intensities as the oxidation of the PSI donor side and NPQ induction.

Table 1: Light utilization properties. The light dependence of different light utilization parameters was determined from light response curves measured with the DUAL-PAM 100 fluorimeter. Mean values ± SD from 8 independent measurements are shown. Significant differences among the species are indicated by upper case letters, differences among growth conditions by lower case letters.

Parameter	Growth light	Tobacco	Arabidopsis	Pea	Spinach
qL LI_{50}	LL	$28.1 \pm 20.7^{AB,a}$	$45.8 \pm 10.6^{B,a}$	$44.5 \pm 35.8^{A,a}$	$47.3 \pm 19.0^{B,a}$
	NL	$101.5 \pm 21.2^{A,b}$	$61.9 \pm 36.2^{A,a}$	$99.6 \pm 56.5^{A,b}$	$111.8 \pm 65.9^{A,b}$
	HL	$95.3 \pm 24.6^{A,b}$	$141.4 \pm 45.6^{A,b}$	$113.1 \pm 25.8^{A,b}$	$111.1 \pm 35.5^{A,b}$
Y(ND) LI_{50}	LL	$54.4 \pm 17.1^{A,a}$	$75.0 \pm 0.0^{A,a}$	$66.8 \pm 16.5^{A,a}$	$65.8 \pm 21.4^{A,a}$
	NL	$125.1 \pm 27.8^{A,b}$	$96.9 \pm 8.8^{A,a}$	$106.8 \pm 62.2^{A,a}$	$155.1 \pm 78.3^{A,b}$
	HL	$101.5 \pm 31.3^{A,b}$	$229.0 \pm 34.9^{B,b}$	$111.0 \pm 49.7^{A,a}$	$48.5 \pm 31.5^{C,a}$
NPQ LI_{50}	LL	$65.8 \pm 21.4^{AB,a}$	$87.5. \pm 13.4^{B,a}$	$42.0 \pm 0.0^{A,a}$	$25.8 \pm 33.4^{AB,a}$
	NL	$119.3 \pm 38.3^{A,ab}$	$96.9 \pm 8.8^{A,a}$	$89.5 \pm 58.8^{A,a}$	$160.3 \pm 97.6^{A,b}$
	HL	$150.1 \pm 78.4^{AB,b}$	$205.9 \pm 42.8^{AB,b}$	$115.3 \pm 76.6^{A,a}$	$226.0 \pm 91.3^{B,b}$
NPQ_{max}	LL	$2.1 \pm 0.2^{AC,a}$	$1.8 \pm 0.1^{B,a}$	$2.0 \pm 0.2^{AB,a}$	$2.3 \pm 0.1^{C,a}$
	NL	$3.4 \pm 0.3^{A,b}$	$2.6 \pm 0.3^{B,b}$	$3.2 \pm 0.5^{AB,b}$	$3.2 \pm 0.7^{AB,b}$
	HL	$4.3 \pm 0.6^{A,c}$	$2.6 \pm 0.4^{B,b}$	$3.1 \pm 0.5^{B,b}$	$2.9 \pm 0.2^{B,b}$
qE_{max}	LL	$1.3 \pm 0.3^{A,a}$	$1.2 \pm 0.1^{A,a}$	$1.6 \pm 0.2^{B,a}$	$1.8 \pm 0.1^{B,a}$
	NL	$3.0 \pm 0.3^{A,b}$	$2.1 \pm 0.4^{B,b}$	$2.8 \pm 0.4^{A,b}$	$2.7 \pm 0.7^{AB,b}$
	HL	$2.9 \pm 0.7^{A,b}$	$2.3 \pm 0.4^{AB,b}$	$2.8 \pm 0.5^{AB,b}$	$2.2 \pm 0.3^{B,ab}$
$(qZ+qI)_{max}$	LL	$0.8 \pm 0.2^{A,a}$	$0.6 \pm 0.1^{B,a}$	$0.4\pm 0.1^{C,a}$	$0.5 \pm 0.1^{BC,ab}$
	NL	$0.5 \pm 0.0^{A,a}$	$0.5 \pm 0.1^{A,a}$	$0.5 \pm 0.1^{A,a}$	$0.5 \pm 0.1^{A,a}$
	HL	$1.4 \pm 0.7^{A,b}$	$0.3 \pm 0.1^{B,b}$	$0.3 \pm 0.1^{B,a}$	$0.7 \pm 0.3^{B,b}$

Pigment composition

The total amount of Chl (a+b) per leaf area did not alter significantly in response to different growth light conditions in Arabidopsis, pea and spinach plants (Table 2). Only in tobacco plants, HL plants showed a significant reduction of the Chl content compared to LL plants. Comparing the different species, highest amounts of Chl per leaf area were found for spinach and pea plants and significantly lower amounts for Arabidopsis and tobacco (Table 2).

The Chl a/b ratio did not show significant differences when comparing LL and NL plants in all species, whereas a significant increase in response to HL conditions was found in Arabidopsis, pea and spinach, but not in tobacco plants (Table 2). Comparing the different species, no significant differences were found between tobacco, Arabidopsis and spinach plants under all growth conditions. Only pea plants showed a significant lower Chl a/b ratio than all other species under LL conditions. Under NL conditions, the Chl a/b ratio of pea plants was significantly lower only in comparison with tobacco plants. In conclusion, all species showed a similar acclimation to different growth light conditions with respect to Chl accumulation, except for HL acclimated tobacco plants.

Table 2: Chlorophyll content. The content of Chl a and Chl b was determined from HPLC analyses of the pigment content of leaves. Mean values ± SD from xy independent measurements are shown. Significant differences among the species are indicated by upper case letters, differences among growth conditions by lower case letters.

Species	Chl (a+b) per cm^2 leaf area				Chl a/b ratio		
	LL	NL	HL		LL	NL	HL
Tobacco	$25 \pm 4^{B,a}$	$22 \pm 10^{C,ab}$	$16 \pm 7^{B,b}$		$3.25 \pm 0.19^{B,a}$	$3.47 \pm 0.20^{B,a}$	$3.67 \pm 0.76^{A,a}$
Arabidopsis	$27 \pm 11^{B,a}$	$27 \pm 11^{BC,a}$	$28 \pm 5^{C,a}$		$3.22 \pm 0.23^{B,a}$	$3.38 \pm 0.33^{AB,a}$	$4.07 \pm 0.30^{A,b}$
Pea	$51 \pm 11^{A,a}$	$50 \pm 8^{A,a}$	$43 \pm 7^{A,a}$		$2.86 \pm 0.29^{A,a}$	$3.08 \pm 0.11^{A,a}$	$3.65 \pm 0.33^{A,b}$
Spinach	$41 \pm 8^{A,a}$	$40 \pm 12^{AB,a}$	$42 \pm 11^{A,a}$		$3.28 \pm 0.26^{B,a}$	$3.30 \pm 0.23^{AB,a}$	$3.77 \pm 0.42^{A,b}$

The amount of the xanthophyll cycle pigments (= VAZ pool size) in relation to total Chl was similar in LL and NL plants in all species (Fig. 3A and B). Compared to LL and NL plants, a significant and about 1.5fold increase of the VAZ pool size was determined for HL acclimated plants of Arabidopsis, pea and spinach, whereas a 2 to 4fold increase was observed for tobacco. Comparing the different species, Arabidopsis plants showed the lowest VAZ pool size under all growth conditions, whereas about 1.5fold and 2fold higher values were found for pea and spinach plants, respectively. Tobacco plants exhibited by far the highest VAZ pool size in HL acclimated plants, but the second lowest pool size in LL plants (Fig. 3A and B). In conclusion, all plant species showed the typical HL acclimation response at the level of the VAZ pool size, but overall VAZ pool sizes and relative changes differed among the species.

The ratio of VAZ pigments per lutein (Lut) was determined to estimate the amount and changes of the VAZ pool size per antenna protein (Fig. 3C and D). No significant changes were detectable for all species when comparing LL and NL plants. In contrast, a significant increase of the VAZ / Lut ratio was found for all species in HL plant compared to LL and NL plants. Spinach plants showed the smallest increase (about 15 %) followed by pea (about 40%) and Arabidopsis (about 65%), whereas tobacco plants showed the by far largest increase (about 130%). When comparing the different species, significantly higher VAZ / Lut ratios were found for spinach under LL and NL conditions, indicating that a fraction of VAZ pigments might be not bound to antenna proteins in spinach even under LL and NL conditions.

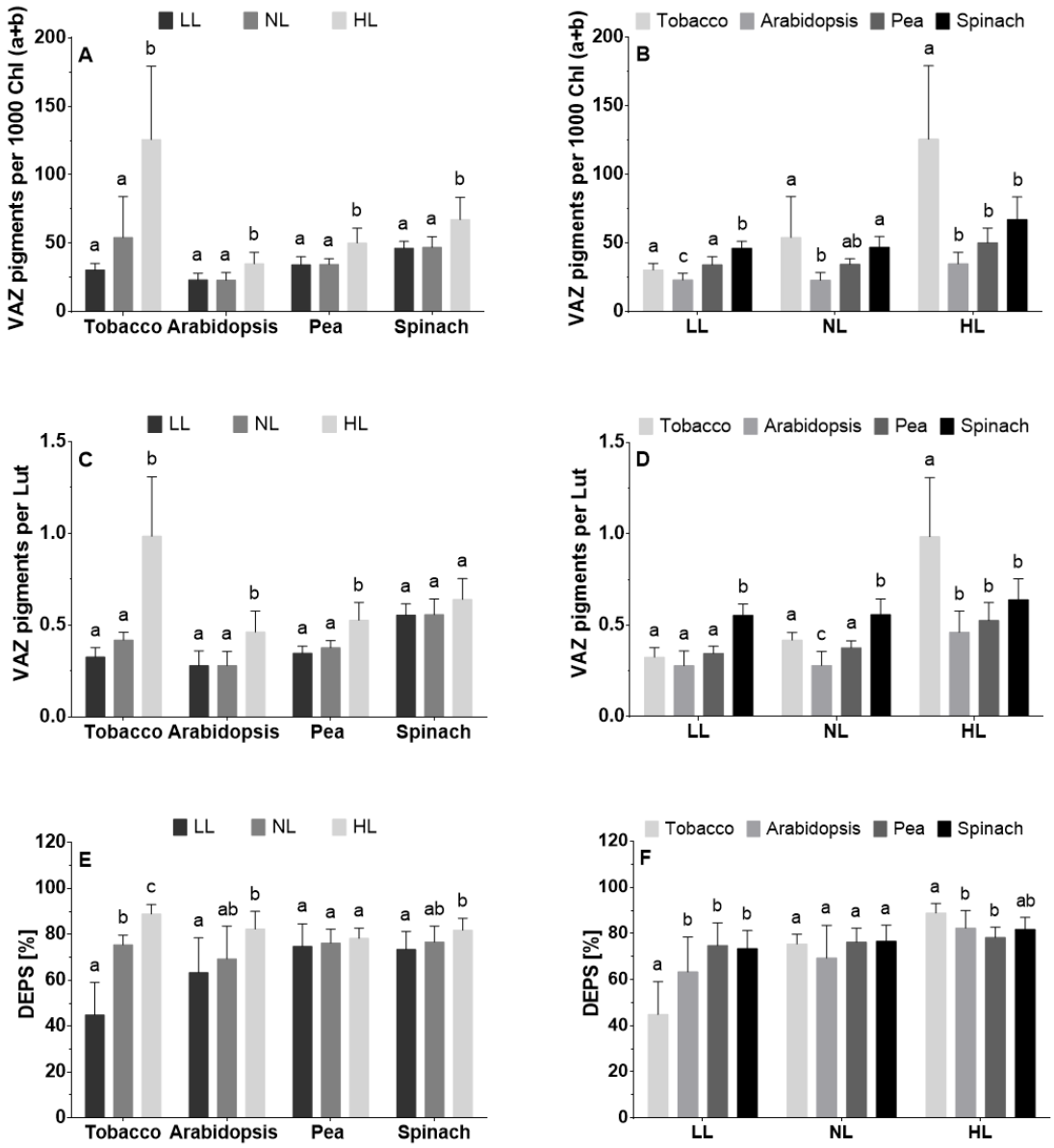

Figure 3. Xanthophyll cycle pigments. The amount of the xanthophyll cycle pigments (VAZ) on Chl basis (**A, B**) and on lutein basis (**C, D**) were derived from pigment analyses of dark-adapted leaves. The maximum de-epoxidation state (DEPS = (0.5 Ax + Zx) / (Vx + Ax + Zx) * 100) of the VAZ pool (**E, F**) was determined in leaves exposed to 8 h of high light (2000 µmol photons m^{-2} s^{-1}). Panels on the left-hand side (A,C,E) show comparison of the growth conditions for each species, panels on the right-hand side (B,D,F) show differences among the species for each growth condition. Mean values ± SD from 8-9 independent measurements are shown. Letters indicate significant differences (One-Way Anova, $p < 0.05$).

The maximum de-epoxidation state (DEPS = (0.5 Ax + Zx) / (Vx + Ax + Zx) * 100) of the VAZ pool (Fig. 3E and F) was determined to obtain information about possible species-specific differences in the amount of Zx in high light. When comparing plants from different growth light conditions (Fig. 3E), a trend for an increase of the maximum DEPS with increasing growth light intensities was visible for each species. However, pea plants showed no significant differences among the growth conditions, whereas

in spinach and Arabidopsis plants, significant differences were found only between LL and HL grown plants. Solely in tobacco plants, the maximum DEPS significantly differed under all growth light conditions. When comparing the different species (Fig. 3F), tobacco plants showed the lowest DEPS in LL acclimated plants, and pea and spinach plants the highest. Under NL conditions, no significant differences among the species were detectable, whereas tobacco plants showed significantly higher DEPS in HL acclimated plants, in comparison with Arabidopsis and pea plants.

High-light induced inactivation of PSII and ZEP

The inactivation of PSII and ZEP activity in response to high light was determined during and after 8 h of illumination at 2000 µmol photons m^{-2} s^{-1}. PSII activity was derived from measurements of the Fv/Fm ratio and ZEP activity from changes in the de-epoxidation state (DEPS) of the xanthophyll cycle pigments (Fig. 4).

As expected, acclimation to different growth light intensities resulted in pronounced changes of the high light sensitivity of PSII and ZEP activity. In general, high light induced inactivation both PSII (Fig. 4A,C,E and G) and ZEP (Fig. 4B,D,F and H) was reduced in response to increasing growth light intensities. In LL acclimated plants, PSII activity was reduced to 5 - 20 % of the maximum activity of dark controls, with tobacco (Fig. 4A) and Arabidopsis (Fig. 4C) being more sensitive than pea (Fig. 4E) and spinach (Fig. 4G). During 12 h recovery at low light (2000 µmol photons m^{-2} s^{-1}), PSII activity partially recovered in all species, but to significantly lower levels in tobacco (7 %) and Arabidopsis (15 %) compared to pea (67 %) and spinach (50 %) (Fig. 4 and Table 3), indicating a much higher high light sensitivity of LL acclimated tobacco and Arabidopsis plants. Similar differences among the species were determined for NL grown plants, though particularly the recovery from PSII inhibition was more efficient in all species (Fig. 4). In HL grown plants, however, inhibition of PSII during 8 h high light exposure was strongly reduced compared to LL and NL plants in all species. Moreover, subsequent low light exposure resulted in nearly full recovery of PSII activity in all species ranging from 72 % (tobacco) to nearly 100 % in Arabidopsis and spinach (Fig. 4 and Table 3), indicating that species specific differences in the high light sensitivity of PSII is attenuated upon long-term acclimation to HL conditions.

High light induced inactivation of ZEP activity was derived from the decrease of the DEPS during the 12 h low light period. Similar to the impact of 8 h high light exposure on PSII activity, a reduction of inhibition with increasing growth light intensities was also found for ZEP activity (Fig. 4). LL acclimated plants showed the lowest ZEP activity for all species. Acclimation to NL and HL conditions led to stepwise decrease of ZEP inhibition in Arabidopsis (Fig. 4D) and spinach (Fig. 4H) plants, whereas no significant differences in ZEP activity in response to different growth light intensities were detectable for tobacco (Fig. 4B) and pea (Fig. 4F). However, ZEP activity in tobacco plants, was strongly inhibited in plants from all acclimation states, whereas pea plants showed similar high ZEP activity in plants from all acclimation states (Fig. 4 and Table 3).

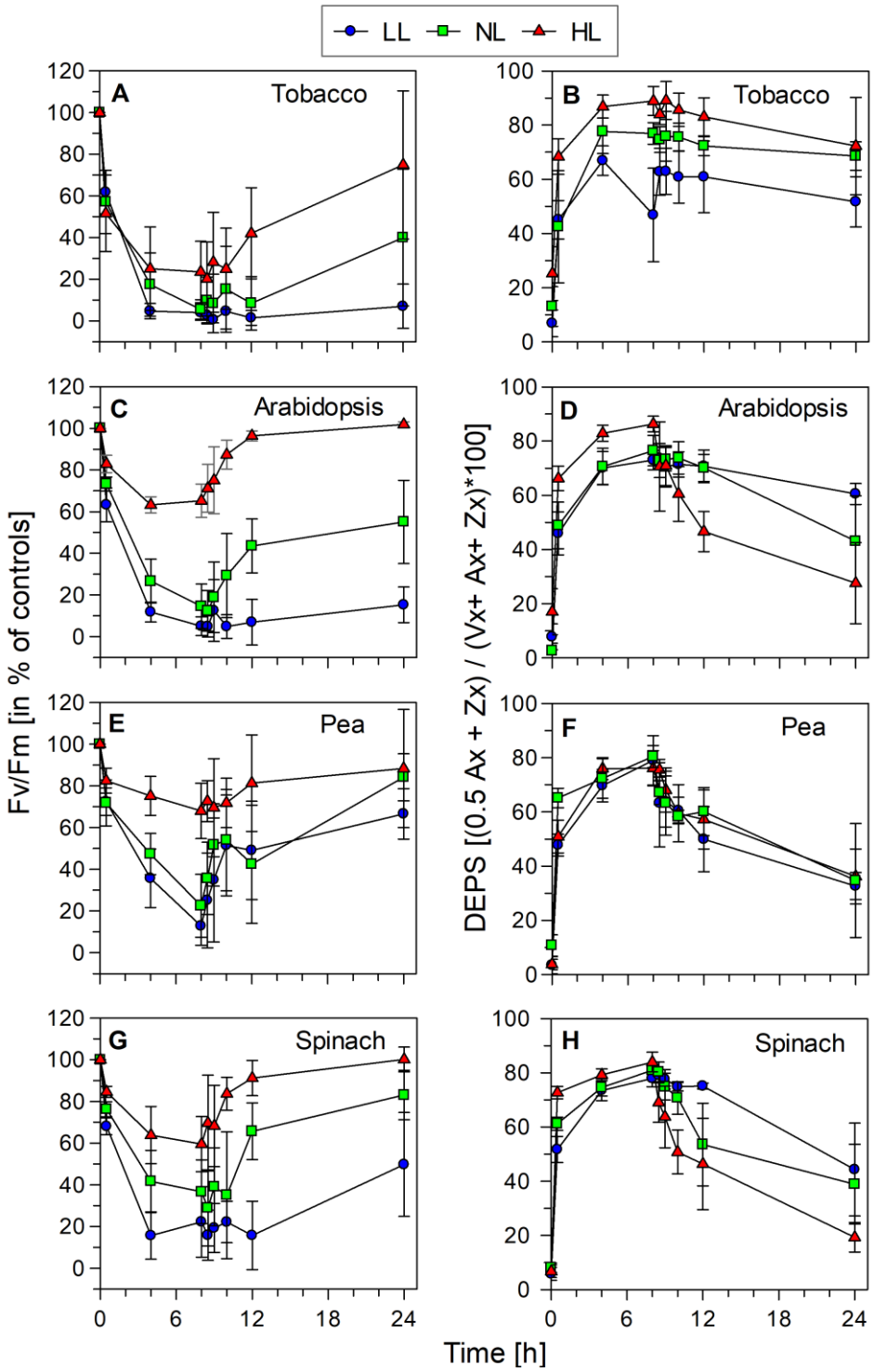

Figure 4. High-light induced inactivation of PSII and ZEP. Leaf discs from dark-adapted plants were floated on water (20°C) and illuminated for 8 h at high light (2000 µmol photons $m^{-2} s^{-1}$), followed by 12 h of low light exposure (10-20 µmol photons $m^{-2} s^{-1}$). At indicated time, Fv/Fm was determined with a DUAL PAM fluorimeter, and the de-epoxidation state (DEPS = (0.5 Ax + Zx) / (Vx + Ax + Zx) * 100) of the VAZ pool was determined from HPLC analyses of the pigment content. Mean values ± SD from 9 independent measurements are shown. For statistical analysis of the data see Table 3.

Table 3: High-light induced inactivation of PSII and ZEP. PSII and ZEP activities were derived from the data shown in Figure 4. PSII activity is expressed as the ratio of Fv/Fm at the end of the low light phase (t = 24 h) and Fv/Fm of dark controls (t = 0 h). ZEP activity is expressed as the ratio of the DEPS at the end of the low light phase (t = 24 h) and the maximum DEPS at the end of the high light phase (t = 8 h). Mean values ± SD from 12 independent measurements are shown. Significant differences among the species are indicated by upper case letters, differences among growth conditions by lower case letters.

Species	PSII activity				ZEP activity		
	LL	NL	HL		LL	NL	HL
Tobacco	$7 \pm 11^{C,a}$	$40 \pm 33^{B,b}$	$72 \pm 32^{B,c}$		$6 \pm 11^{B,a}$	$30 \pm 31^{A,a}$	$20 \pm 19^{B,a}$
Arabidopsis	$15 \pm 8^{C,a}$	$57 \pm 22^{B,b}$	$99 \pm 4^{A,c}$		$17 \pm 8^{B,a}$	$46 \pm 23^{A,b}$	$64 \pm 20^{A,b}$
Pea	$67 \pm 12^{A,a}$	$67 \pm 11^{A,ab}$	$85 \pm 26^{AB,b}$		$58 \pm 7^{A,a}$	$46 \pm 9^{A,a}$	$52 \pm 29^{AB,a}$
Spinach	$50 \pm 25^{B,a}$	$83 \pm 12^{A,b}$	$98 \pm 4^{A,b}$		$43 \pm 23^{A,a}$	$52 \pm 19^{A,ab}$	$77 \pm 9^{A,b}$

In conclusion, the high light induced inactivation of PSII and ZEP shows a similar response to different growth light conditions in all species, supporting the co-regulation of both enzymes in response to high light stress. Comparing the high light sensitivity of the different species, tobacco plants showed the strongest high light sensitivity and the weakest capacity of acclimation to high light. In pea and spinach plants, the acclimation response to different growth light intensities was rather weak as well, but these two species are characterized by a pronounced resistance against high light stress already in LL acclimated plants. Arabidopsis plants exhibited the most pronounced acclimation response to increasing growth light intensities, with LL plants being highly sensitive to high light, while HL acclimated plants developed a high light resistance similar to pea and spinach.

High-light induced degradation of D1 and ZEP protein

The degradation of D1 and ZEP protein was investigated by immunoblot analyses of total leaf protein extracts under the same conditions as applied before for studying the high light induced inactivation of D1 and ZEP. Figure 5 shows representative blots with antibodies against the D1 and ZEP protein. An antibody raised against the large subunit of RubisCO (RbcL) was used as loading control for chloroplast proteins. Although the obtained band intensities showed some variations, it is clearly visible that ZEP protein became largely degraded in tobacco plants in response to high light under all growth conditions (Fig. 5A). Strong degradation was detectable after 4 h of high light. Degradation of the D1 protein was particularly detectable in LL grown plants (Fig. 5A). In NL and HL grown tobacco plants, however, D1 degradation was clearly attenuated. Hence, 8 h high light exposure induced more pronounced degradation of ZEP proteins compared to D1 protein in tobacco.

Also in Arabidopsis, degradation of ZEP and D1 was detectable (Fig. 5B). Both proteins were degraded to similar extent in LL and NL grown plants after about 8 h of high light exposure, whereas no clear degradation was observable for HL grown plants. Compared to tobacco, degradation of ZEP was thus less pronounced in LL and NL plants, and acclimation to HL further reduced ZEP degradation. In pea (Fig. 5C) and spinach (Fig. 5D), a similar pattern of ZEP and D1 protein amounts were detectable in plants form all growth conditions. In contrast to tobacco and Arabidopsis, only weak degradation of ZEP was found, even in LL acclimated plants. Degradation of D1 protein was slightly more pronounced in

both species compared to ZEP degradation. In conclusion, the four species differed particularly with respect to the degradation of ZEP protein, which was most pronounced in tobacco and less pronounced in pea and spinach.

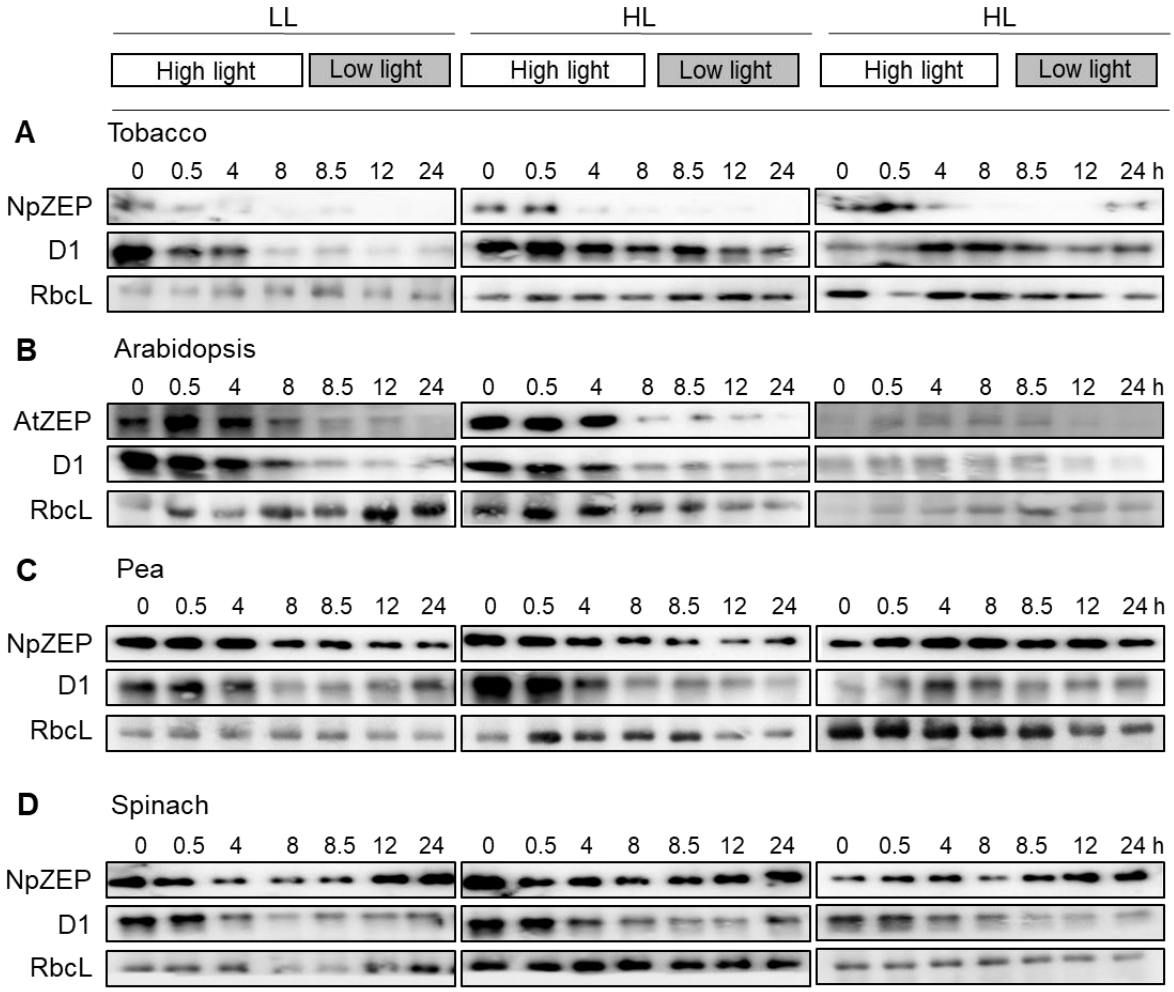

Figure 5. Immunoblot analysis of the D1 and ZEP protein content. Leaf discs from dark-adapted tobacco (**A**), Arabidopsis (**B**), pea (**C**) and spinach (**D**) plants were floated on water (20°C) and illuminated for 8 h at high light (2000 µmol photons m^{-2} s^{-1}), followed by 12 h of low light exposure (10-20 µmol photons m^{-2} s^{-1}). At indicated time points, 3 leaf discs were used for protein extraction. Total protein extracts equivalent to 5 µg protein were separated by SDS-PAGE. The abundance of ZEP and D1 protein, as well as of the large subunit of RubisCO (RbcL) was assessed by immunoblotting with specific antibodies. For ZEP protein, two different antibodies were used. For tobacco, pea and spinach, an antibody raised against a peptide specific for tobacco ZEP (NpZEP) was used, for Arabidopsis samples an antibody against a peptide specific for Arabidopsis ZEP (AtZEP). Representative blots from at least 3 biological replicates are shown.

Discussion

Long-term acclimation to different growth light intensities involves a large set of adjustments at different levels (Anderson 1986; Boardman 1977; Schoettler and Toth 2014). In line with expectations, the present work showed that all four studied species followed a similar trend of acclimation to different light with respect to most of the investigated parameters. Irrespective of the differences in absolute values, the following general trends of acclimation were determined in response to increasing growth light intensities:

- Increase of leaf thickness (Fig. 1) and reduction of grana width (Fig. 2)
- Increased amount of Chl per leaf area and increased Chl a/b ratio (Table 2)
- Increased light saturation of photosynthetic electron transport (Table 1)
- Increased energy dissipation capacity (NPQ and qE) (Table 1)
- Reduced HL sensitivity of PSII and ZEP activity (Fig. 4)

Hence, all four investigated species have the general capacity to acclimate to different growth light intensities in a well-known manner, ranging from morphological changes to the adjustment of photosynthetic light utilization. Although all species followed the same trend of acclimation, the phenotypical plasticity was different among the species and rather variable when comparing the different measuring parameters. Arabidopsis and tobacco plants grown under NL conditions have been shown to be more prone to HL-induced photoinhibition of PSII and ZEP inactivation than pea and spinach plants (Bethmann et al. 2019). It was just of particular interest whether these two species show possibly specific deficiencies or peculiarities in long-term acclimation to different growth light intensities. Comparative inspection of the data with respect to the acclimation properties of each species was thus performed to clarify this aspect. For that, the values determined for the most relevant parameters were encoded by colors (Figs 6 and 7) to allow an easy and comprehensive comparison of the different data sets. Within a data set for one parameter, similar colors reflect similar ratios of the values among all species under all growth light intensities. These plots thus allow an easy visualization not only of relative changes in response to different growth light intensities for each individual species but also of relative differences among the species. Figure 6 depicts those parameters, for which Arabidopsis and tobacco both showed clearly different (lower or higher) values at one or more growth light intensities compared to pea and spinach. These parameters might thus represent parameters that are related to the more pronounced HL sensitivity of PSII in Arabidopsis and tobacco compared to pea and spinach. Figure 7 highlights those parameters, which showed a quite variable difference among the four species. It is obvious from Fig. 6 that in particular LL acclimated plants from Arabidopsis and tobacco showed similar values, which however clearly differed from LL grown pea and spinach plant. Hence, the parameters leaf thickness (Fig. 6A), Chl per leaf area (Fig. 6B), VAZ pool size (Fig. 6C) and qE capacity (Fig. 6D) are likely critical determinants for the vulnerability to the HL induced inhibition of PSII (Fig. 6E) and ZEP (Fig. 6F) activity. Interestingly, the leaf thickness increased significantly with increased growth light intensities in all species when comparing HL and LL plants (Figs. 1 and 6A), whereas the Chl content per leaf area (Fig. 6B, Table 2) decreased or remained nearly unchanged in all species. Since the increase of leaf thickness is related to an increased size of parenchyma cells and/or an increased number of parenchyma cell layers (Fig. S1), the similar (or reduced) Chl content per leaf area allows a location of chloroplasts further

away from the leaf surface and a higher degree of self-shading. Chloroplast movement to the side of parenchyma cells and chloroplast self-shading are well-known efficient photoprotective short-term (10-20 min) mechanisms (Kagawa et al. 2001; Kasahara et al. 2002; Li et al. 2009). Increasing the leaf thickness in combination with a decrease or an unchanged amount of Chl per leaf area can thus be an efficient strategy to reduce photo-oxidative stress. The thicker leaves of LL grown pea and spinach plants might therefore be essential for their lower HL sensitivity when compared to LL grown Arabidopsis and tobacco plants.

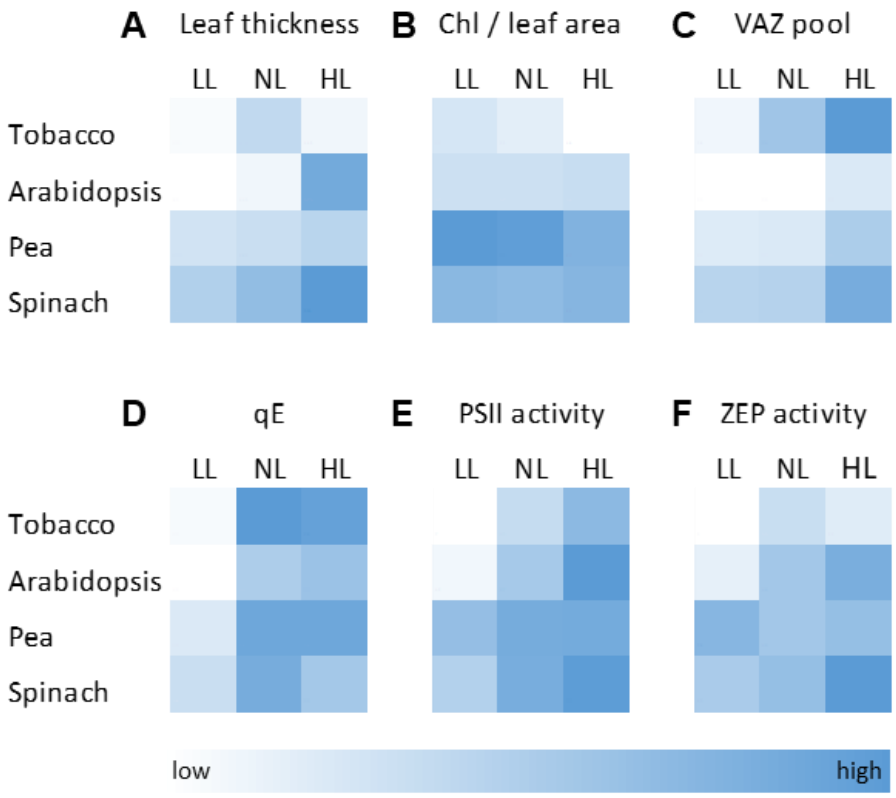

Figure 6. Species specific differences in light acclimation: Summary 1. Comparison of relative changes of LL, NL and HL acclimated plants from tobacco, Arabidopsis, pea and spinach plants for: **(A)** Leaf thickness (data from Fig.1), **(B)** Chl (a+b) content per leaf area (= Chl / leaf area; data from Table 2), **(C)** the amount of xanthophyll cycle pigments per Chl (a+b) (VAZ pool; data from Fig. 3) **(D)** the capacity of pH-dependent quenching (qE; data from Table 1), **(E)** PSII activity (data from Fig. 4) and **(F)** ZEP activity (data from Fig. 4). The color code indicates the range from the lowest (white) to the highest (dark blue) value within each parameter set.

The qE capacity and in particular the VAZ pool size are well-known determinants of the photoprotective capacity. Since the maximum DEPS was found to be very similar in all species (Fig. 3F), the VAZ pool size determines the amount of Zx that can be accumulated in the membrane. The amount of Zx in the thylakoid membrane is known to modulate the qE capacity (Kalituho et al. 2007; Nilkens et al. 2010), which can at least partially explain the correlation of the VAZ pool size and the qE capacity. With respect to qE regulation, however, a high Zx amount might reduce the relaxation kinetics of qE upon the transfer from HL to LL (Ruban and Horton 1999; Ruban and Johnson 2010). However, this might be particularly

important for plants growing under natural, fluctuating light conditions. Characterization of photosynthetic light utilization and photoprotection under fluctuating light conditions would thus be required to clarify whether the higher VAZ pool size of pea and spinach plants has negative impact under more natural growth conditions. Higher amounts of Zx in the thylakoid membrane and hence an increased VAZ pool size will further contribute to photoprotection independent of NPQ (Havaux et al. 2007; Havaux and Niyogi 1999). The NPQ-independent photoprotective function of Zx is likely related to non-protein bound Zx (Havaux et al. 2004). The increase of the VAZ pool size in response to increasing growth light intensities (Figs. 3 and 6) occurred in parallel with an increase of the Chl a/b ratio (Fig. 7 and Table 2). An increase of the Chl a/b ratio reflects the reduction of the Chl a/b binding proteins, which also provide the xanthophyll binding sites. It is thus reasonable to assume that the amount of non-protein bound Zx will be distinctly increased upon acclimation to higher growth light intensities.

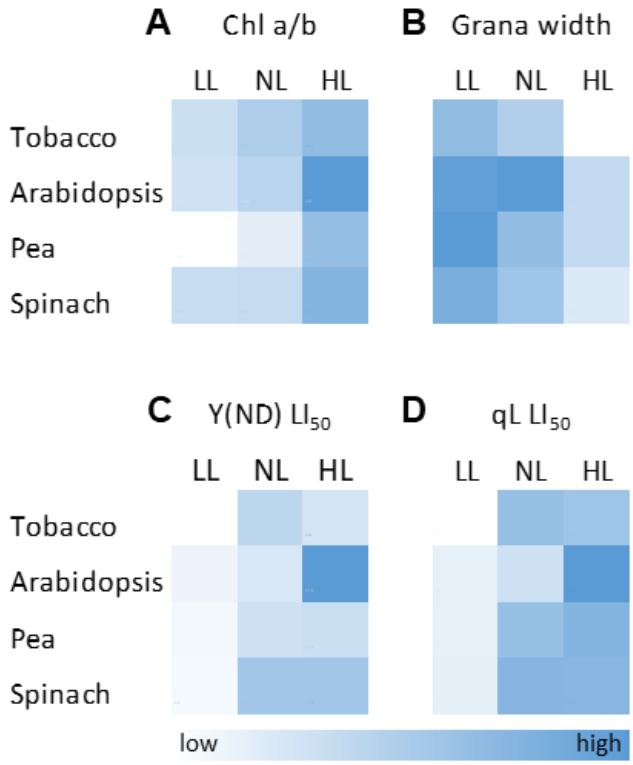

Figure 7. Species specific differences in light acclimation: Summary 2. Comparison of relative changes of LL, NL and HL acclimated plants from tobacco, Arabidopsis, pea and spinach plants for: **(A)** Chl a/b ratio (data from Table 2), **(B)** grana width (data from Fig. 2) and he light intensity of the half-saturation of **(C)** NPQ (NPQ LI_{50}) and **(D)** qL (qL LI_{50}) (both data sets from Table 1). The color code indicates the range from the lowest (white) to the highest (dark blue) value within each parameter set.

This further supports the critical role of the VAZ pool size for photoprotection. Moreover, the down-regulation or inactivation of ZEP activity in response to HL stress is supposed to ensure that high levels of Zx are retained in the thylakoid membrane under photoinhibitory conditions (Bethmann et al. 2019). Indeed, a quite similar response of the HL sensitivity of PSII and ZEP activity has been found in all four

species and in plants under all growth light conditions (Figs. 4 and 6) supporting the close correlation of PSII and ZEP activity. In addition, parallel degradation of D1 protein and ZEP during photoinhibition has been shown in former work (Bethmann et al. 2019). The much less pronounced degradation of ZEP in pea and spinach plants compared to Arabidopsis and tobacco D1 (particularly obvious for LL grown plants, Fig. 5) supports not only the lower HL sensitivity of these two species but also the important role of ZEP regulation in close relation to photoinhibition of PSII.

When comparing the relative changes of the different parameters in response to increasing growth light intensities for each species on basis of Figures 6 and 7, it is quite obvious that particularly Arabidopsis plants show the most pronounced phenotypic plasticity among the four species. In contrast, pea and spinach plants exhibited a much more attenuated acclimation response. This reduced plasticity seems to be mainly determined by the rather high HL resistance of LL grown pea and spinach plants. Again, in particular leaf thickness, VAZ pool size and qE capacity can thus be assumed to be the critical determinant for the reduced vulnerability of these two species to photoinhibition and thus the inactivation of ZEP in response to HL exposure.

In conclusion, our data show that each of the four species is able to acclimate to different growth light intensities. The higher HL sensitivity of Arabidopsis and tobacco plants compared to pea and spinach is even more pronounced in LL acclimated plants, but attenuated in HL acclimated plants. The regulation of ZEP activity in close correlation with PSII activity is maintained in all species and under all growth light conditions. Leaf thickness, the VAZ pool size and qE capacity seem to be the critical determinants for HL sensitivity.

Data availability

All data are contained within the article.

Acknowledgments

This work was supported by the Deutsche Forschungsgemeinschaft (JA 665/12-1 to P.J.).

Author Contributions

S.B., M.M. and P.J. designed the research; S.B. and A.H.K performed the experiments; S.B. and M.M. analyzed data; S.B. and P.J. wrote the original draft; S.B., A.K.H, M.M. and P.J. reviewed and edited the manuscript.

References

Adams, W.W., Demmig-Adams, B., Rosenstiel, T.N., Brightwell, A.K. and Ebbert, V. (2002) Photosynthesis and photoprotection in overwintering plants. Plant Biol 4: 545-557.

Adams, W.W., Demmig-Adams, B., Verhoeven, A.S. and Barker, D.H. (1995) 'Photoinhibition' during winter stress: involvement of sustained xanthophyll cycle-dependent energy dissipation. Aust. J. Plant Physiol. 22: 261-276.

Adams, W.W., Zarter, C.R., Ebbert, V. and Demmig-Adams, B. (2004) Photoprotective strategies of overwintering evergreens. Bioscience 54: 41-49.

Anderson, J.M. (1986) Photoregulation of the composition, function, and structure of thylakoid membranes. Annu Rev Plant Physiol Plant Mol Biol 37: 93-136.

Aro, E.M., Virgin, I. and Andersson, B. (1993) Photoinhibition of Photosystem II. Inactivation, protein damage and turnover. Biochim Biophys Acta 1143: 113–134

Bailey, S., Walters, R.G., Jansson, S. and Horton, P. (2001) Acclimation of Arabidopsis thaliana to the light environment: the existence of separate low light and high light responses. Planta 213: 794-801.

Bailey, S., Horton, P. and Walters, R.G. (2004) Acclimation of Arabidopsis thaliana to the light environment: the relationship between photosynthetic function and chloroplast composition. Planta 218: 793-802.

Bethmann, S., Melzer, M., Schwarz, N. and Jahns, P. (2019) The zeaxanthin epoxidase is degraded along with the D1 protein during photoinhibition of photosystem II. Plant Direct 3, https://doi.org/10.1002/pld3.185.

Boardman, N.K. (1977) Comparative photosynthesis of sun and shade plants. Annu Rev Plant Physiol Plant Mol Biol 28: 355-377.

Brugnoli, E., Cona, A. and Lauteri, M. (1994) Xanthophyll cycle components and capacitiy for non-radiative energy dissipation in sun and shade leaves of Ligustrum ovalifolium exposed to conditions limiting photosynthesis. Photosynth Res 41: 451-463.

Demmig-Adams, B., Cohu, C.M., Muller, O. and Adams, W.W., III (2012) Modulation of photosynthetic energy conversion efficiency in nature: from seconds to seasons. Photosynth Res 113: 75-88.

Färber, A., Young, A.J., Ruban, A.V., Horton, P. and Jahns, P. (1997) Dynamics of xanthophyll-cycle activity in different antenna subcomplexes in the photosynthetic membranes of higher plants: the relationship between zeaxanthin conversion and nonphotochemical fluorescence quenching. Plant Physiol. 115: 1609-1618.

Garcia-Molina, A. and Leister, D. (2020) Accelerated relaxation of photoprotection impairs biomass accumulation in Arabidopsis. Nature Plants 6: 9-12.

Havaux, M., Dall'Osto, L. and Bassi, R. (2007) Zeaxanthin has enhanced antioxidant capacity with respect to all other xanthophylls in Arabidopsis leaves and functions independent of binding to PSII antennae. Plant Physiol 145: 1506-1520.

Havaux, M., Dall'Osto, L., Cuine, S., Giuliano, G. and Bassi, R. (2004) The effect of zeaxanthin as the only xanthophyll on the structure and function of the photosynthetic apparatus in Arabidopsis thaliana. J Biol Chem 279: 13878-13888.

Havaux, M. and Niyogi, K.K. (1999) The violaxanthin cycle protects plants from photooxidative damage by more than one mechanism. Proc Natl Acad Sci USA 96: 8762-8767.

Horton, P., Ruban, A.V. and Walters, R.G. (1996) Regulation of light harvesting in green plants. Annu Rev Plant Physiol Plant Mol Biol 47: 655-684.

Kagawa, T., Sakai, T., Suetsugu, N., Oikawa, K., Ishiguro, S., Kato, T., et al. (2001) Arabidopsis NPL1: A phototropin homolog controlling the chloroplast high-light avoidance response. Science 291: 2138-2141.

Kalituho, L., Beran, K.C. and Jahns, P. (2007) The transiently generated nonphotochemical quenching of excitation energy in Arabidopsis leaves is modulated by zeaxanthin. Plant Physiol 143: 1861-1870.

Kasahara, M., Kagawa, T., Oikawa, K., Suetsugu, N., Miyao, M. and Wada, M. (2002) Chloroplast avoidance movement reduces photodamage in plants. Nature 420: 829-832.

Kramer, D.M., Johnson, G., Kiirats, O. and Edwards, G.E. (2004) New fluorescence parameters for the determination of Q(A) redox state and excitation energy fluxes. Photosynth Res 79: 209-218.

Krause, G.H. (1988) Photoinhibition of photosynthesis. An evaluation of damaging and protective mechanisms. Physiol Plant 74: 566-574.

Krause, G.H. and Jahns, P. (2004) Non-photochemical energy dissipation determined by chlorophyll fluorescence quenching: characterization and function. In Chlorophyll a fluorescence: A signature of photosynthesis. Edited by Papageorgiou, G.C. and Govindjee pp. 463-495. Kluwer Acadamic Publishers, Dordrecht.

Kromdijk, J., Glowacka, K., Leonelli, L., Gabilly, S.T., Iwai, M., Niyogi, K.K., et al. (2016) Improving photosynthesis and crop productivity by accelerating recovery from photoprotection. Science 354: 857-861.

Kyhse-Andersen, J. (1984) Electroblotting of multiple gels - A simple apparatus without buffer tank for rapid transfer of proteins from polyacrylamide to nitrocellulose. J Biochem Biophys Methods 10: 203-209.

Laemmli, U.K. (1970) Cleavage of structural proteins during the assembly of the head of bacteriophage T4. Nature 227: 680-685.

Li, X.-P., Björkman, O., Shih, C., Grossman, A.R., Rosenquist, M., Jansson, S., et al. (2000) A pigment-binding protein essential for regulation of photosynthetic light harvesting. Nature 403: 391-395.

Li, X.P., Gilmore, A.M. and Niyogi, K.K. (2002) Molecular and global time-resolved analysis of a psbS gene dosage effect on pH- and xanthophyll cycle-dependent nonphotochemical quenching in photosystem II. J Biol Chem 277: 33590-33597.

Li, Z.R., Wakao, S., Fischer, B.B. and Niyogi, K.K. (2009) Sensing and Responding to Excess Light. Annu Rev Plant Biol 60: 239-260.

Lichtenthaler, H.K., Buschmann, C., Doll, M., Fietz, H.J., Bach, T., Kozel, U., et al. (1981) Photosynthetic activity, chloroplast ultrastructure, and leaf characteristics of high-light and low-light plants and of sun and shade leaves. Photosynth Res 2: 115-141.

Mishra, Y., Jankanpaa, H.J., Kiss, A.Z., Funk, C., Schroder, W.P. and Jansson, S. (2012) Arabidopsis plants grown in the field and climate chambers significantly differ in leaf morphology and photosystem components. BMC Plant Biol 12.

Moller, I.M., Jensen, P.E. and Hansson, A. (2007) Oxidative modifications to cellular components in plants. Annu Rev Plant Biol 58: 459-481.

Nilkens, M., Kress, E., Lambrev, P.H., Miloslavina, Y., Müller, M., Holzwarth, A.R., et al. (2010) Identification of a slowly inducible zeaxanthin-dependent component of non-photochemical quenching of chlorophyll fluorescence generated under steady state conditions in Arabidopsis. Biochim Biophys Acta 1797: 466-475.

Niyogi, K.K. (1999) Photoprotection revisited: genetic and molecular approaches. Annu Rev Plant Physiol Plant Mol Biol 50: 333-359.

Niyogi, K.K., Grossman, A.R. and Björkman, O. (1998) Arabidopsis mutants define a central role for the xanthophyll cycle in the regulation of photosynthetic energy conversion. Plant Cell 10: 1121-1134.

Öquist, G. and Huner, N.P.A. (2003) Photosynthesis of overwintering evergreen plants. Annu Rev Plant Biol 54: 329-355.

Park, Y.I., Chow, W.S., Anderson, J.M. and Hurry, V.M. (1996) Differential susceptibility of Photosystem II to light stress in light-acclimated pea leaves depends on the capacity for photochemical and non-radiative dissipation of light. Plant Sci 115: 137-149.

Powles, S.B. (1984) Photoinhibition of photosynthesis induced by visible light. Annu Rev Plant Physiol 35: 15-44.

Reinhold, C., Niczyporuk, S., Beran, K. and Jahns, P. (2008) Short-term down-regulation of zeaxanthin epoxidation in Arabidopsis thaliana in response to photo-oxidative stress conditions. Biochim Biophys Acta 1777: 462-469.

Ruban, A.V. and Horton, P. (1999) The xanthophyll cycle modulates the kinetics of nonphotochemical energy dissipation in isolated light-harvesting complexes, intact chloroplasts, and leaves of spinach. Plant Physiol 119: 531-542.

Ruban, A.V. and Johnson, M.P. (2010) Xanthophylls as modulators of membrane protein function. Arch Biochem Biophys 504: 78-85.

Ruban, A.V., Johnson, M.P. and Duffy, C.D. (2012) The photoprotective molecular switch in the photosystem II antenna. Biochim Biophys Acta 1817: 167-181.

Schoettler, M.A. and Toth, S.Z. (2014) Photosynthetic complex stoichiometry dynamics in higher plants: environmental acclimation and photosynthetic flux control. Front Plant Sci 5:188. doi:10.3389/fpls.2014.00188.

Schumann, T., Paul, S., Melzer, M., Doermann, P. and Jahns, P. (2017) Plant growth under natural light conditions provides highly flexible short-term acclimation properties toward high light dtress. Front Plant Sci 8: 681. doi:10.3389/fpls.2017.00681.

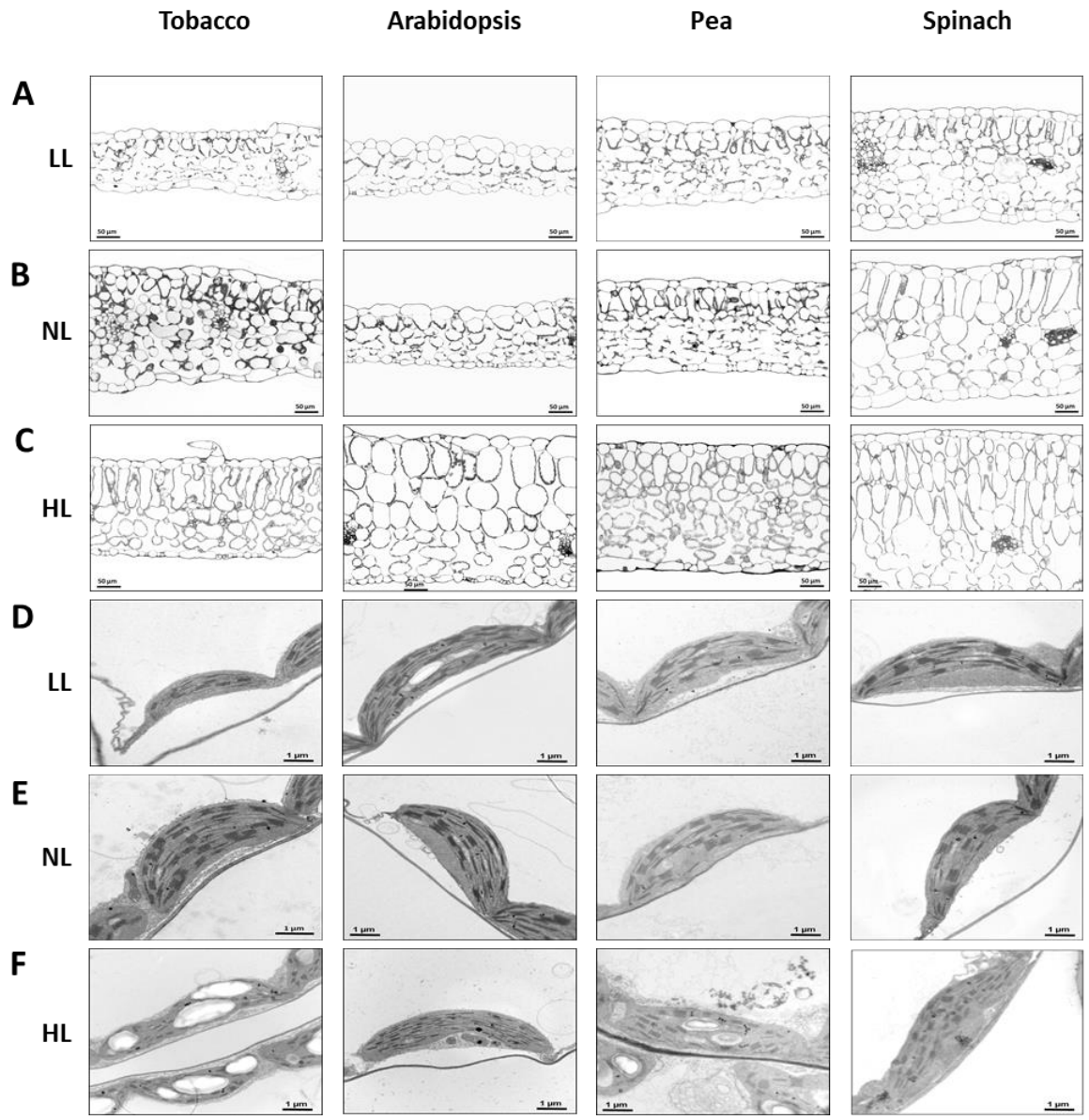

Figure S1. Leaf morphology and chloroplast structure. Light microscopic images of leaf cross-sections (**A-C**) and electron microscopic images of chloroplasts (**D-F**) from plants grown under LL (**A,D**), NL (**B,E**) and LL (**C,F**). All samples were prepared from dark-acclimated leaves. Representative images form 6-65 images are shown.

8. Manuscript 3

Zeaxanthin Epoxidase Activity is Down-regulated by Hydrogen Peroxide

Dimitrij Holzmann, Stephanie Bethmann and Peter Jahns

Status: under revision

Contributions:

S.B. and P.J. designed and supervised the research; D.H. performed most the experiments; S.B. performed some of the experiments; S.B. and D.H. analyzed data; P.J. wrote the original draft; D.H., S.B. and P.J. reviewed and edited the manuscript.

Title:

Zeaxanthin Epoxidase Activity is Down-regulated by Hydrogen Peroxide

Running head:

Down-Regulation of Zeaxanthin Epoxidase by H_2O_2

Corresponding author:

P. Jahns

Photosynthesis and Stress Physiology of Plants, Heinrich-Heine-University Düsseldorf

Universitaetsstr. 1, 40225 Düsseldorf, Germany

Tel.: +49-211-8113862

Fax: +49-211-8113706

E-mail: pjahns@hhu.de

Subject areas:

Environmental and stress response

Photosynthesis, respiration and bioenergetics

Number of black and white figures: 5

Colour figures: 0

Tables: 0

Supplementary material: 3 Figures

Zeaxanthin Epoxidase Activity is Down-regulated by Hydrogen Peroxide

Running Head:

Down-Regulation of Zeaxanthin Epoxidase by H_2O_2

Dimitrij Holzmann, Stephanie Bethmann and Peter Jahns*

Photosynthesis and Stress Physiology of Plants, Heinrich-Heine-University Düsseldorf, 40225 Düsseldorf, Germany

*Corresponding author: E-mail, pjahns@hhu.de; Fax, +49-211-8113706

Abstract

The xanthophyll zeaxanthin (Zx) serves important photoprotective functions in chloroplasts and is particularly involved in the dissipation of excess light energy as heat in the antenna of photosystem II (PSII). Zx accumulates under high light conditions in thylakoid membranes and is reconverted to violaxanthin by zeaxanthin epoxidase (ZEP) in low light or darkness. ZEP activity is completely inhibited under long-lasting high light stress and ZEP protein becomes degraded along with the PSII subunit D1 during photoinhibition of PSII. This ZEP inactivation ensures that high levels of Zx are maintained under harsh high light stress. The mechanism of ZEP inactivation is unknown. Here, we investigated ZEP inactivation by reactive oxygen species (ROS) under *in vitro* conditions. Our results show that ZEP activity is completely inhibited by hydrogen peroxide (H_2O_2), but not by singlet oxygen. Our data further support the view that superoxide generated at the acceptor site of PSI does not accumulate to reasonable levels in presence of thylakoid-associated superoxide dismutase. Hence, high-light induced inactivation of ZEP is likely based on H_2O_2 accumulation.

Keywords: Photo-oxidative stress, Photoprotection, Reactive oxygen species, Xanthophyll cycle, Zeaxanthin epoxidase

Introduction

Photo-oxidative stress is one of the most challenging stress factors for plants, because reactive oxygen species (ROS) are inevitably produced on daily basis in chloroplasts along with photosynthetic light utilization (Moller et al. 2007). Consequently, several strategies have been developed in plants to manage this challenge, either by reducing ROS formation or by increasing ROS detoxification (Li et al. 2009). The xanthophyll zeaxanthin (Zx) which is formed in thylakoid membranes under high light (HL) conditions (Jahns et al. 2009) serves a number of photoprotective functions. Zx is known to be involved in the energy-dependent and Zx-dependent mechanisms of non-photochemical quenching (NPQ) of excitation energy, by which excessively absorbed light energy can be dissipated as heat in the antenna proteins of photosystem II (PSII) (Horton et al. 2005; Nilkens et al. 2010). In addition, Zx is supposed to be required for the protection of damaged PSII reaction centers during the photoinhibition and repair cycle (Bethmann et al. 2019). Moreover, Zx contributes to photoprotection independent of NPQ possibly as antioxidant in the lipid phase of the membrane (Havaux and Niyogi 1999) or related to its function as modulator of thylakoid membrane properties (Havaux 1998).

The amount of Zx accumulating in the thylakoid membrane is determined by the equilibrium of the two reactions of the xanthophyll cycle: (i) the de-epoxidation of violaxanthin (Vx) to Zx catalyzed by Vx de-epoxidase (VDE) and (ii) the epoxidation of Zx to Vx catalyzed by the Zx epoxidase (ZEP). The VDE is localized in the thylakoid lumen and requires ascorbate as cofactor (Hager 1966, 1969; Yamamoto et al. 1971). VDE activity is strictly regulated by the lumen pH and becomes fully activated at pH values below 6.0, but is inactive at pH > 6.5 (Hager 1969; Pfündel and Dilley 1993). Thus, VDE activity is largely regulated by light-induced acidification of the thylakoid lumen. ZEP is localized in the chloroplast stroma and requires NADPH and O_2 as cofactors (Siefermann and Yamamoto 1975). ZEP activity is only moderately affected by pH in the physiological pH range (pH 7-8) in the chloroplast stroma (Siefermann and Yamamoto 1975). The maximum VDE activity is 5-10 times faster than the maximum ZEP activity (Hartel et al. 1996), Consequently, Zx accumulates to maximum levels, when photosynthetic electron transport is light-saturated and hence a low lumen pH is established. In contrast, Zx reconversion to Vx only occurs, when VDE activity is low, and hence under low light or in the dark.

ZEP activity is differentially regulated by light. Initial pioneering work on ZEP already showed that Zx epoxidation in intact leaves proceeds faster in low light compared to darkness (Hager 1966). It has been proposed that this is related to the requirement of NADPH and/or oxygen, which are both produced along with photosynthetic electron transport. So far, however, it is still unclear whether ZEP has the same activity in the dark- and light-acclimated state. A possibly different activity of ZEP in the dark-and light-acclimated state can be suggested due to recent characterization of mutants with defects in NADPH thioredoxin reductase C (NTRC) (Naranjo et al. 2016) or m-type thioredoxins (TRX-m) (Da et al. 2017). Studies on the *ntrc1* mutants revealed that recombinant ZEP protein is prone to thiol oxidation, but no indications for that was found so far under *in vivo* conditions (Naranjo et al. 2016). Nevertheless, redox regulation might explain the observed lower ZEP activity under low light, which could be derived from the increased accumulation of Zx under non-saturating light intensities compared to wild-type plants (Naranjo et al. 2016). Redox regulation of ZEP activity is further supported by the phenotype of *TRX-m* silenced Arabidopsis mutants (Da et al. 2017). Down-regulation of TRX-m resulted in increased Zx levels in the dark-acclimated state, lower ZEP activity and reduced ZEP stability. TRX-m was further

identified as interaction partner of ZEP and TRX-m was supposed to control ZEP oligomerization (Da et al. 2017). These data suggest that ZEP activity might be redox-regulated and possibly light-activated by the TRX system.

Moreover, ZEP activity is down-regulated under HL conditions in parallel with the inactivation of PSII. Several studies showed that Zx reconversion to Vx is kinetically closely correlated with the recovery of the slowly relaxing NPQ components qZ and qI (Hoang et al. 2020; Jahns and Miehe 1996; Kim et al. 2017; Kress and Jahns 2017; Nilkens et al. 2010; Verhoeven et al. 1996). The NPQ component qZ represents a reversible inactivation of PSII. qZ is likely identical with the rapid phase of recovery from photoinhibition, which was shown to be independent of D1 turnover (Leitsch et al. 1994; Thiele et al. 1996). Severe HL stress increases the portion of irreversible photoinhibition of PSII, which requires degradation and repair of the D1 protein. Recent work showed that ZEP is gradually down-regulated with increasing photoinhibition (Reinhold et al. 2008) and ZEP protein is degraded in parallel with D1 protein under severe high-light stress (Bethmann et al. 2019).

The molecular mechanism of ZEP inactivation / down-regulation is still unclear. Based on the observed partial inhibition of Zx epoxidation in presence of the phosphatase inhibitor NaF, protein phosphorylation has been proposed to be involved in ZEP inactivation (Kim et al. 2017; Xu et al. 1999). However, it is still unclear (i) whether ZEP protein or other proteins become phosphorylated and (ii) whether phosphorylation is involved in regulation of the reversible and/or the irreversible inactivation of ZEP. An alternative mechanism of ZEP inactivation may be related to direct modification of ZEP (or other proteins) by ROS. Such a scenario has been suggested at least for the irreversible inactivation of ZEP activity (Bethmann et al. 2019; Reinhold et al. 2008).

In this work, we investigated ZEP activity in the dark- and light-acclimated state and determined the impact of ROS on ZEP activity. Our results indicate that ZEP is fully active in the dark-adapted state and thus not responsive to thiol modulation. Furthermore, ZEP activity was found to be sensitive to hydrogen peroxide (H_2O_2) but not to singlet oxygen.

Results

In vitro ZEP activity in the light- and dark-acclimated state

To study the regulation of ZEP activity, we applied established *in vitro* analysis of ZEP activity (Färber and Jahns 1998) using thylakoid membranes isolated from spinach leaves. The increased accumulation of Zx in dark-acclimated *trxm* mutants compared to wild-type plants and the interaction of TRX-m with ZEP (Da et al. 2017) may indicate the down-regulation of ZEP activity in darkness due to oxidation through the TRX system. Determination of ZEP activity in the dark-adapted state is rather challenging, since synthesis of Zx, which is the substrate of ZEP, requires illumination of leaves under *in vivo* conditions, which would result also in light activation of ZEP. To overcome this limitation, we induced Zx synthesis in isolated thylakoids in darkness by lowering the medium pH to 5.8 and addition of 20 mM ascorbate. 10 min of low pH treatment resulted in full activation of VDE and hence conversion of about 50 % of the total VAZ pool to Zx, resulting in a de-epoxidation state (DEPS) of about 50% (Fig. 1*A*). Subsequent adjustment of the medium pH to values of about 7.5 led to inactivation of VDE and allowed measurement of Zx epoxidation in darkness after addition of NADH and FAD (Fig. 1*A*). Within 30 min

of epoxidation, the DEPS decreased to about 25%, corresponding to a net change of the DEPS of 30% within 30 min (Fig. 1*C*). This result supports that ZEP is active in the dark-acclimated state. Addition of 1 mM DTT or TCEP did not increase ZEP activity (Fig. 1*A*), while higher concentrations of both reductants resulted in reduced ZEP activity (not shown). This demonstrates that ZEP activity cannot be enhanced by the reduction of putative disulfide bridges in the dark-acclimated state. ZEP activity in the light-acclimated state was determined with thylakoids isolated from pre-illuminated (30 min, 900 µmol photons $m^{-2}s^{-1}$) spinach leaves. Also, this treatment induced an increase of the DEPS to values of about 50% (Fig. 1*B*). Zx epoxidation was again induced by addition of NADH and FAD. Within 30 min of epoxidation, the DEPS decreased to values of about 25%, as before shown for the dark-acclimated enzyme (Fig. 1*A*). This corresponds to a similar net change of the DEPS (34%; Fig. 1*C*) as determined for the dark-acclimated ZEP. As expected, addition of DTT and TCEP did not result in significant changes of ZEP activity in the light-acclimated state (Fig. 1*B*). Although the net change of the DEPS was slightly (but not significantly) reduced in the dark-acclimated state, we thus conclude, that ZEP has similar activity in both acclimation states.

However, closer inspection of the characteristics of the two steps of epoxidation (Zx to antheraxanthin (Ax) and Ax to Vx) indicated that specifically the second step of epoxidation (Ax to Vx conversion) was altered in the dark state compared to the light state (Fig. 2 *A* and *B*). In fact, comparison of the net changes of the three xanthophylls showed, that the conversion of Zx to Ax was identical in both acclimation states (Fig. 2*C*), with initial (first 10 min) rates of Zx to Ax conversion of about 1.8 and 1.9 Zx / 1000 Chl (a+b) and min (Fig. 2*C*) in the dark-and light-acclimated state, respectively. In contrast, the intermediate Ax accumulated to significantly higher levels in the dark-acclimated state after 30 min of epoxidation (Fig. 2*D*), resulting in a reduced accumulation of Vx compared to the light-acclimated state of ZEP (Fig. 2*E*). Hence, only the second step of epoxidation (Ax to Vx) is slightly retarded in the dark-acclimated state.

The impact of ROS on ZEP activity

HL induced down-regulation of Zx epoxidation is supposed to be based either on phosphorylation or ROS modification of ZEP protein. To address the possible inactivation of ZEP by ROS, we examined the impact of singlet oxygen, superoxide and H_2O_2 on Zx epoxidation under *in vitro* conditions. For all following experiments, thylakoids from pre-illuminated leaves (30 min, 900 µmol photons $m^{-2}s^{-1}$) were used, and hence light-acclimated ZEP. It should further be noted that the initial DEPS obtained after pre-illumination differed among the experiments between about 40% and 50%, due to natural variations of leaf properties.

Singlet oxygen can be generated by rose bengal (RB) under illumination at moderate light intensities of about 150 µmol photons $m^{-2}s^{-1}$, superoxide by methyl viologen (MV) under the same illumination conditions, whereas H_2O_2 can be added directly to the assay medium. In presence of RB, a small but not significant reduction of ZEP activity was detected under conditions that have been applied successfully in earlier work to induce programmed cell death in Arabidopsis (Gutierrez et al. 2014) (Fig. 3*A*). Although we did not prove to which extent singlet oxygen was formed, this result suggests, that ZEP activity is not affected by singlet oxygen. It is further worth noting, that already 30 min illumination of thylakoids in absence of RB resulted in reduction of ZEP activity, indicating a general high sensitivity

of ZEP activity in diluted isolated thylakoid membranes. In contrast, addition of MV under the same illumination conditions resulted in nearly complete inhibition of Zx epoxidation (Fig. 3*B*), implying that ZEP activity is prone to either superoxide or H_2O_2. MV is reduced at the acceptor side of photosystem I (PSI) and rapidly transfers electrons to oxygen, leading to superoxide formation. However, superoxide can be efficiently dismutated to H_2O_2, either by superoxide dismutase (SOD) or non-enzymatically. To test, whether superoxide is converted to H_2O_2 we performed oxygen measurements with a Clark-type electrode. Efficient dismutation of superoxide to H_2O_2 should result in the consumption of two molecules of oxygen per electron transferred to MV. As control, we determined the rate of oxygen evolution from water oxidation at PSII in presence of ferricyanide (Fecy) as electron acceptor. Provided that MV and Fecy have similar efficiencies as electron acceptor at PSI, one would expect similar rates of oxygen consumption with MV compared to rates of oxygen evolution with Fecy, given that superoxide is completely dismutated to H_2O_2. Indeed, nearly same rates of oxygen evolution (76 µmol O_2 / mg Chl and h) in the presence of Fecy) and oxygen consumption (67 µmol O_2/mg Chl*h) in the presence of MV were determined (Fig. 4). Therefore, the presence of MV leads rather to accumulation of H_2O_2 than to accumulation of superoxide.

To test whether inhibition of Zx epoxidation by MV is based on H_2O_2 accumulation, we analyzed Zx epoxidation in presence of catalase and SOD inhibitors. Addition of catalase (1300 U/ml) led to inhibition of oxygen consumption in presence of MV (Fig. 4), indicating a complete conversion of superoxide to H_2O_2. Two SOD isoforms are known to be localized in plastids, Cu/ZnSOD and FeSOD (Kliebenstein et al. 1998). Cu/ZnSOd is known to be inhibited by KCN and FeSOD by H_2O_2 (Kliebenstein et al. 1998). Any inhibitory effect of these effectors on SOD activity should be reflected by inhibition of oxygen consumption in presence of MV. Addition of 1 mM KCN had no effect on oxygen consumption in presence of MV (Fig. 4*A*), indicating that Cu/ZnSOD does not contribute to superoxide conversion under our experimental conditions and implies that only FeSOD is active in isolated spinach thylakoids and thus responsible for superoxide conversion to H_2O_2. Addition of 1 mM H_2O_2 led to reduction of oxygen consumption (Fig. 4*A*), indicating that H_2O_2 is partially decomposed to H_2O and O_2 in the assay. This H_2O_2 decomposition was light-independent, but required the presence of thylakoid membranes (not documented). Due to this superimposed oxygen production by H_2O_2 decomposition, it was not possible to evaluate the specific impact of H_2O_2 on MV-dependent oxygen consumption.

Inhibition of Zx epoxidation by MV was not affected by addition of either KCN or H_2O_2 (Fig. 4*B*). This was expected for KCN, since CuZnSOD did not contribute to superoxide conversion to H_2O_2. In presence of both MV and H_2O_2, however, inhibition of ZEP could be related either to superoxide (due to inhibited conversion of superoxide to H_2O_2) or to H_2O_2 itself. To discriminate between these two possibilities, we thus tested the impact of catalase, which efficiently removes H_2O_2, on Zx epoxidation. Strikingly, inhibition of Zx epoxidation by MV was nearly completely abolished in presence of catalase (Fig. 4*B*). It can thus be concluded that inhibition of Zx epoxidation by MV is based on the formation of H_2O_2 and is not related to superoxide accumulation.

ZEP activity is sensitive to H_2O_2

To characterize in more detail the inhibitory effect of H_2O_2 on ZEP activity, we studied the direct impact of H_2O_2 on Zx epoxidation *in vitro*. In initial experiments, H_2O_2 was added at concentrations between 0.1

and 1 mM to thylakoids isolated from pre-illuminated leaves and Zx epoxidation was started without any time of pre-incubation. Under these conditions, significant inhibition of Zx epoxidation was observed after 30 min of epoxidation at the highest concentration of 1 mM H_2O_2 (Fig. 5*A*). The inhibitory effect was more pronounced after 30 min of pre-incubation with H_2O_2 (Fig. 5*B*). We thus conclude that ZEP activity is efficiently inhibited by H_2O_2 in a concentration-dependent way. Detailed analyses of the two steps of epoxidation indicated that H_2O_2 affects both steps of epoxidation (Figs. S1 and S2). However, the second step of epoxidation (Ax to Vx) was more affected than the first step (Zx to Ax) when epoxidation was analyzed without pre-incubation of thylakoids with H_2O_2 (Fig. S1). The same trend was observable after 30 min of pre-incubation with H_2O_2, but the overall extent of inhibition was more pronounced (Fig. S2). In fact, nearly no Vx formation was detectable within 30 min of epoxidation in presence of the highest H_2O_2 concentration of 1 mM (Fig. S2). When comparing the control samples without (Fig. 5*A*) and with (Fig. 5*B*) pre-incubation, it is obvious that also simply 30 min pre-incubation of thylakoid membranes in darkness resulted in partial inhibition of ZEP activity. This supports again the vulnerability of ZEP activity in diluted isolated thylakoid membranes. Finally, we tested the possible reversibility of the H_2O_2 induced inhibition of ZEP activity. To this end, thylakoids from pre-illuminated leaves were incubated for 5 min with H_2O_2 (10 mM). This high concentration was chosen to induce a strong inhibition of ZEP activity without long incubation. After short centrifugation, thylakoids were resuspended in epoxidation medium in absence of H_2O_2 and tested for ZEP activity. Under these conditions, ZEP activity could not be restored, even after addition of 1 mM DTT (Fig. S3), indicating that H_2O_2 induces irreversible inactivation of ZEP.

Discussion

ZEP activity is known to be regulated by light. Former work indicated that ZEP might have reduced activity in the dark-acclimated state (Da et al. 2017; Naranjo et al. 2016) and that ZEP is inactivated in response to HL stress (Bethmann et al. 2019; Kim et al. 2017; Reinhold et al. 2008). In the present *in vitro* study, we tested the activity of ZEP in the dark state and further investigated the possible role of ROS in ZEP inactivation.

Our data clearly show that ZEP is fully active in the dark-acclimated state under *in vitro* conditions. Moreover, addition of reductants, such as DTT or TCEP, had no stimulating effect on ZEP activity (Fig. 1). This supports the view that ZEP is not light-regulated by thiol modulation like other chloroplast proteins (Javier Cejudo et al. 2021; Knuesting and Scheibe 2018). The accumulation of Zx in darkness described in mutants affected in key enzymes of redox regulation in chloroplasts, such as NTRC (Naranjo et al. 2016) or TRXm (Da et al. 2017), is thus not related to direct thiol modulation of ZEP protein, but rather based on an indirect effect. Both studies provided evidence, that ZEP protein in Arabidopsis may form oligomers under non-reducing conditions, likely through intermolecular disulfide bonds (Da et al. 2017; Naranjo et al. 2016). In the work by Naranjo et al. (2016), oligomeric ZEP was found for recombinant ZEP protein only, but not for total leaf extracts (Naranjo et al. 2016), whereas Da et al. (2017) determined the oligomeric form in leaf extracts (Da et al. 2017). In both cases, however, these oligomers were convertible to monomers upon reduction by NTRC (Naranjo et al. 2016) or DTT (Da et al. 2017). The full activity of ZEP in spinach thylakoids thus implies, that ZEP protein is present in its monomeric form only.

Down-regulation of ZEP activity under pronounced HL stress has been proposed to be related to ROS formation (Bethmann et al. 2019; Reinhold et al. 2008). Here, we tested the impact on ROS on ZEP activity *in vitro*. Our analyses strongly support the view that ZEP is irreversibly inactivated by H_2O_2. ZEP activity is likely not inhibited by singlet oxygen, as can be judged from the unchanged Zx epoxidation after treatment with RB (Fig. 3). Our analyses further showed that superoxide is very unlikely to accumulate to reasonable levels due to efficient removal of this ROS, likely by thylakoid associated SOD.

The applied H_2O_2 concentrations are about 1000fold higher than those that have been estimated recently to occur in chloroplasts under *in vivo* conditions (Gerken et al. 2020). Nevertheless, it is reasonable to assume that the observed inhibition of ZEP activity is not related to unspecific reactions without biological relevance for several reasons: (i) We did not observe any impact of H_2O_2 on photosynthetic electron transport activity or VDE activity, excluding random unspecific inactivation of other proteins. (ii) The incubation time is likely a critical determinant for ZEP inactivation (Fig. 5). Compared to the 8 h HL treatment required for inactivation of ZEP in leaves (Bethmann et al. 2019), incubation for up to 30 min under *in vitro* conditions is rather short. It can thus be expected that longer exposure to much lower H_2O_2 concentrations may result in similar inactivation of ZEP under *in vivo* conditions. (iii) In presence of MV (Fig. 3*B*), ZEP was nearly completely inactivated, although the amount of H_2O_2 produced under these conditions can be estimated to be in the 10-100 µM range. Therefore, site and mode of H_2O_2 formation are likely critical for the impact on ZEP activity. In fact, it was recently shown that superoxide formation in the Mehler reaction occurs at the phylloquinone of the A-branch rather than at the distal iron-sulfur clusters of PSI (Kozuleva et al. 2021). This indicates the existence of a specific release valve for electrons when $NADP^+$ is fully reduced in HL. It can be assumed that local H_2O_2 concentration gradients exist in the chloroplast stroma depending on the distance to the site of H_2O_2 formation and ZEP localization. Hence, ZEP might be transiently exposed to much higher H_2O_2 concentrations at its binding site. Identification of the specific localization of ZEP at the stroma side of the thylakoid membrane is thus essential for the understanding of ZEP regulation. Since ZEP protein has no access to the appressed grana regions of the membrane, it is reasonable to assume that ZEP might be in close proximity to PSI. (iv) Oxygen measurements upon addition of 1 mM H_2O_2 showed that reasonable amounts of H_2O_2 are rapidly decomposed to H_2O and O_2 (Fig 4A). Hence, the effective H_2O_2 concentration in the assay is likely much lower than the added amount. (v) Compared to Arabidopsis or tobacco plants, the ZEP protein of spinach plants is less sensitive to HL induced inactivation (Bethmann et al. 2019) and might thus require higher H_2O_2 concentrations for inactivation. Comparative analyses in these two species might clarify this aspect. However, *in vitro* ZEP activity in isolated thylakoids of these two species were too low to allow reliable analyses. Conversely, the loss of ZEP activity after isolation of thylakoid membranes may reflect specific membrane properties that are required for the maintenance of ZEP activity *in vitro*, and which are missing in Arabidopsis and tobacco chloroplasts. These feature might also be related to the higher light stress sensitivity of ZEP in these two species compared to spinach and pea, which have been reported recently (Bethmann et al. 2019).

Our work further showed that ZEP activity is quite unstable in diluted isolated thylakoids, independent of illumination or treatment with inhibitors. In light of the specific inactivation of ZEP activity by H_2O_2, it seems reasonable to assume that ZEP is generally prone to oxidation under these conditions. Whether

this is related to oxidation of specific amino acids involved in substrate binding or conversion, or to destabilization of the interaction with the membrane, remains elusive.

Material and methods

Plant material

Spinach (*Spinacia oleracea*) was grown for 6-8 weeks under short-day conditions (8 h light / 16 h dark) in the greenhouse at light intensities of 250-300 µmol photons $m^{-2}s^{-1}$ and at temperatures between about 15 and 25 °C.

Isolation of thylakoid membranes and oxygen measurements

Thylakoid membranes were isolated from spinach leaves as described in (Krause et al. 1985). Chlorophyll content was determined according to (Porra et al. 1989). Changes in the oxygen concentration were determined by a Clark-type electrode. Thylakoids equivalent to 30 µg Chl / mL were suspended in a medium containing 0.33 M sorbitol, 40 mM Hepes/NaOH pH 7.5, 10 mM NaCl and 5 mM $MgCl_2$. $K_3[Fe(CN)_6]^{3-}$ (Fecy, 1 mM) or methyl viologen (MV, 10 µM) were added as electron acceptor, as indicated, and 2 µM Gramicidin D and 5 mM NH_4Cl were added as uncouplers. Samples were illuminated at a light intensity of 1,000 µmol photons m^{-2} s^{-1} for induction of maximum electron transport rates, and at a light intensity of 150 µmol photons m^{-2} s^{-1} in all other experiments.

In vitro assay of Zx epoxidation

For analysis of Zx epoxidation, thylakoid membranes equivalent to 30 µg chlorophyll were resuspended in 1 mL reaction medium consisting of 0.4 M sorbitol, 50 mM Hepes/NaOH pH 7.5, 0.3 mg/ml BSA and 5 mM NH_4Cl. Epoxidation was started by addition of 0.5 mM NADH and 1 mM FAD. To assess ZEP activity in the dark-acclimated state, thylakoids were isolated from leaves of 16 h dark-adapted plants. To induce Zx formation in darkness, thylakoid membranes were first incubated for 10 min in a medium containing 0.4 M sorbitol, 10 mM MES, pH 5.4, and 20 mM ascorbate. Subsequently, the pH was adjusted to 7.5 by addition of Hepes buffer to a final concentration of 50 mM, and epoxidation was started by addition of 0.5 mM NADH and 1 mM FAD. ZEP activity in the light-acclimated state was determined with thylakoid membranes isolated from leaves that were pre-illuminated for 30 min at a light intensity of 1000 µmol photons m^{-2} s^{-1}. In all cases, the reaction was stopped at indicated time by rapid cooling of an aliquot of 200 µl in liquid nitrogen.

Pigment analyses

The xanthophyll content was determined by HPLC analysis of the pigment content according to (Färber et al. 1997). Frozen thylakoid samples were thawed at 4°C and collected by short centrifugation (2 min, 10,000 x g). Pigments were extracted by addition of 1 ml 100% acetone and proteins were removed by centrifugation for 5 min at 10,000 x g. After filtration (0.2 µm pores size), the supernatant was directly used for HPLC analysis. To quantify ZEP activity, the conversion of Zx to Vx was evaluated in two different ways: (1) as change of the de-epoxidation state (DEPS = [(Zx+0.5Ax) / (Vx+Ax+Zx)] x 100), which reflects the percentage of epoxy groups. (2) As changes of the content of the single xanthophyll cycle pigments (Vx, Ax and Zx) on Chl basis.

Statistical analyses

Statistical analyses of pigment composition were performed using GraphPad Prism (version 6.01). ANOVA was used to test significant differences between diverse conditions (light conditions, electron acceptors, ROS). The post hoc test (Tukey HSD) or Dunnett's test were performed for multiple comparison analysis. Significant differences were marked by asterisk (* = $p < 0.05$; ** = $p < 0.01$; ***$p<0.001$) or by different letters ($p < 0,5$).

Data availability

All data are contained within the article.

Acknowledgments

This work was supported by the Deutsche Forschungsgemeinschaft (JA 665/12-1 to P.J.).

Author Contributions

S.B. and P.J. designed and supervised the research; D.H. and S.B. performed the experiments; S.B. and D.H. analyzed data; P.J. wrote the original draft; D.H., S.B. and P.J. reviewed and edited the manuscript.

References

Bethmann, S., Melzer, M., Schwarz, N. and Jahns, P. (2019) The zeaxanthin epoxidase is degraded along with the D1 protein during photoinhibition of photosystem II. Plant Direct 3, https://doi.org/10.1002/pld3.185.

Da, Q., Sun, T., Wang, M., Jin, H., Li, M., Feng, D., et al. (2017) M-type thioredoxins are involved in the xanthophyll cycle and proton motive force to alter NPQ under low-light conditions in Arabidopsis. Plant Cell Rep., https://doi.org/10.1007/s00299-017-2229-6.

Färber, A. and Jahns, P. (1998) The xanthophyll cycle of higher plants: influence of antenna size and membrane organization. Biochim. Biophys. Acta 1363: 47-58.

Färber, A., Young, A.J., Ruban, A.V., Horton, P. and Jahns, P. (1997) Dynamics of xanthophyll-cycle activity in different antenna subcomplexes in the photosynthetic membranes of higher plants: the relationship between zeaxanthin conversion and nonphotochemical fluorescence quenching. Plant Physiol. 115: 1609-1618.

Gerken, M., Kakorin, S., Chibani, K. and Dietz, K.-J. (2020) Computational simulation of the reactive oxygen species and redox network in the regulation of chloroplast metabolism. Plos Comp. Biol. 16, e1007102.

Gutierrez, J., Gonzalez-Perez, S., Garcia-Garcia, F., Daly, C.T., Lorenzo, O., Revuelta, J.L., et al. (2014) Programmed cell death activated by Rose Bengal in Arabidopsis thaliana cell suspension cultures requires functional chloroplasts. J. Exp. Bot. 65: 3081-3095.

Hager, A. (1966) Die Zusammenhänge zwischen lichtinduzierten Xanthophyll- Umwandlungen und der Hill-Reaktion. Ber. Dtsch. Bot. Ges. 79: 94-107.

Hager, A. (1969) Light dependent decrease of the pH-value in a chloroplast compartment causing the enzymatic interconversion of violaxanthin to zeaxanthin; relations to photophosphorylation. Planta 89: 224-243.

Härtel, H., Lokstein, H., Grimm, B. and Rank, B. (1996) Kinetic studies on the xanthophyll cycle in barley leaves - Influence of antenna size and relations to nonphotochemical chlorophyll fluorescence quenching. Plant Physiol. 110: 471-482.

Havaux, M. (1998) Carotenoids as membrane stabilizers in chloroplasts. Trends Plant Sci. 3: 147-151.

Havaux, M. and Niyogi, K.K. (1999) The violaxanthin cycle protects plants from photooxidative damage by more than one mechanism. Proc. Natl. Acad. Sci. USA 96: 8762-8767.

Hoang, M.H., Kim, H.-S., Zulfugarov, I.S. and Lee, C.-H. (2020) Down-Regulation of zeaxanthin epoxidation in vascular plant leaves under normal and photooxidative stress conditions. J. Plant Biol. https://doi.org/10.1007/s12374-020-09260-8.

Horton, P., Wentworth, M. and Ruban, A. (2005) Control of the light harvesting function of chloroplast membranes: The LHCII-aggregation model for non-photochemical quenching. FEBS Lett. 579: 4201-4206.

Jahns, P., Latowski, D. and Strzalka, K. (2009) Mechanism and regulation of the violaxanthin cycle: The role of antenna proteins and membrane lipids. Biochim Biophys Acta 1787: 3-14.

Jahns, P. and Miehe, B. (1996) Kinetic correlation of recovery from photoinhibition and zeaxanthin epoxidation. Planta 198: 202-210.

Javier Cejudo, F., Gonzalez, M.-C. and Manuel Perez-Ruiz, J. (2021) Redox regulation of chloroplast metabolism. Plant Physiol. 186: 9-21.

Kim, H.-S., Minh Hien, H., Jeon, Y.A., Wu, G. and Lee, C.-H. (2017) Differential down-regulation of zeaxanthin epoxidation in two rice (*Oryza sativa* L.) cultivars with different chilling sensitivities. J. Plant Biol. 60: 413-422.

Kliebenstein, D.J., Monde, R.A. and Last, R.L. (1998) Superoxide dismutase in Arabidopsis: An eclectic enzyme family with disparate regulation and protein localization. Plant Physiol. 118: 637-650.

Knuesting, J. and Scheibe, R. (2018) Small molecules govern thiol redox switches. Trends Plant Sci. 23: 769-782.

Kozuleva, M., Petrova, A., Milrad, Y., Semenov, A., Ivanov, B., Redding, K.E., et al. (2021) Phylloquinone is the principal Mehler reaction site within photosystem I in high light. Plant Physiol. 186: 1848-1858.

Krause, G.H., Köster, S. and Wong, S.Y. (1985) Photoinhibition of photosynthesis under anaerobic conditions studied with laves and chloroplasts of *Spinacia oleracea* L. Planta 165: 430-438.

Kress, E. and Jahns, P. (2017) The dynamics of energy dissipation and xanthophyll conversion in Arabidopsis indicate an indirect photoprotective role of zeaxanthin in slowly inducible and relaxing components of non-photochemical quenching of excitation energy. Front. Plant Sci. 8: 2094.

Leitsch, J., Schnettger, B., Critchley, C. and Krause, G.H. (1994) Two mechanisms of recovery from photoinhibition in vivo: Reactivation of photosystem II related and unrelated to D1 protein turnover. Planta 194: 15-21.

Li, Z.R., Wakao, S., Fischer, B.B. and Niyogi, K.K. (2009) Sensing and responding to excess light. Annu. Rev. Plant Biol. 60: 239-260.

Moller, I.M., Jensen, P.E. and Hansson, A. (2007) Oxidative modifications to cellular components in plants. Annu. Rev. Plant Biol. 58: 459-481.

Naranjo, B., Mignee, C., Krieger-Liszkay, A., Hornero-Mendez, D., Gallardo-Guerrero, L., Javier Cejudo, F., et al. (2016) The chloroplast NADPH thioredoxin reductase C, NTRC, controls non-photochemical quenching of light energy and photosynthetic electron transport in Arabidopsis. Plant Cell Environ. 39: 804-822.

Nilkens, M., Kress, E., Lambrev, P.H., Miloslavina, Y., Müller, M., Holzwarth, A.R., et al. (2010) Identification of a slowly inducible zeaxanthin-dependent component of non-photochemical quenching of chlorophyll fluorescence generated under steady state conditions in Arabidopsis. Biochim. Biophys. Acta 1797: 466-475.

Pfündel, E.E. and Dilley, R.A. (1993) The pH dependence of violaxanthin deepoxidation in isolated pea chloroplasts. Plant Physiol. 101: 65-71.

Porra, R.J., Thompson, W.A. and Kriedemann, P.E. (1989) Determination of accurate extinction coefficients and simultaneous equations for assaying chlorophyll a and b extracted with four different solvents: verification of the concentration of chlorophyll standards by atomic absorption spectroscopy. Biochim. Biophys. Acta 975: 384-394.

Reinhold, C., Niczyporuk, S., Beran, K. and Jahns, P. (2008) Short-term down-regulation of zeaxanthin epoxidation in *Arabidopsis thaliana* in response to photo-oxidative stress conditions. Biochim. Biophys. Acta 1777: 462-469.

Siefermann, D. and Yamamoto, H.Y. (1975) Properties of NADPH and oxygen-dependent zeaxanthin epoxidation in isolated chloroplasts. Arch. Biochem. Biophys. 171: 70-77.

Thiele, A., Schirwitz, K., Winter, K. and Krause, G.H. (1996) Increased xanthophyll cycle activity and reduced D1 protein inactivation related to photoinhibition in two plant systems acclimated to excess light. Plant Sci. 115: 237-250.

Verhoeven, A.S., Adams, W.W.I. and Demmig-Adams, B. (1996) Close relationship between the state of the xanthophyll cycle pigments and photosystem II efficiency during recovery from winter stress. Physiol. Plant. 96: 567-576.

Xu, C.C., Jeon, Y.A., Hwang, H.J. and Lee, C.H. (1999) Suppression of zeaxanthin epoxidation by chloroplast phosphatase inhibitors in rice leaves. Plant Sci. 146: 27-34.

Yamamoto, H.Y., Wang, Y. and Kamite, L. (1971) Chloroplast absorbance change from violaxanthin de-Epoxidation. A possible component of 515 nm changes. Biochem. Biophys. Res. Comm. 42: 37-42.

Figure 1

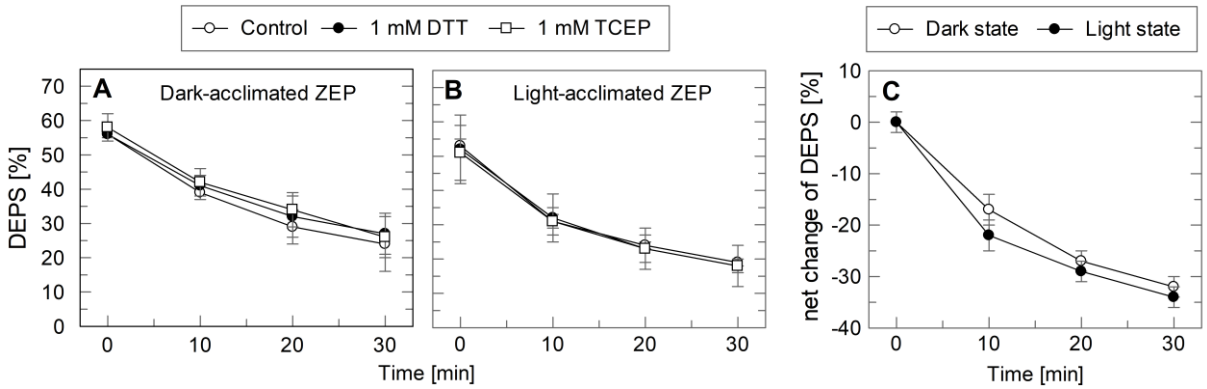

Figure 1. ZEP activity in the dark- and light-acclimated state. Changes in the de-epoxidation state (DEPS) of the xanthophyll cycle pigments, calculated as DEPS = (0.5 Ax+Zx)/(Vx+Ax+Zx)*100. **(A)** ZEP activity in the dark-acclimated state. Dark synthesis of Zx in thylakoid membranes isolated from dark-adapted plants was induced by lowering the medium pH to 5.8 in presence of ascorbate. After adjustment of the medium pH to 7.5, Zx epoxidation was started by addition of NADH and FAD. **(B)** ZEP activity in the light-acclimated state. Synthesis of Zx was induced by 30 min illumination of intact leaves at a light intensity of 1000 µmol photons m^{-2} s^{-1}. After isolation of thylakoid membranes, Zx epoxidation was started by addition of NADH and FAD. (**C**) Net changes of the DEPS. Initial DEPS values were normalized to 0 and absolute values of the differences are shown for each time point. Mean values ± SD of 3 independent biological replicates are shown.

Figure 2

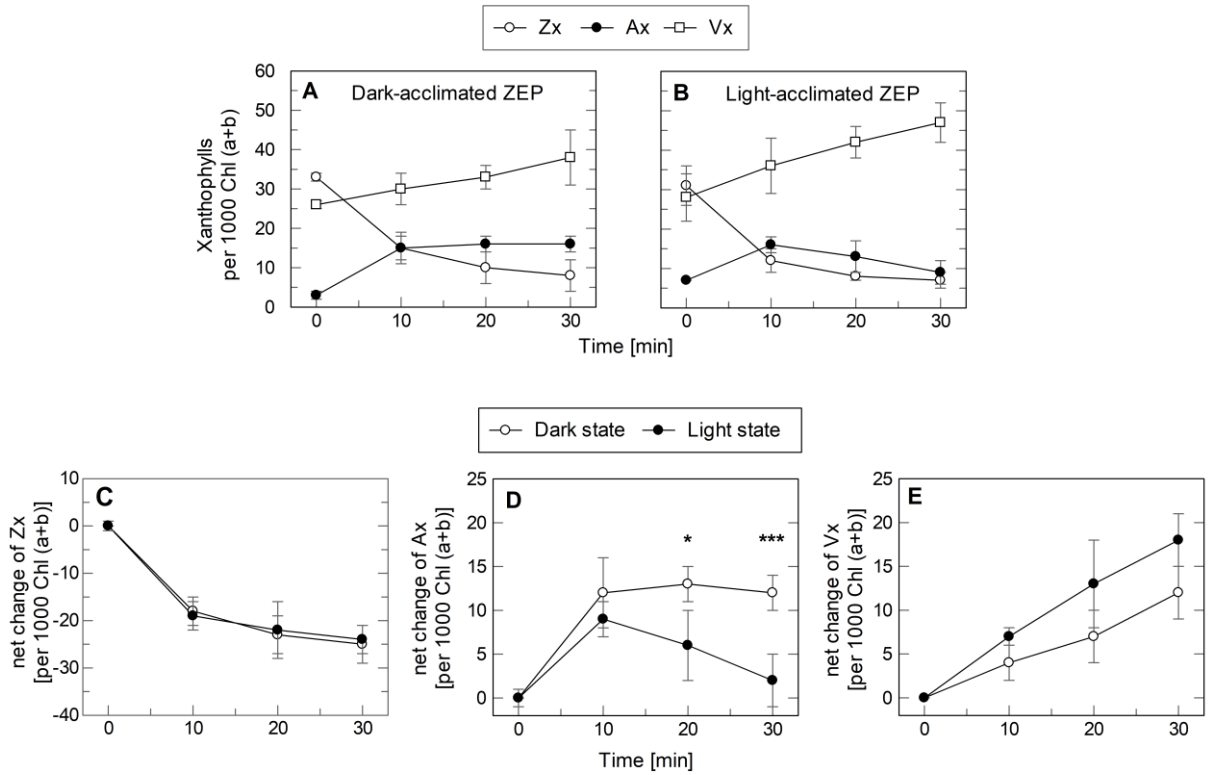

Figure 2. Epoxidation reactions in the dark- and light-acclimated state. (A, B) Changes in the amount of the xanthophyll cycle pigments violaxanthin (Vx), antheraxanthin (Ax) and zeaxanthin (Zx) during epoxidation in the dark-acclimated (A) and the light-acclimated (B) state. **(C, D, E)** Net changes of the xanthophyll cycle pigments. Initial amounts of the xanthophylls were normalized to 0 and absolute values of the differences are shown for Zx (C), Ax (D) and Vx (E) for each time point. Mean values ± SD of 3 independent biological replicates are shown. Asterisks indicate significant differences (* = $p < 0.05$; *** = $p < 0.001$) between the corresponding values in the dark- and light state.

Figure 3

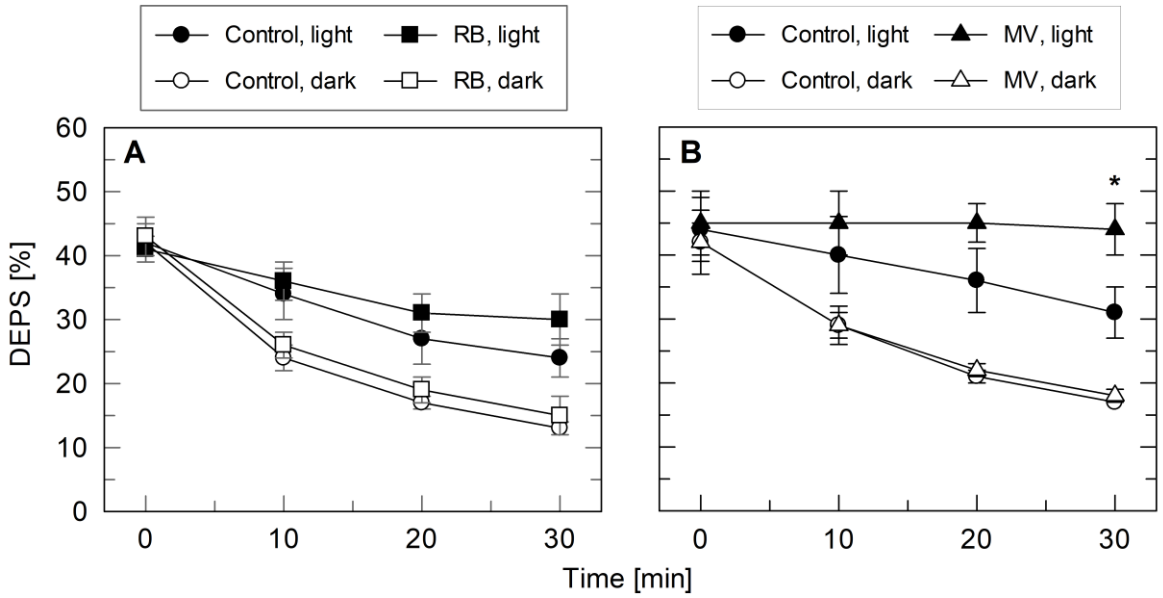

Figure 3. Impact of singlet oxygen and superoxide formation on ZEP activity. Synthesis of Zx was induced by 30 min illumination of intact leaves (1000 µmol photons m^{-2} s^{-1}). Isolated thylakoids resuspended in epoxidation medium were treated with **(A)** 5 µM rose bengal (RB) or **(B)** 10 µM methyl viologen (MV) and then exposed for 30 min in light (150 µmol photons m^{-2} s^{-1}). After addition of NADH and FAD, epoxidation was measured for up to 30 min. For dark samples, epoxidation was measured without 30 min pre-incubation. Mean values ± SD of 3 independent biological replicates are shown. The asterisk indicates significant differences (*= $p < 0.05$) between the values of the control and MV-treated samples in the light-exposed samples.

Figure 4

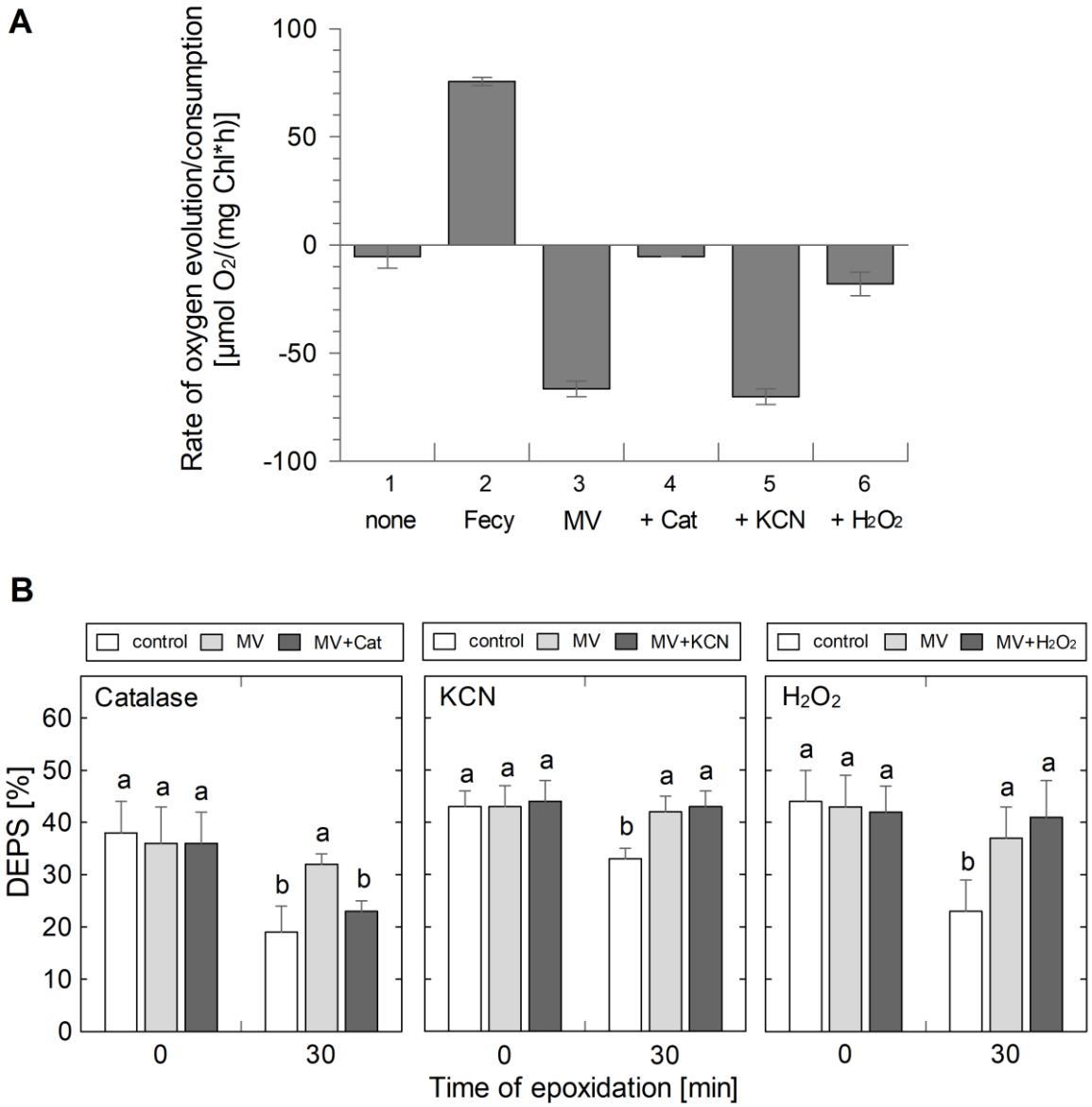

Figure 4. Impact of inhibitors on oxygen evolution and ZEP activity. (A) The rate of light-induced oxygen evolution measured with isolated thylakoid membranes with following additions 1: No artificial electron acceptor (none); 2: 1 mM $K_3[Fe(CN)_6]^{3-}$ (Fecy); 3: 10 µM methyl viologen (MV); 4: MV + 1300 units/ml catalase (Cat); 5: MV + 1 mM KCN (KCN), 6: MV + 1 mM H_2O_2. **(B)** ZEP activity was derived from determination of the de-epoxidation state (DEPS) of the xanthophyll cycle pigments before (0) and after 30 min epoxidation (30) in presence of 1300 units/ml catalase, 1 mM KCN or 1 mM H_2O_2, as indicated. Letters indicate significant differences ($p < 0.05$). Mean values ± SD of 3 independent biological replicates are shown.

Figure 5

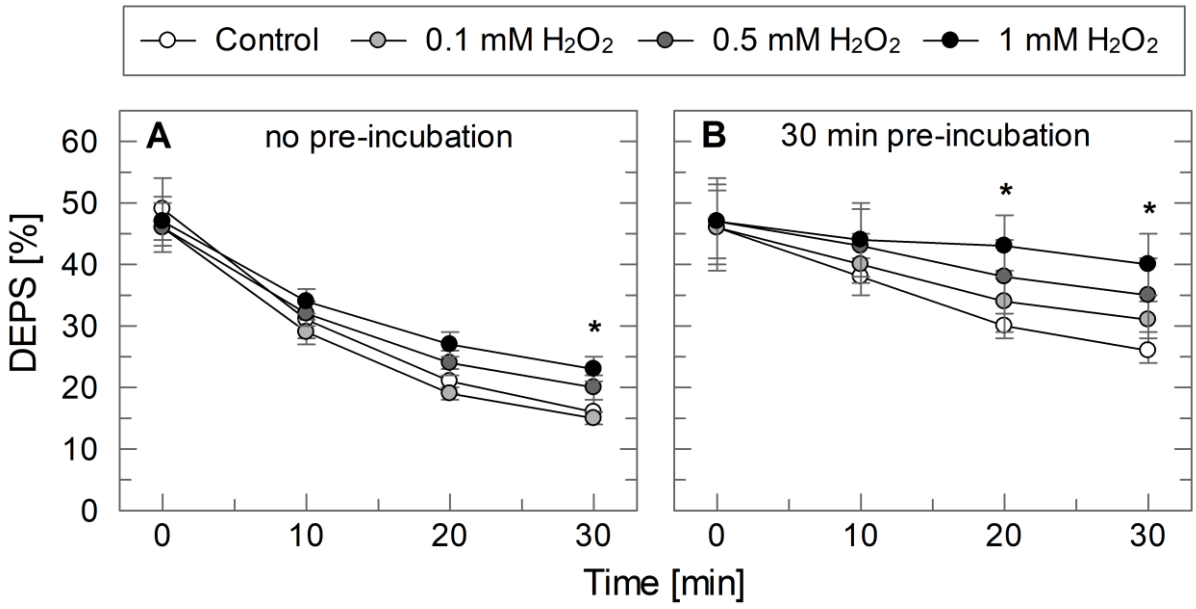

Figure 5. Impact of H_2O_2 on ZEP activity. Synthesis of Zx was induced by 30 min illumination of intact leaves (1000 µmol photons m^{-2} s^{-1}). Isolated thylakoids resuspended in epoxidation medium were treated in the dark with different H_2O_2 concentrations. Epoxidation was started by addition of NADH and FAD directly after addition of H_2O_2 **(A)** or after 30 min of incubation with H_2O_2 **(B).** Mean values ± SD of 3 independent biological replicates are shown. Asterisks indicate significant differences (*= $p < 0.05$) between control values and values of samples treated with 1 mM H_2O_2.

Figure S1

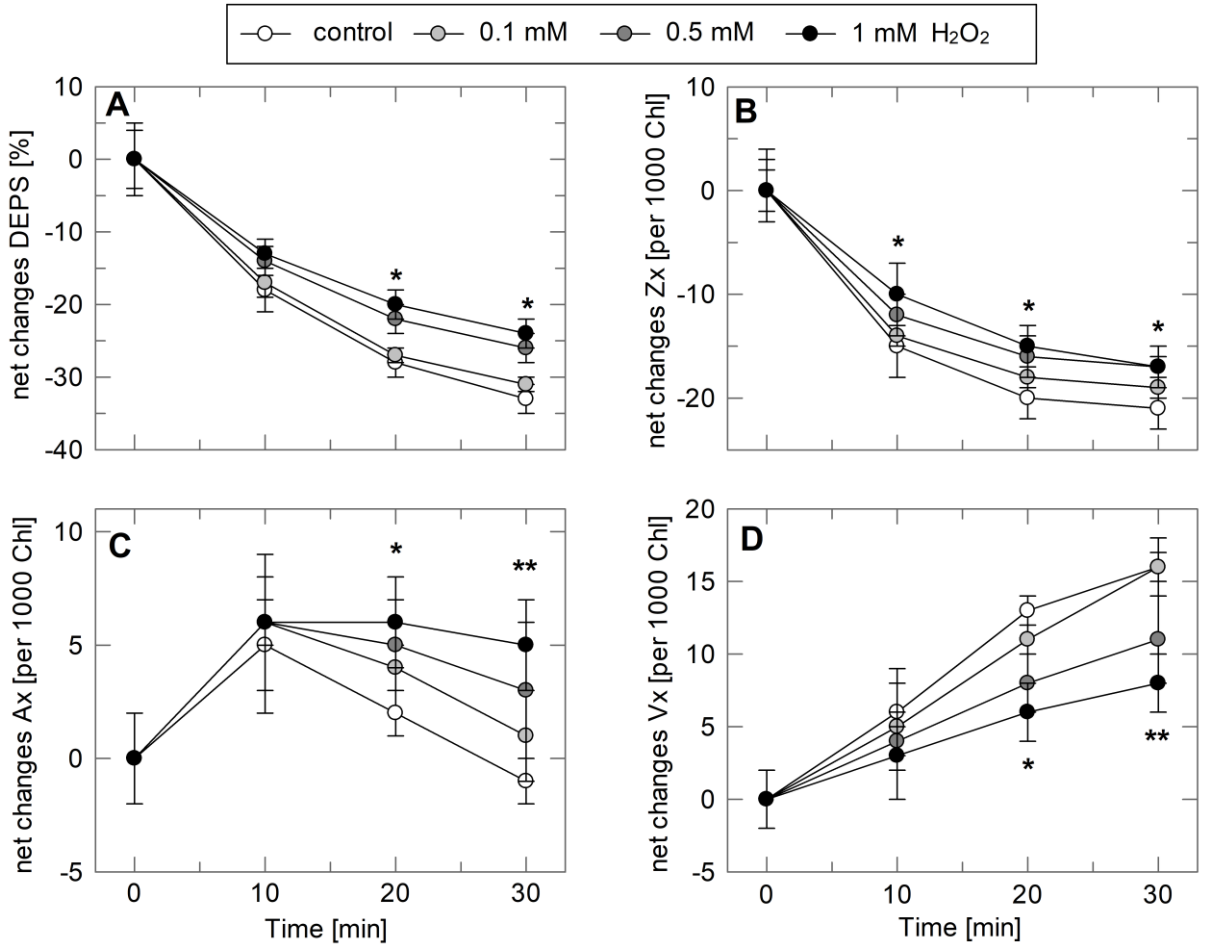

Figure S1. Impact of H_2O_2 without pre-incubation on the epoxidation reactions. Net changes of **(A)** the de-epoxidation state (DEPS) of the xanthophyll cycle pigments, **(B)** the zeaxanthin (Zx) content, **(C)** the antheraxanthin (Ax) content and **(D)**, the violaxanthin (Vx) content are shown. Mean values ± SD of 3 independent biological replicates are shown. For clarity, significant differences (* = $p < 0.05$; ** = $p < 0.01$) are indicated by asterisks only between the values of the highest H_2O_2 concentration (1 mM) and control values.

Figure S2

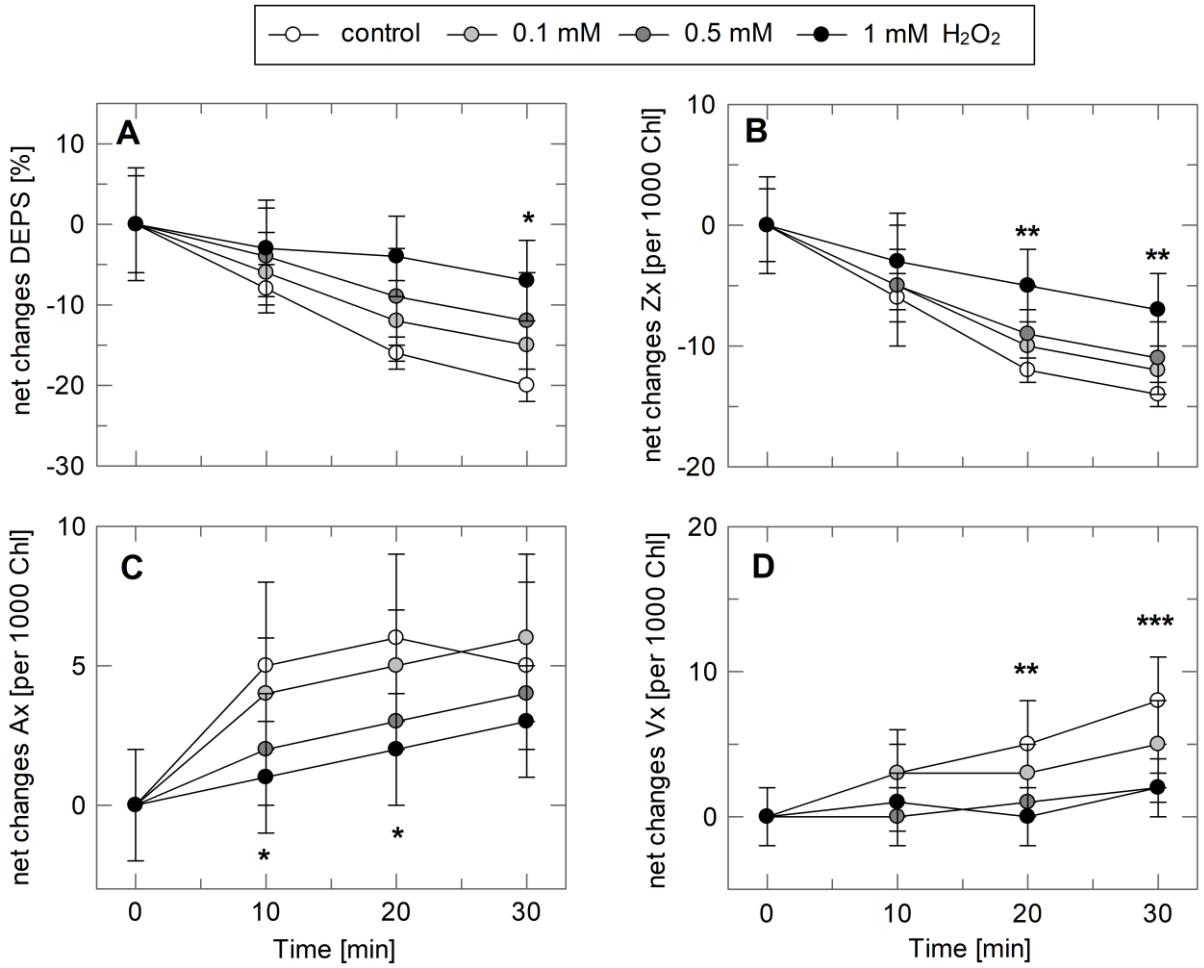

Figure S2. Impact of H_2O_2 after 30 min pre-incubation on the epoxidation reactions. Net changes of **(A)** the de-epoxidation state (DEPS) of the xanthophyll cycle pigments, **(B)** the zeaxanthin (Zx) content, **(C)** the antheraxanthin (Ax) content and **(D)**, the violaxanthin (Vx) content are shown. Mean values ± SD of 3 independent biological replicates are shown. For clarity, significant differences (* = $p < 0.05$; ** = $p < 0.01$; ***$p<0.001$) are indicated by asterisks only between the values of the highest H_2O_2 concentration (1 mM) and control values.

Figure S3

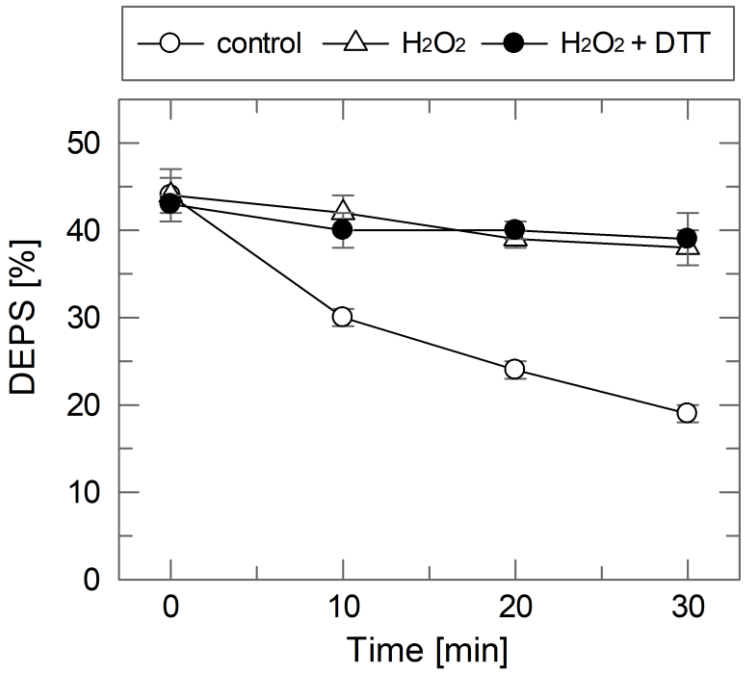

Figure S3. Reversibility of ZEP inactivation by H_2O_2. Synthesis of Zx was induced by 30 min illumination of intact leaves (1000 µmol photons m^{-2} s^{-1}). Isolated thylakoids resuspended in epoxidation medium were treated in the dark without and with 10 mM H_2O_2 for 5 min. After incubation, thylakoids were spun down by short centrifugation and resuspended in epoxidation medium. Epoxidation was started by addition of NADH and FAD. Mean values ± SD of 3 independent biological replicates are shown.

9. Conclusions

Photo-oxidative stress is one of the most challenging abiotic stress factors since ROS are inevitably produced in the chloroplast along with photosynthetic light utilization (Mller et al., 2007). Hence, the acclimation to short-term and long-term HL stress as well as to fluctuating light conditions is essential for plant fitness in the field. To achieve this goal, plants have developed many strategies, aiming either at the reduction of ROS formation or at the detoxification of ROS (Li et al., 2009). The photoprotective pigment Zx serves crucial functions in this context since Zx is involved in both the qE and the qZ mechanism of NPQ and hence, in the dissipation of excess energy and consequently the formation of ROS (Horton et al., 2005; Nilkens et al., 2010). Also, Zx acts as antioxidant in the lipid phase of the thylakoid membrane by detoxifying ROS independently of NPQ (Havaux and Niyogi, 1999). Furthermore, a close correlation of Zx epoxidation and relaxation of the qI component of NPQ (= photoinhibition) has been shown (Jahns and Miehe, 1996; Verhoeven et al., 1996; Kress and Jahns, 2017). In the present work, the concerted down-regulation of ZEP and PSII activity during photoinhibition has been further analyzed in different plant species (Arabidopsis, tobacco, pea and spinach) in context with the short-term acclimation (manuscript 1) and the long-term acclimation (manuscript 2I) to HL. Moreover, the role of redox-regulation and ROS-induced inactivation of ZEP has been analyzed in detail under *in vitro* conditions (manuscript 3). Although this work revealed a number of important results, it also raised questions that should be addressed in future work:

1. The possible target sites of the H_2O_2-induced post-translational modification of ZEP are still unknown and need to be identified.
2. The close correlation of ZEP and D1 degradation may reflect a direct functional link of both processes. Mutants that are affected in different components of the PSII repair cycle might help to prove or disprove this close correlation of ZEP/D1 degradation.
3. To better understand ZEP regulation, the impact of increased ZEP amounts on the regulation of ZEP activity and ZEP degradation should be investigated.

1. Possible post-translational modifications of ZEP by H_2O_2

   The inactivation of ZEP by H_2O_2 occurs in a concentration- and time-dependent manner. To gain a better understanding of the molecular basis of ZEP inactivation, possible targets (likely Cys and/or methionine (Met) residues) of H_2O_2 oxidation need to be identified. The structure of ZEP protein is not solved, but it is known that ZEP consists of a C-terminal cTP, a central lipocalin/monooxygenase domain and a N-terminal FHA-domain (Fig. 10, introduction). An alignment of ZEP sequences of six different species (Arabidopsis, pea, spinach, tobacco, rice and barley) revealed that five Cys and seven Met residues are

conserved among those species (data not shown). According to Barrero et al. (2005), three of the conserved Cys residues (Fig. 10, introduction) and six of the conserved Met residues are localized in the central lipocalin/monooxygenase domain in *A. thaliana*. The predicted structure of ZEP in *Oryza sativa* (AlphaFold Protein Structure Database) was used to better visualize the localization of possible target sites in ZEP. As depicted in Figure 12, most conserved Cys and Met residues are located in a rather narrow area in the lipocalin/monooxygenase domain, which contains the catalytic site of ZEP. All of these Cys and Met residues are thus potential targets for H_2O_2 oxidation, which might be involved in the HL-induced inactivation of ZEP.

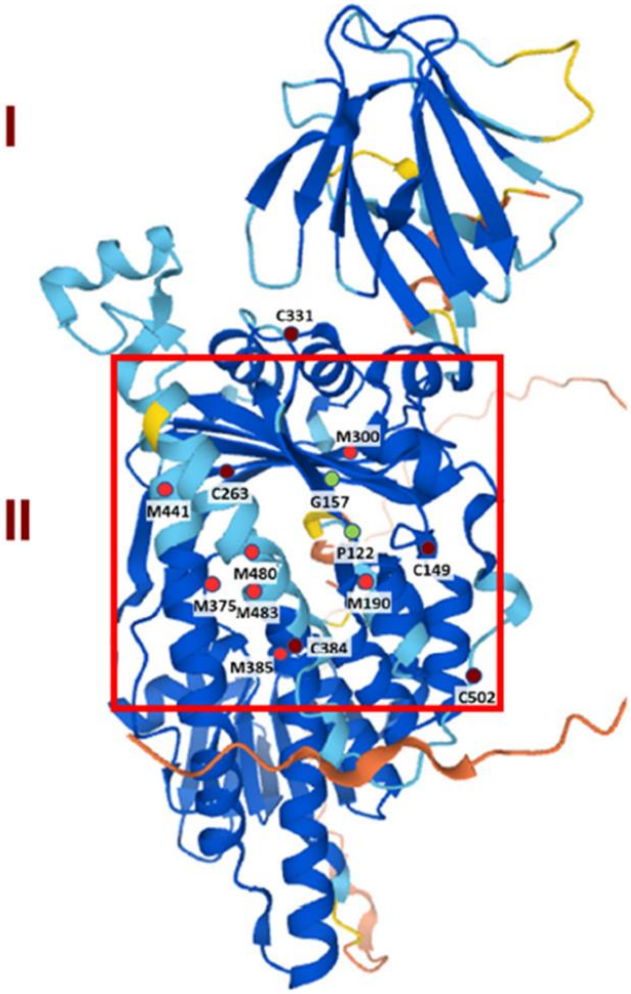

Figure 12: Predicted structure of ZEP protein from rice (*Oryza sativa*) (AlphaFold Protein Structure Database). The overall structure of ZEP with the N-terminal FHA-domain (I) and the central lipocalin/monooxygenase domain (II) is depicted. Seven conserved Met residues (M, light red) and five conserved Cys residues (C, dark red) are represented as dots. Moreover, the two residues proline P122 (light green) and glycine G157 (light green), whose mutation leads to inactivation of ZEP, are shown. The lipocalin/monooxygenase domain (red box) likely represents the active site.

Mass spectrometric (MS) analyses (performed by Molecular Proteomics Laboratory (MPL), Heinrich Heine University) of spinach thylakoids treated with H_2O_2 identified oxidations of Met residues but no oxidations of any Cys residues. Although Met oxidation is frequently observed in proteins during MS analyses and thus were partly visible in dark-acclimated ZEP, increased oxidation of these Met was found in HL treated samples (not shown). This supports a possible role of Met oxidation during HL-induced inactivation of ZEP. Since the amount of ZEP protein is rather low in chloroplasts (about 1 ZEP per 10 PSII, Schwarz et al., 2015), ZEP overexpressing (OE) lines should be included in this approach to confirm this assumption. Moreover, site-directed mutagenesis of the conserved Cys and Met residues should be performed to identify those residues that are involved in the regulation of ZEP activity. Ideally, such experiments should be applied to recombinant ZEP protein. However, it was impossible so far in several laboratories to purify enzymatically active recombinant ZEP. Therefore, the impact of mutagenesis on ZEP regulation has to be analyzed after transient expression *in vivo*.

Besides post-translational modification by ROS, the phosphorylation of ZEP or of other proteins represents an additional way to regulate ZEP activity upon light stress. So far, MS-based analyses did not identify any amino acids of ZEP protein that were phosphorylated in response to HL. Nevertheless, this analysis should also be repeated with ZEP OE lines, to overcome possible limitations by low ZEP protein amounts. The N-terminal FHA-domain might be involved in the putative regulation of ZEP activity by phosphorylation of e.g. other thylakoid membrane proteins, since FHA domains are known to recognize phosphothreonine epitopes (Durocher and Jackson, 2002). Hence, identification of ZEP interaction partners is required to identify such proteins.

2. Degradation of ZEP

Earlier studies already showed a close correlation of ZEP activity and PSII activity under photoinhibitory conditions (Jahns and Miehe, 1996; Verhoeven et al., 1996; Kress and Jahns, 2017). The present work further identified a parallel degradation of ZEP and D1 protein. It seems obvious, that crucial components of the D1 turnover, like proteases or kinases, might also be involved in the inactivation and degradation of ZEP protein. To test whether the knockout of these components of the D1 turnover maintains or abolishes the close correlation of ZEP degradation and D1 turnover and to identify possible enzymes that are involved in ZEP degradation, different *A. thaliana* mutants that are affected in D1 turnover were analyzed concerning their HL responses. The mutants *var1* and *var2*, that are lacking the proteases FtsH5 and FtsH2, respectively, displayed a complete inactivation of PSII, but only a partial inhibition of ZEP (data not shown). However, a partial degradation

of both, D1 and ZEP protein, was detectable in both mutants to similar levels as the corresponding wildtype (data not shown), indicating that FtsH2 and FtsH5 alone are not responsible for ZEP degradation. Since FtsH proteases form complexes (type A = FtsH1 and 5, type B = FtsH2 and 8) it might be possible that FtsH complex type A compensates for the function of type B in *var2* mutants and that FtsH complex type B compensates for the function of type A in *var1* mutants. Similar results were obtained when performing the same experiments with *deg2* mutants (data not shown). The downregulation of PSII and ZEP activity occurred simultaneously while D1 and ZEP were degraded in parallel in similar levels compared to the wildtype. These results indicate that the protease Deg2 is not exclusively responsible for ZEP degradation. Hence, ZEP degradation is probably not based on one single protease but rather on a network of several proteases. To verify this assumption, recombinant ZEP protein and different recombinant proteases (Deg2, FtsH1, FtsH2, FtsH5 and FtsH8) should be studied to test whether ZEP protein is a target protein for one or several of these proteases. Furthermore, the response of *stn7*, *stn8* and *stn7xstn8* mutants, which are affected in protein kinases involved in PSII proteins, to HL treatment revealed an unchanged correlation between D1 turnover and ZEP degradation. *stn8* and *stn7xstn8* mutants exhibited a higher susceptibility to photoinhibition as well as a reduced degradation of D1 protein, but ZEP activity and degradation were unaltered, which indicates that ZEP inactivation is independent of phosphorylation upon the D1 turnover.

3. Overexpression of ZEP

This present work revealed that the tested plant species were able to acclimate to different growth conditions in order to improve the photosynthetic light utilization and hence, plant fitness. It would be of interest to determine, to what extent the amount of ZEP protein might influence the impact on ZEP regulation and/or photoprotection. Plants with increased amounts of ZEP protein should therefore be analyzed with respect to (1) ZEP regulation in response to HL and (2) HL sensitivity and ZEP degradation. To address this aspect, so-called VPZ overexpression lines, that have been generated in *A. thaliana* (Garcia-Molina and Leister, 2020) and *Nicotiana tabacum* (Kromdijk et al., 2016) to improve photosynthesis, were investigated. These mutants were shown to have a higher amount of VDE (30-fold higher in tobacco, 5.2-fold higher in Arabidopsis), PsbS (4-fold in tobacco, 2.4-fold in Arabidopsis) and ZEP (74-fold in tobacco, 5.1-fold in Arabidopsis), which resulted in higher NPQ capacity (especially qE) and a faster induction and relaxation of qE (Kromdijk et al., 2016; Garcia-Molina and Leister, 2020). Moreover, the relaxation of qZ occurred faster than in the corresponding wildtype (Kromdijk et al., 2016; Garcia-Molina and Leister, 2020). In order to evaluate the impact of higher ZEP levels on xanthophyll

cycle conversion during and after HL exposure, photoprotective parameters as well as ZEP accumulation and regulation were determined. In contrast to the results from Kromdijk et al. (2016), MS-based analyses revealed an only 3.5- to 6-fold higher amount of ZEP in the three independent VPZ lines (VPZ #23: 6-fold higher, VPZ #34: 3.5-fold higher, VPZ #56: 4.5-fold higher), whereas the Arabidopsis VPZ lines #2, #4 and #7 displayed a 4-fold higher amount of ZEP protein (data not shown). Studies on the distribution of ZEP showed that the additional pool of ZEP predominantly interacts with the thylakoid membrane (Fig. 13), indicating that the binding capacity of the thylakoid membrane is not limiting the amount of ZEP protein.

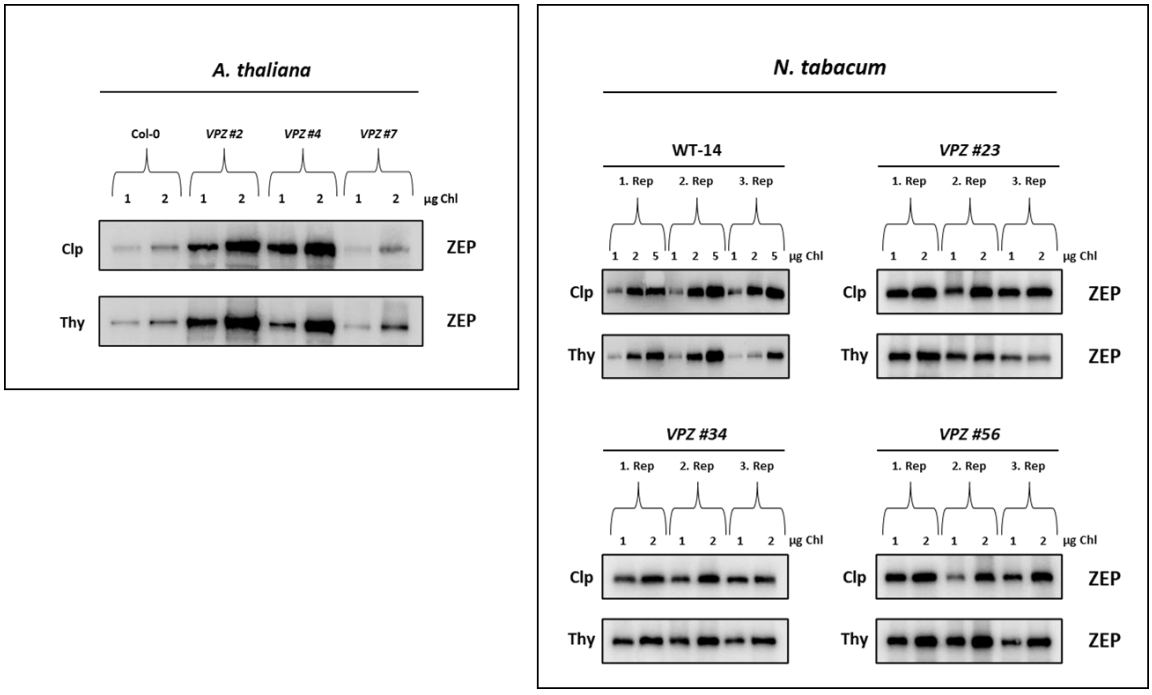

Figure 13: Immunoblot analysis of ZEP contribution within the chloroplast in the VPZ overexpression lines of *A. thaliana* and *N. tabacum*. Tobacco plants were grown under long day conditions (16 h at 150-200 µmol photons m-2 s-1 µmol / 8 h dark), Arabidopsis plants were grown under short day conditions (8 h at ~ 100 µmol photons m-2 s-1/16 h dark). Prior to isolation of chloroplasts, plants were dark-adapted overnight. Thylakoids were isolated from a fraction of the chloroplast by removing the stroma. For Arabidopsis and tobacco VPZ lines, a total chlorophyll amount of 1 µg and 2 µg was loaded onto the gel. For tobacco wildtype a total chlorophyll amount of 1 µg, 2 µg and 5 µg was loaded onto the gel. Tobacco wildtype was detected separately. One biological replicate for Arabidopsis and three biological replicates for tobacco are depicted. Chl: chlorophyll, Clp: chloroplast, Thy: thylakoids.

Moreover, analysis of tobacco and Arabidopsis VPZ lines revealed a lower reduction of PSII activity and a better recovery of PSII activity compared to the corresponding wildtype in response to HL (data not shown). This could be explained by the higher qE capacity determined for these mutants. Hence, VPZ OE lines of both species show an increased potential to overcome prolonged HL stress. ZEP activity was found to be downregulated in

Arabidopsis and tobacco VPZ mutants as well, but to less extent as the corresponding wildtypes. As expected, the overall ZEP activity was increased in both species, as a consequence of the additional ZEP pool. The increased ZEP activity resulted in a lower DEPS value and a faster epoxidation in LL compared to the wildtypes (data not shown). Inhibition of chloroplast protein biosynthesis by lincomycin (LM) led to the complete inactivation of PSII activity in Arabidopsis and tobacco VPZ lines. However, ZEP activity partly persisted even in presence of LM in all mutants (data not shown). This indicates that the efficiency of HL-induced down-regulation of ZEP might depend on the amount of ZEP protein. In Arabidopsis, a parallel degradation of D1 and ZEP was observable under control conditions and in presence of LM in all mutants (data not shown). Although these data indicate that the amount of ZEP does not alter the general correlation of PSII and ZEP activity as well as the relation of D1 and ZEP degradation, these mutants represent an important source for further analysis on ZEP regulation. With respect to the identification of possible interaction partners of ZEP, these mutants further provide a useful tool to increases the protein yield in future Co-IP and cross-linking studies.

10. References

Albanese, P., Manfredi, M., Meneghesso, A., Marengo, E., Saracco, G., Barber, J., et al. (2016). Dynamic reorganization of photosystem II supercomplexes in response to variations in light intensities. Biochim. Biophys. Acta 1857: 1651–1660.

Albertsson, P. (2001). A quantitative model of the domain structure of the photosynthetic membrane. Trends Plant Sci 6 (8): 349–354.

Allen, J.F., & Forsberg, J. (2001). Molecular recognition in thylakoid structure and function. Trends in Plant Science 6 (7): 317-326.

Allen, J.F. (2017). Why we need to know the structure of phosphorylated chloroplast light-harvesting complex II. Physiol Plant 161: 28–44.

Amunts, A., Drory, O., Nelson, N. (2007). The structure of a plant photosystem I supercomplex at 3.4 Å resolution. Nature 447 (7140): 58–63.

Amunts, A., Nelson, N. (2008). Functional organization of a plant Photosystem I: Evolution of a highly efficient photochemical machine. Plant Physiol Biochem 46 (3): 228–237.

Amunts, A., Toporik, H., Borovikova, A., Nelson, N. (2010). Structure Determination and Improved Model of Plant Photosystem I. J Biol Chem 285 (5): 3478–3486.

Ananyev, G., Renger, G., Wacker, U., Klimov, V. (1994). The photoproduction of superoxide radicals and the superoxide-dismutase activity of Photosystem II—the possible involvement of cytochrome b559. Photosynth Res 41: 327–338.

Anderson, J.M. (1986). Photoregulation of the Composition, Function, and Structure of Thylakoid Membranes. Annu. Rev. Plant Physiol. 37: 93–136.

Anderson, J.M., Goodchild, D.J., Boardman, N.K. (1973). Composition of photosystems and chloroplast structure in extreme shade plants. Biochim. Biophys. Acta 325: 573–585.

Armbruster, U., Labs, M., Pribil, M., Viola, S., Xu, W., Scharfenberg, M., Hertle, A.P., Rojahn, U., Jensen, P.E., Rappaport, F., Joliot, P., Dörmann, P., Wanner, G., and Leister, D. (2013). Arabidopsis CURVATURE THYLAKOID1 Proteins Modify Thylakoid Architecture by Inducing Membrane Curvature. The Plant Cell 25 (7): 2661–2678.

Aro, E.M., Virgin, I., Andersson, B. (1993). Photoinhibition of photosystem II. Inavtivation, protein damage and turnover. Biochimica et Biophysica Acta – Bioenergetics 1143: 113-134.

Arsova, B., Hoja, U., Wimmelbacher, M., Greiner, E., Ustun, S., Melzer, M., Petersen, K., Lein, W., Bornke, F. (2010). Plastidial thioredoxin z interacts with two fructokinase-like proteins in a thiol-dependent manner: evidence for an essential role in chloroplast development in Arabidopsis and Nicotiana benthamiana. Plant Cell 22: 1498–1515.

Asada, K. (2000). The water-water cycle as alternative photon and electron sinks. Philos Trans R Soc Lond B Biol Sci. 355(1402): 1419–1431.

Asada, K. (2006). Production and Scavenging of Reactive Oxygen Species in Chloroplasts and Their Functions. Plant Physiol 141: 391–396.

Avenson, T.J., Cruz, J.A., Kanazawa, A., Kramer, D.M. (2005). Regulating the proton budget of higher plant photosynthesis. PNAS 27 (102): 9709–9713.

Bailey, S., Horton, P., & Walters, R. G. (2004). Acclimation of Arabidopsis thaliana to the light environment: the relationship between photosynthetic function and chloroplast composition. Planta 218: 793-802.

Ballottari, M., Dall'Osto, L., Morosinotto, T., Bassi, R. (2007). Contrasting Behavior of Higher Plant Photosystem I and II Antenna Systems during Acclimation. J Biol Chem 282 (12): 8947–8958.

Barrero, J.M., Piqueras, P., González-Guzmán, M., Serrano, M., Rodriguez, P.L., Ponce, M.R., Micol, J.L. (2005). A mutational analysis of the ABA1 gene of Arabidopsis thaliana highlights theinvolvement of ABA in vegetative development. Journal of Experimental Botany 56(418): 2071-2083.

Bartsch, S., Monnet, J., Selbach, K., Quigley, F., Gray, J., von Wettstein, D., Reinbothe, S., Reinbothe, C. (2008). Three thioredoxin targets in the inner envelope membrane of chloroplasts function in protein import and chlorophyll metabolism. PNAS 105(12): 1-6.

Bellafiore, S., Barneche, F., Peltier, G., Rochaix, J.D. (2005). State transitions and light adaptation require chloroplast thylakoid protein kinase STN7. Nature 433, 892–895.

Ben-Shem, A., Frolow, F., Nelson, N. (2003). Crystal structure of plant photosystem I. Nature 426: 630–635.

Björkman, O., Holmgren, P. (1963). Adaptability of photosynthetic apparatus to light intensity in ecotypes from exposed and shaded habitats. Physiol. Plant 16: 889–914.

Boardman, N.K. (1977). Comparative photosynthesis of sun and shade plants. Annu. Rev. Plant Physiol. Plant Mol. Biol. 28: 355–377.

Bouvier, F., d'Harlingue, A., Hugueney, P., Marin, E., Marion-Poll, A., Camara, B. (1996). Xanthophyll biosynthesis: Cloning, expression, functional reconstitution, and regulation of β- cyclohexenyl carotenoid epoxidase from pepper (Capsicum annuum). Journal of Biological Chemistry 271: 28861-28867.

Bratt, C.E., Arvidsson, P.O., Carlsson, M., Åkerlund, H.E. (1995). Regulation of violaxanthin de-epoxidase activity by pH and ascorbate concentration. Photosynth. Res. 45: 169–175.

Broser, M., Gabdulkhakov, A., Kern, J., Guskov, A., Müh, F., Saenger, W., Zouni, A. (2010). Crystal structure of monomeric photosystem II from Thermosynechococcus elongatus at 3.6-Å resolution. J. Biol. Chem. 285: 26255–26262.

Brugnoli, E., Cona, A., Lauteri, M. (1994). Xanthophyll cycle components and capacitiy for non-radiative energy dissipation in sun and shade leaves of Ligustrum ovalifolium exposed to conditions limiting photosynthesis. Photosynth. Res. 41, 451–463.

Büch, K., Stransky, H., Hager, A. (1995). FAD is a further essential cofactor of the NAD(P)H and O_2-dependent zeaxanthin-epoxidase. FEBS letter 376: 45-48.

Buchanan, B.B. (2016). The Path to Thioredoxin and Redox Regulation in Chloroplasts. Annu. Rev. Plant Biol. 67:1–24

Bugos, R., Hieber, A.D., Yamamoto, H. (1998). Xanthophyll cycle enzymes are members of the lipocalin family, the first identified from plants. Journal of Biological Chemistry 273: 15321-15324.

Caffarri, S., Croce, R., Breton, J., Bassi, R. (2001). The Major Antenna Complex of Photosystem II Has a Xanthophyll Binding Site Not Involved in Light Harvesting. J. Biol. Chem. 276 (38): 35924–35933.

Cavalier-Smith, T. (2000). Membrane heredity and early chloroplast evolution. Trends Plant Sci 5 (4): 174–182.

Choquet, Y., Vallon, O. (2000). Synthesis, assembly and degradation of thylakoid membrane proteins. Biochimie 82: 615–634.

Collin, V., Issakidis-Bourguet, E., Marchand, C., Hirasawa, M., Lancelin, J.M., Knaff, D.B., Miginiac-Maslow, M. (2003). The Arabidopsis plastidial thioredoxins new functions and new insights into specificity. The Journal of Biological Chemistry 278: 23747–23752.

Collin, V., Lamkemeyer, P., Miginiac-Maslow, M., Hirasawa, M., Knaff, D.B., Dietz, K.J., Issakidis-Bourguet, E. (2004). Characterization of plastidial thioredoxins from Arabidopsis belonging to the new y-type. Plant Physiol. 136: 4088–4095.

Croce, R., Weiss, S. (1999). Membranes And Bioenergetics: Carotenoid-binding Sites of the Major Light-harvesting Complex II of Higher Plants. J. Biol. Chem. 274: 29613–29623.

Da, Q., Sun, T., Wang, M., Jin, H., Li, M., Feng, D., Wang, J., Wang, H., & Liu, B. (2018). M-type thioredoxins are involved in the xanthophyll cycle and proton motive force to alter NPQ under low-light conditions in Arabidopsis. Plant Cell Rep 37: 279-291.

Dal Corso, G., Pesaresi, P., Masiero, S., Aseeva, E., Schunemann, D., Finazzi, G., Joliot, P., Barbato, R., and Leister, D. (2008). A complex containing PGRL1 and PGR5 is involved in the switch between linear and cyclic electron flow in Arabidopsis. Cell 132: 273-285.

Dall'Osto, L., Caffarri, S., Bassi, R.A. (2005). Mechanism of non-photochemical energy dissipation, independent from PsbS, revealed by a conformational change in the antenna protein CP26. Plant Cell 17: 1217–1232.

Danielsson, R., Albertsson, P.A., Mamedov, F., Styring, S. (2004). Quantification of photosystem I and II in different parts of the thylakoid membrane from spinach. Biochimia et Biophysica Acta – Bioenergetics 1608: 53-61.

Dekker, J., Boekema, E. (2005). Supramolecular organization of thylakoid membrane proteins in green plants. Biochimica et biophysica acta 1706: 12-39.

Demmig-Adams, B., Adams, W.W., Heber, U., Neimanis, S., Winter, K., Krüger, A., Czygan, F.C., Bilger, W., Björkman, O. (1990). Inhibition of Zeaxanthin Formation and of Rapid Changes in Radiationless Energy Dissipation by Dithiothreitol in Spinach Leaves and Chloroplasts. Plant Physiol. 92: 293–301.

Demmig-Adams, B., Adams, W.W. (1996). The role of xanthophyll cycle carotenoids in the protection of photosynthesis. Trends Plant Sci 1 (1): 21–26.

Demmig-Adams, B., Gilmore, A., Adams, W. (1996). In vivo functions of carotenoids in higher plants. Faseb 10: 403-412.

Dietz, K.J. (2010). Peroxiredoxins in Plants and Cyanobacteria. ANTIOXIDANTS & REDOX SIGNALING 15(4): 1129-1159.

Durocher, D., Jackson, S. (2002). The FHA domain. FEBS Letters 513: 58-66

Formaggio, E., Cinque, G., Bassi, R. (2001). Functional Architecture of the Major Light-harvesting Complex from Higher Plants. J Mol Biol 314: 1157–1166.

Foyer, C.H., Noctor, G. (2009). Redox regulation in photosynthetic organisms: signaling, acclimation, and practical implications. Antioxidants & Redox Signaling 11: 861–905.

Galvez-Valdivieso, G., Mullineaux, P.M. (2010). The role of reactive oxygen species in signalling from chloroplasts to the nucleus. Physiol Plant 138 (4): 430–439.

Garcia-Molina, A., Leister, D. (2020). Accelerated relaxation of photoprotection impairs biomass accumulation in Arabidopsis. Nature Plants 6: 9-12.

Gisselsson, A., Szilágyi, A., Åkerlund, H.E. (2004). Role of histidines in the binding of violaxanthin de-epoxidase to thylakoid membrane as studied by site-directed mutagenesis. Physiol Plant 122: 337–43.

Hager, A. (1969). Lichtbedingte pH-Erniedrigung in einem Chloroplasten-Kompartiment als Ursache der enzymatischen Violaxanthin- -> Zeaxanthin-Umwandlung; Beziehungen zur Photophosphorylierung. Planta 89: 224–243.

Härtel, H., Lokstein, H., Grimm, B., Rank, B. (1996). Kinetic studies on the xanthophyll cycle in barley leaves. Influence of antenna size and relations to nonphotochemical chlorophyll fluorescence quenching. Plant Physiol 110: 471–482.

Havaux, M., Dall'Osto, L., Bassi, R. (2007). Zeaxanthin Has Enhanced Antioxidant Capacity with Respect to All Other Xanthophylls in Arabidopsis Leaves and Functions Independent of Binding to PSII Antennae. Plant Physiol. 145 (4): 1506–1520.

Havaux, M., Niyogi, K.K. (1999). The violaxanthin cycle protects plants from photooxidative damage by more than one mechanism. Proc. Natl. Acad. Sci. U. S. A. 96, 8762–7.

Horton, P., Johnson, M.P., Perez-Bueno, M.L., Kiss, A.Z., Ruban, A.V. (2008). Photosynthetic acclimation: Does the dynamic structure and macro-organisation of photosystem II in higher plant grana membranes regulate light harvesting states? FEBS J 275: 1069–1079.

Horton, P., Wentworth, M., & Ruban, A. (2005). Control of the light harvesting function of chloroplast membranes: The LHCII-aggregation model for non-photochemical quenching. FEBS Letters 579: 4201-4206.

Ifuku, K., Endo, T., Shikanai, T., and Aro, E.M. (2011). Structure of the chloroplast NADH dehydrogenase-like complex: nomenclature for nuclear-encoded subunits. Plant Cell Physiol 52: 1560-1568.

Ikegami, A., Yoshimura, N., Motohashi, K., Takahashi, S., Romano, P.G., Hisabori, T., Takamiya, K., Masuda, T. (2007). The CHLI1 subunit of Arabidopsis thaliana magnesium chelatase is a target protein of the chloroplast thioredoxin. J Biol Chem 282: 19282–19291.

Jackson-Constan, D. Akita, M., Keegstra, K. (2001). Molecular chaperones involved in chloroplast protein import. Biochim Biophys Acta 1541: 102–113.

Jacquot J., Vidal J., Gadal P., Schürmann P. (1978). Evidence for existence of several enzyme-specific thioredoxins in plants. FEBS Letters 96: 243–246.

Jahns, P. (1995). The Xanthophyll Cycle in Intermittent Light-Crown Pea Plants. Plant Physiol. 108: 149–156.

Jahns, P., Holzwarth, A.R. (2012). The role of the xanthophyll cycle and of lutein in photoprotection of photosystem II. Biochimia et Biophysica Acta – Bioenergetics 1817: 182-193.

Jahns, P., Latowski, D., Strzalka, K. (2009). Mechanism and regulation of the violaxanthin cycle: The role of antenna proteins and membrane lipids. Biochimica et Biophysica Acta – Bioenergetics 1787(1): 3-14.

Jahns, P., Miehe, B. (1996). Kinetic correlation of recovery from photoinhibition and zeaxanthin epoxidation. Planta 198: 202-210.

Jahns, P., Wehner, A., Paulsen, H., Hobe, S. (2001). De-epoxidation of Violaxanthin after Reconstitution into Different Carotenoid Binding Sites of Light-harvesting Complex II. J Biol Chem 276 (25): 22154–22159.

Jansson, S. (1994). The light-harvesting chlorophyll a/b-binding proteins. Biochimica et Biophysica Acta – Bioenergetics 1184: 1-19.

Jarvis, P., Robinson, C. (2004). Mechanisms of protein import and routing in chloroplasts. CurrentBiology 14: 1064-1077.

Johnson, M. P., Davison, P. A., Ruban, A. V., & Horton, P. (2008). The xanthophyll cycle pool size controls the kinetics of non-photochemical quenching in Arabidopsis thaliana. FEBS Letters 582: 262-266.

Joliot, P., Johnson, G.N. (2011). Regulation of cyclic and linear electron flow in higher plants. Proc Natl Acad Sci 108: 13317–13322.

Junge, W., Sielaff, H., Engelbrecht, S. (2009). Torque generation and elastic power transmission in the rotary FOF1-ATPase. Nature 459 (7245): 364–370.

Kalituho, L., Rech, J., Jahns, P. (2007). The roles of specific xanthophylls in light utilization. Planta 225: 423–39.

Kato, Y., Sakamoto, W. (2009). Protein quality control in chloroplasts: A current model of D1 protein degradation in the photosystem II repair cycle. Journal of Biochemistry 146(4): 463-469.

Kato, Y., Sun, X., Zhang, L., Sakamoto, W. (2012). Cooperative D1 degradation in the photosystem II repair mediated by chloroplastic proteases in Arabidopsis. Plant Physiology 159(4): 1429-1439**.**

Kim, H.S., Minh Hien, H., Jeon, Y.A., Wu, G., Lee, C.H. (2017). Differential down-regulation of zeaxanthin epoxidation in two rice (Oryza sativa L.) cultivars with different chilling sensitivities. J. Plant Biol. 60: 413-422.

Kirchhoff, H., Hall, C., Wood, M., Herbstova, M., Tsabari, O., Nevo, R., Charuvi, D., Shimoni, E., and Reich, Z. (2011). Dynamic control of protein diffusion within the granal thylakoid lumen. PNAS 108 (50): 20248–20253.

Kobayashi, N., DellaPenna, D. (2008). Tocopherol metabolism, oxidation and recycling underhigh light stress in Arabidopsis. The Plant Journal 55: 607–618.

Koochak, H., Puthiyaveetil, S., Mullendore, D.L., Li, M., Kirchhoff, H. (2019). The structural and functional domains of plant thylakoid membranes. Plant Journal 97(3): 412-429.

Koorneef, M., Jorna, M.L., Brinkhorst-van der Swan, D.L.C., Karssen, C.M. (1982). The isolation of abscisic acid (ABA) deficient mutants by selection of induced revertants in non-germinating giberellin sensitive lines of Arabidopsis thaliana (L.) Theor. Appl. Genet. 61: 385-393.

Kovács-Bogdán, E., Soll, J., Bölter B. (2010). Protein import into chloroplasts: The Tic complex and its regulation. Biochimica et Biophysica Acta 1803: 740-747.

Kramer, D.M., Avenson, T.J., Edwards, G.E. (2004). Dynamic flexibility in the light reactions of photosynthesis governed by both electron and proton transfer reactions. Trends Plant Sci 9 (7): 349–357.

Krause, G.H., Jahns, P. (2004). Non-photochemical energy dissipation determined by chlorophyll fluorescence quenching: characterization and function. In: Chlorophyll a Fluorescence, Springer Netherlands: 463-495.

Kress, E., Jahns, P. (2017). The dynamics of energy dissipation and xanthophyll conversion in Arabidopsis indicate an indirect photoprotective role of zeaxanthin in slowly inducible and relaxing components of non-photochemical quenching of excitation energy. Front. Plant Sci. 8: 1-17.

Krieger-Liszkay, A. (2005). Singlet oxygen production in photosynthesis. J Exp Bot 56: 337–346.

Kromdijk, J., Glowacka, K., Leonelli, L., Gabilly, S.T., Iwai, M., Niyogi, K.K., & Long, S.P. (2016). Improving photosynthesis and crop productivity by accelerating recovery from photoprotection. Science 354 (6314): 857-860.

Kühlbrandt, W., Wang, D.N., Fujiyoshi, Y. (1994). © 19 9 4 Nature Publishing Group. Nature 367: 532–8.

Latowski, D., Kruk, J., Burda, K., Skrzynecka-Jaskier, M., Kostecka-Gugala, A., Strzalka, K. (2002). Kinetics of violaxanthin de-epoxidation by violaxanthin de-epoxidase, a xanthophyll cycle enzyme, is regulated by membrane fluidity in model lipid bilayers. Eur. J. Biochem. 269.4656–4665.

Li, X., Björkman, O., Shih, C., Grossman, A.R., Rosenquist, M., Jansson, S., and Niyogi, K.K. (2000). A pigment-binding protein essential for regulation of photosynthetic light harvesting. Nature 403: 391-395.

Li, Z., Wakao, S., Fischer, B.B., Niyogi, K.K. (2009). Sensing and responding to excess light. Annual Review of Plant Biology 60: 239-260.

Lichtenthaler, H.K., Buschmann, C., Döll, M., Fietz, H., Bach, T., Kozel, U., Meier, D., Rahmsdorf, U. (1981). Photosynthetic activity, chloroplast ultrastructure, and leaf characteristics of high-light and low-light plants and of sun and shade leaves. Photosynth Res 2: 115–141.

Liebthal, M., Maynard, D., and Dietz, K.-J. (2018). Peroxiredoxins and Redox Signaling in Plants. Antioxid. Redox Signal. 28: 609–624.

Liu, Z., Yan, H., Wang, K., Kuang, T., Zhang, J., Gui, L., An, X., Chang, W. (2004). Crystal structure of spinach major light-harvesting complex at 2.72 Å resolution. Nature 428: 287–292.

Loll, B., Kern, J., Saenger, W., Zouni, A. Biesiadka, J. (2005). Towards complete cofactor arrangement in the 3.0 A resolution structure of photosystem II. Nature 438: 1040-1044.

Ludlow, M.M., Wilson, G.L. (1971). Photosynthesis of tropical pasture plants. 2. Temperature and illuminance history. Aust. J. Biol. Sci. 24: 1065–1075.

Malnoë, A. (2018). Photoinhibition or photoprotection of photosynthesis? Update on the (newly termed) sustained quenching component qH. Environmental and Experimental Botany 154: 123-133.

Marin, E., Nussaume, L., Quesada, A., Gonneau, M., Sotta, B., Hugueney, P., Frey, A., Marion-Poll, A. (1996). Molecular identification of zeaxanthin epoxidase of Nicotiana plumbaginifolia, a gene involved in abscisic acid biosynthesis and corresponding to the ABA locus of Arabidopsis thaliana. The EMBO Journal 15(10): 2331-2342.

Mazor, Y., Borovikova, A., Nelson, N. (2015). The structure of plant photosystem I super-complex at 2.8 Å resolution. eLife 4: 1-18.

Mehler, A.H. (1951). Studies on reactions of illuminated chloroplasts. Archives of Biochemistry and Biophysics 33: 65-77.

Melis, A. (1999). Photosystem-II damage and repair cycle in chloroplasts: what modulates the rate of photodamage in vivo? Trends Plant Sci 4 (4): 130–135.

Mishra, Y., Jänkänpää, H.P., Kiss, A.Z., Funk, C., Schröder, W.P., Jansson, S. (2012). Arabidopsis plants grown in the field and climate chambers significantly differ in leaf morphology and photosystem components. BMC Plant Biol 12 (6): 1-18.

Mittler, R., Vanderauwera, S., Gollery, M., van Breusegem, F. (2004). Reactive oxygen gene network of plants. Trends in Plant Science 9 (10): 490–498.

Miyake, C. (2010). Alternative electron flows (water-water cycle and cyclic electron flow around PSI) in photosynthesis: Molecular mechanisms and physiological functions. Plant and Cell Physiology 51(12): 1951-1963.

Møller, I. M., Jensen, P. E., & Hansson, A. (2007). Oxidative modifications to cellular components in plants. Annual Review of Plant Biology 58: 459-481

Morosinotto, T., Caffarri, S.,Dall'Osto, L., Bassi, R. (2003). Mechanistic aspects of the xanthophyll dynamics in higher plant thylakoids. Physiol. Plant. 119: 347–354.

Müller, P., Li, X., Niyogi, K.K. (2001). Non-photochemical quenching. A response to excess light energy. Plant physiology 125(April): 1558-1566.

Munekage, Y., Hashimoto, M., Miyake, C., Tomizawa, K.-I., Endo, T., Tasaka, M., and Shikanai, T. (2004). Cyclic electron flow around photosystem I is essential for photosynthesis. Nature 429: 579-582.

Naranjo, B., Mignée, C., Krieger-Liszkay, A., Hornero-Méndez, D., Gallardo-Guerrero, L., Cejudo, F.J., Lindahl, M. (2016). The chloroplast NADPH thioredoxin reductase C, NTRC, controls non-photochemical quenching of light energy and photosynthetic electron transport in Arabidopsis. Plant, Cell and Environment 39(4): 804-822.

Nath, K., Jajoo, A., Poudyal, R.S., Timilsina, R., Park, Y.S., Aro, E.M., Nam, H.G., Lee, C.H. (2013). Towards a critical understanding of the photosystem II repair mechanism and its regulation during stress conditions. FEBS Letters 587(21): 3372-3381.

Nawrocki, W.J., Santabarbara, S., Mosebach, L., Wollman, F.A., Rappaport, F. (2016). State transitions redistribute rather than dissipate energy between the two photosystems in Chlamydomonas. Nat Plants 2: 1-7.

Nelson, N., and Junge, W. (2015). Structure and energy transfer in photosystems of oxygenic photosynthesis. Annu Rev Biochem 84: 659-683.

Nikkanen, L., Guinea Diaz, M., Toivola, J., Tiwari, A., Rintamäki, E. (2019). Multilevel regulation of non-photochemical quenching and state transitions by chloroplast NADPH-dependent thioredoxin reductase. Physiologia Plantarum 166: 211-225.

Nikkanen, L., Rintamäki, E. (2019). Chloroplast thioredoxin systems dynamically regulate photosynthesis in plants. Biochemical Journal 476: 1159-1172.

Nilkens, M., Kress, E., Lambrev, P., Miloslavina, Y., Müller, M., Holzwarth, A.R., Jahns, P. (2010). Identification of a slowly inducible zeaxanthin-dependent component of non-photochemical quenching of chlorophyll fluorescence generated under steady-

state conditions in Arabidopsis. Biochimica et Biophysica Acta – Bioenergetics 1797(4): 466-475.

Niyogi, K.K., Grossman, A.R., Björkman, O. (1998). Arabidopsis Mutants Define a Central Role for the Xanthophyll Cycle in the Regulation of Photosynthetic Energy Conversion. The Plant Cell 10(July): 1121-1134.

North, H. M., Frey, A., Boutin, J., Sotta, B., & Marion-Poll, A. (2005). Analysis of xanthophyll cycle gene expression during the adaptation of Arabidopsis to excess light and drought stress: Changes in RNA steady-state levels do not contribute to short-term responses. Plant Science 169: 115-124.

Okegawa, Y., Motohashi, K. (2015). Chloroplastic thioredoxin m functions as a major regulator of Calvin cycle enzymes during photosynthesis in vivo. Plant J. Cell Mol. Biol. 84, 900–913.

Öquist, G., Huner, N.P.A. (2003). Photosynthesis of overwintering evergreen plants. Annual Review of Plant Biology 54:329-355.

Ort, D.R. (2001). When There Is Too Much Light. Plant Physiol. 125: 29–32.

Paila, Y.D., Richardson, L.G.L., Schnell, D.J. (2015). New insights into the mechanism of chloroplast protein import and its integration with protein quality control, organelle biogenesis and development. J. Mol. Biol. 427, 1038–1060.

Park, Y. I., Chow, W. S., Anderson, J. M., Hurry, V. M. (1996). Differential susceptibility of Photosystem II to light stress in light-acclimated pea leaves depends on the capacity for photochemical and non-radiative dissipation of light. Plant Sci. 115, 137–149.

Park, H., Seok, H., Park, B., Kim, S., Goh, C., Lee, B., Lee, C., & Moon, Y. (2008). Overexpression of Arabidopsis ZEP enhances tolerance to osmotic stress. Biochemical and Biophysical Research Communications 375: 80-85.

Pérez-Ruiz, J.M., Naranjo, B., Ojeda, V., Guinea, M., Cejudo, F.J. (2017). NTRC-dependent redox balance of 2-Cys peroxiredoxins is needed for optimal function of the photosynthetic apparatus. Proc. Natl. Acad. Sci. 114: 12069–12074.

Pogson, B.J., Niyogi, K.K., Björkman, O., DellaPenna, D. (1998). Altered xanthophyll compositions adversely affect chlorophyll accumulation and nonphotochemical quenching in Arabidopsis mutants. Proc. Natl. Acad. Sci. U. S. A. 95, 13324–13329.

Pospíšil, P., Arató, A., Krieger-Liszkay, A., Rutherford, A.W. (2004). Hydroxyl radical generation by photosystem II. Biochemistry 43: 6783–6792.

Qin, X., Suga, M., Kuang, T., Shen, J. (2015). Structural basis for energy transfer pathways in the plant PSI-LHCI supercomplex. Science 438 (6238): 989–995.

Reinhold, C., Niczyporuk, S., Beran, K.C., Jahns, P. (2008). Short-term down-regulation of zeaxanthin epoxidation in Arabidopsis thaliana in response to photo-oxidative stress conditions. Biochimica et Biophysica Acta – Bioenergetics 1777: 462-469.

Richter A.S., Peter E., Rothbart M., Schlicke H., Toivola J., Rintamaki E., Grimm B. (2013). Posttranslational influence of NADPH-dependent thioredoxin reductaseC on enzymes in tetrapyrrole synthesis. Plant Physiology 162: 63–73.

Rochaix, J.D. (2014). Regulation and Dynamics of the Light-Harvesting System. Annu Rev Plant Biol 65: 287–309.

Rock, C.D., Zeevart, J.A.D. (1991). The aba mutant of Arabidopsis thaliana is impaired in epoxy-carotenoid biosynthesis. Proc. Natl Acad. Sci. USA 88: 7496–7499.

Ruban, A.V., Lee, P.J., Wentworth, M., Young, A.J., Horton, P. (1999). Determination of the Stoichiometry and Strength of Binding of Xanthophylls to the Photosystem II Light Harvesting Complexes. J. Biol. Chem. 274: 10458–10465.

Schöttler, M.A., Albus, C.A., Bock R. (2011). Photosystem I: Its biogenesis and function in higher plants. J Plant Physiol 168 (12): 1452–1461.

Schöttler, M.A., Tóth, S.Z. (2014). Photosynthetic complex stoichiometry dynamics in higher plants: environmental acclimation and photosynthetic flux control. Front. Plant Sci. 5 (188): 1–15.

Schumann, T., Paul, S., Melzer, M., Dörmann, P., & Jahns, P. (2017). Plant growth under natural light conditions provides highly flexible short-term acclimation properties toward high light stress. Frontiers in Plant Science 8: 1-18.

Schwarz, N., Armbruster, U., Iven, T., Brückle, L., Melzer, M., Feussner, I., Jahns, P. (2015). Tissue-Specific Accumulation and Regulation of Zeaxanthin Epoxidase in Arabidopsis Reflect the Multiple Functions of the Enzyme in Plastids. Plant and Cell Physiology 56(2): 346-357.

Seo, M., Koshiba, T. (2002). Complex regulation of ABA biosynthesis in plants. Trends in Plant Science 7(1): 41-48.

Shikanai, T. (2007). Cyclic electron transport around photosystem I: genetic approaches .Annu. Rev. Plant Biol. 58: 199 – 217.

Siefermann, D., Yamamoto, H.Y. (1975). Properties of NADPH and oxygen-dependent zeaxanthin epoxidation in isolated chloroplasts. Arch. Biochem. Biophys. 171: 70-77.

Standfuss, J., van Scheltinga,, A.C.T., Lamborghini, M., Kühlbrandt, W. (2005). Mechanisms of photoprotection and nonphotochemical quenching in pea light-harvesting complex at 2.5 Å resolution. EMBO J 24: 919–928.

Suorsa, M., Jarvi, S., Grieco, M., Nurmi, M., Pietrzykowska, M., Rantala, M., Kangasjarvi, S., Paakkarinen, V., Tikkanen, M., Jansson, S., Aro, E.M. (2012). Proton Gradient Regulation5 Is Essential for Proper Acclimation of Arabidopsis Photosystem I to Naturally and Artifi-cially Fluctuating Light Conditions. Plant Cell 24: 2934-2948

Taiz, L. & Zeiger, E. (2010). Plant Physiology. 5th Edition.Sunderland, MA: Sinauer Associates.

Takahashi, H., Watanabe, A., Tanaka, A., Hashida, S.N., Kawai-yamada, M., Sonoike, K., Uchimiya, H. (2006). Chloroplast NAD kinase is essential for energy transduction through the xanthophyll cycle in photosynthesis. Plant Cell Physiol. 47: 1678–1682.

Tikkanen, M., Piippo, M., Suorsa, M., Sirpio, S., Mulo, P., Vainonen, J., Vener, A.V., Allahverdiyeva, Y., and Aro, E.M. (2006). State transitions revisited-a buffering system for dynamic low light acclimation of Arabidopsis. Plant Mol Bio 62: 779-793.

Triantaphylidès, C., Havaux, M. (2009). Singlet oxygen in plants: production, detoxification and signaling. Trends in Plant Science 14 (4): 219–228.

Triantaphylidès, C., Krischke, M., Hoeberichts, F.A., Ksas, B., Gresser, G., Havaux, M., Van Breusegem, F., Mueller, M.J. (2008). Singlet oxygen is the major reactive oxygen species involved in photooxidative damage to plants. Plant Physiol. 148: 960–968.

Tyystjärvi, E., Aro, E.M. (1996). The rate constant of photoinhibition, measured in lincomycin-treated leaves, is directly proportional to light intensity. Proceedings of the National Academy of Sciences of the United States of America 93: 2213-2218.

Umena, Y., Kawakami, K., Shen, J.R., Kamiya, N. (2011). Crystal structure of oxygen-evolving photosystem II at 1.9 Å resolution. Nature 473: 55–60

Verhoeven, A., Adams, W., Demmig-Adams, B. (1996). Close relationship between the state of the xanthophyll cycle pigments and photosystem II efficiency during recovery from winter stress. Physiologia Plantarum 96: 567-576.

Walters, R.G., Horton, P. (1991). Resolution of components of non-photochemical fluorescence quenching in barley leaves. Photosynth Res 27: 121-133.

Wei, X., Su, X., Cao, P., Liu, X., Chang, W., Li, M., Zhang, X., Liu, Z. (2016). Structure of spinach photosystem II–LHCII supercomplex at 3.2 Å resolution. Nature 1: 1-18.

Welti, R., Li, W. Q., Li, M. Y., Sang, Y. M., Biesiada, H., Zhou, H. E., et al. (2002). Profiling membrane lipids in plant stress responses–role of phospholipase alpha in freezing-induced lipid changes in Arabidopsis. J. Biol. Chem. 277: 31994–32002.

Weston, E., Thorogood, K., Vinti, G., López-Juez, E. (2000). Light quantity controls leaf-cell and chloroplast development in Arabidopsis thaliana wild type and blue-light-perception mutants. Planta 211: 807–815.

Wild, A. (1980). Phyiology of photosynthesis in higher plants– adaptation to light-intensity and light quality. Ber. Dtsch. Bot. Ges. 92: 341–364.

Wild, A., Wolf, G. (1980). The effect of different light intensities on the frequency and size of stomata, the size of cells, the number size and chlorophyll content of chloroplasts in the mesophyll and the guard-cells during the ontogeny of primary leaves of Sinapis alba. Z. Pflanzenphys. 97: 325–342.

Wolosiuk R., Crawford N., Yee B., Buchanan B.B. (1979). Isolation of 3 thioredoxins from spinach leaves. Journal of Biological Chemistry 254: 1627–1632.

Wood, W.H.J., MacGregor-Chatwin, C., Barnett, S.F.H., Mayneord, G.E., Huang, X., Hobbs, J.K., Hunter, C.N., Johnson, M.P. (2018). Dynamic thylakoid stacking regulates the balance between linear and cyclic photosynthetic electron transfer. Nat Plants 4:116–127.

Xiong, L., Lee, H., Ishitani, M., Zhu, J.K. (2002). Regulation of osmotic stress-responsive gene expression by the LOS6/ABA1 locus in Arabidopsis. J. Biol. Chem. 277: 8588–8596.

Xu, C.C., Jeon, Y.A., Hwang, H.J., Lee, C.H. (1999). Suppression of zeaxanthin epoxidation by chloroplast phosphatase inhibitors in rice leaves. Plant Science 146: 27-34.

Yakushevska, A.E., Jensen, P.E., Keegstra, W., van Roon, H., Scheller, V.H., Boekema, E.J., Dekker, J.P. (2001). Supermolecular organization of photosystem II and its associated lightharvesting antenna in Arabidopsis thaliana. Eur J Biochem 268: 6020–6028.

Yamamoto, Y. (2016). Quality Control of Photosystem II: The Mechanisms for Avoidance and Tolerance of Light and Heat Stresses are Closely Linked to Membrane Fluidity of the Thylakoids. Front Plant Sci 7: 1–13

Yoshioka-Nishimura, M. (2016). Close Relationships Between the PSII Repair Cycle and Thylakoid Membrane Dynamics. Plant & cell physiology 57(6): 1115-1122.

Zaltsman, A., Ori, N., & Adam, Z. (2005). Two types of FtsH protease subunits are required for chloroplast biogenesis and photosystem II repair in Arabidopsis. The Plant Cell, 17(10): 2782-2790.

Zarter, C.R., Adams, W.W., Ebbert, V., Adamska, I., Jansson, S., Demmig-Adams, B. (2006). Winter acclimation of PsbS and related proteins in the evergreen Arctostaphylos uva-ursi as influenced by altitude and light environment. Plant, Cell Environ. 29: 869–878.

11. Acknowledgement

First of all, I want to thank my supervisor Prof. Dr. Peter Jahns, who gave me the opportunity to work in his lab. Your balance between support and autonomy helped me to grow and to become the person that I am today.

I would also like to thank Prof. Dr. Georg Groth for being my co-supervisor and mentor and for supporting me during my PhD time.

I also give thanks to Dr. Gereon Poschmann for being my co-supervisor. Thanks to you and Nina Prescher, for performing the MS-analyses for us and always being contactable whenever I had questions concerning this topic.

Special thanks to Michael Melzer who performed the electron microscopy and spent so much time in the lab with me. It was a pleasure for me being your lab partner.

At this point, I would like to address myself to all my bachelor and master students: Lukas Willing, Katrin Sammet, Emin Dülger, Melody Haarmann, Francesca Bongiovanni, Ann-Kathrin Haas, Jan Eichner, Dimitrij Holzmann and Lukas Küster. Thank you so much for being part of the ZEP team and for spending so much time end effort into this topic. You all made a great job and I am happy to see how all of you have evolved.

I want to thank all present and former members of the AG Jahns. You have made working being much easier and more fun. Emin, thanks for your technical and organizational support and for the times when we were singing in the lab. Fritz, thanks for your experimental advices. Although I am not particularly interested in sports, I enjoyed talking about football with you. And damn, I have won our betting game!

Natalie Rothhausen, Natascha Rothhausen, Nicole Eggink, Melody Haarmann, Ann-Kathrin Haas, Janine Meyer and Anastasiia Bovdilova. I would like to thank all of you for beautifying my days in the lab. Thank you for always listening to my sorrows and helping me to overcome these, and especially for becoming my friends.

Maria Graf and Lukas Küster, what can I say? Without you, I wouldn't have survived the last two years. Thank you for always listening to me, supporting me, taking me as I am (as you know sometimes very emotionally), making me laugh and also for letting me cry when it was necessary. I can't imagine better friends.

Big thanks to my sister Sina, to my father and my grandmother. Thank you for supporting and for always loving me. Without you, I wouldn't be where I am without you. Also, I would like to thank David Haas for proofreading my thesis. You are family!

The best comes last: Björn Westhäuser. I am so grateful that you came into my life. You have made me feel so much better during the last two years. Thanks to you, I am a different person than I was before I met you. Thank you for always being there for me and especially for being that patient. I know that I can be very difficult and still, you stay with me. Thank you for loving me exactly as I am. I can no longer imagine life without you. I love you!